

CANADA
DEPARTMENT OF ENERGY, MINES AND RESOURCES
Observatories Branch

PUBLICATIONS
of the
DOMINION OBSERVATORY
OTTAWA

Volume XXXV • No. 7

MAGNETOTELLURIC TWO- AND THREE-LAYER MASTER CURVES

S. P. Srivastava

This document was produced
by scanning the original publication.

Ce document est le produit d'une
numérisation par balayage
de la publication originale.

Price 25 cents

Magnetotelluric Two- and Three-Layer Master Curves S.P. Srivastava

Abstract;—The curve matching method given by Cagniard (1953) to interpret magnetotelluric data in terms of layered resistivity models requires a set of master curves for two, three, or more layers. In this paper the master curve technique is extended to include the theoretical developments of Wait (1962) and Price (1962) in which the dimensions of the inducing field are considered as well as the vertical distribution of resistivity. A large number of two- and three-layer master curves are given for the interpretation of field data. The calculations were done on a computer using the formula given by Srivastava (1965). Curves for both apparent resistivity and phase are plotted as functions of period for various values of horizontal wave-length of the source and various layered models. Some cases in which it is difficult to interpret magnetotelluric data by master curves are mentioned.

Résumé:—La méthode nomographique de Cagniard (1953) pour l'interprétation des données magnétotelluriques relatives aux modèles de couches de résistivité nécessite une série d'abaques pour deux, trois ou plusieurs couches. Dans cette étude, l'auteur étend la technique des abaques aux développements théoriques de Wait (1962) et de Price (1962) qui tiennent compte des dimensions du champ inducteur aussi bien que la répartition verticale de la résistivité. Il y indique un grand nombre d'abaques pour deux ou trois couches, pouvant servir à l'interprétation des données recueillies sur le terrain. Les calculs ont été faits en incorporant la formule de Srivastava (1965) à un ordinateur. Les abaques, pour des valeurs apparentes de résistivité et de phase, sont tracées comme fonctions de période pour diverses valeurs de la longueur d'onde horizontale de la source et pour divers modèles de couches. L'auteur mentionne également certains cas où il est difficile d'interpréter les données magnétotelluriques à l'aide des abaques.



Introduction

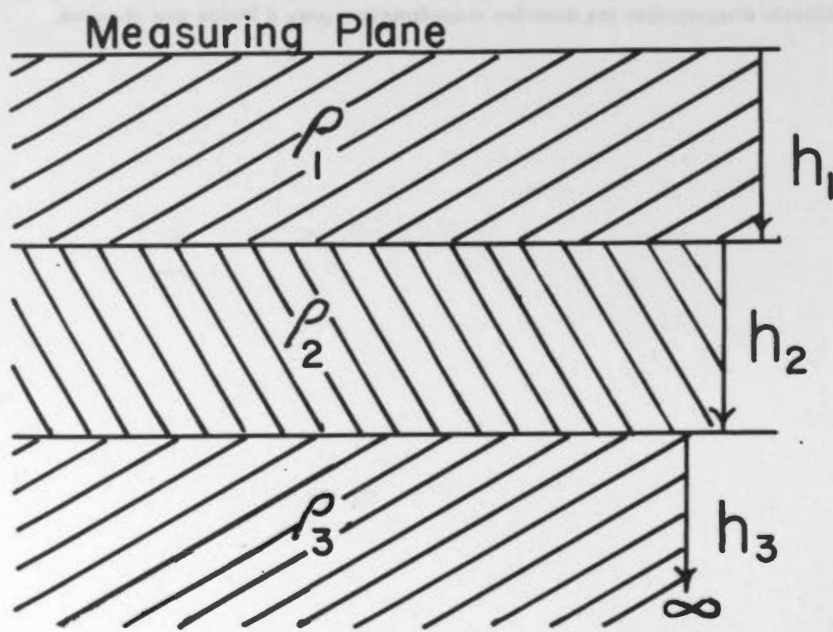
An important problem encountered in all geophysical methods is the interpretation of the data. In many methods interpretation involves comparison of a field curve with a set of master curves, both drawn to the same scale. These master curves are theoretical curves computed for simple geological structures. When a close fit of the field curve with a master curve is obtained the parameters of the mathematical model, such as resistivity, layer depths, etc., that are assumed for the model may be used as estimates of the real earth parameters for the area where the observations are made.

Such a method was suggested by Cagniard (1953) for the analysis of magnetotelluric data. In this method the amplitude and phase relationships between naturally varying electric and magnetic fields at a point on the earth's surface are analysed in order to gain information about the electrical conductivity of the rock strata below. In Cagniard's idealized model, the rock was assumed to lie in horizontal homogeneous layers so that conductivity varies with depth only as one passes from one layer to the next. A further assumption that the electromagnetic field variations are uniform over an infinite horizontal plane simplified the theory but also placed some severe restrictions on its application in geophysical interpretation. However, Wait (1954, 1962) and Price (1962) have shown that Cagniard's theory can be extended to take into account the dimensions of the inducing field. A method of interpretation based on the developments of Wait and Price also requires a comparison of the field curve with a set of master curves. The purpose of this paper is to supply a catalog of such standard curves.

Computation

The amplitude and phase relationships between tangential components of the telluric field E and the magnetic field H which are used for analysis are found from the complex ratios $\frac{E_x}{H_y}$ and $\frac{E_y}{H_x}$. When the tangential components of E and H are mutually perpendicular, these ratios are equivalent except for sign and are frequently referred to as the field impedance, $Z(0)$, at the surface.

The field impedance for a three-layer resistivity model, (shown below), can be written in the form



Three-layer resistivity model

$$Z(0) = \frac{i\omega}{\theta_1} \coth \left\{ \theta_1 h_1 + \coth^{-1} \left[\frac{\theta_1}{\theta_2} \coth \left(\theta_2 h_2 + \coth^{-1} \frac{\theta_2}{\theta_3} \right) \right] \right\} \quad (1)$$

(Srivastava 1965), where

ν is a constant whose reciprocal ($2\pi/\nu$) is a measure of the horizontal scale of the source field, and

$$\theta_m^2 = \nu^2 + 4\pi i \omega \sigma_m \quad (2)$$

Equation (1) can be written in the form

$$Z(0) = \frac{i\omega}{\theta_1} \cdot \frac{G + iH}{Q + iR} \quad (3)$$

where G and Q are the real and H and R the imaginary parts of the right-hand side of (1). Taking the amplitude and phase of (3) we get

$$|Z(0)|^2 = \frac{\rho_1}{2T} \cdot \frac{1}{(1 + \nu^4/k_1^4)^{1/2}} \cdot \frac{G^2 + H^2}{Q^2 + R^2} \quad (4)$$

$$\tan \phi = \frac{x_1(GQ + HR) - y_1(GR - HQ)}{x_1(GR - HQ) + y_1(GQ + HR)} \quad (5)$$

where

$$T = 2\pi/\omega$$

$$G = au(cr+p) - bu(dr+q) + s(r+cp-qd) - t(pd+cq) \quad (6)$$

$$H = au(dr+q) + bu(cr+p) + s(pd+cq) + t(r+cp-qd) \quad (7)$$

$$Q = ru + u(cp-qd) + (as-bt)(cr+p) - (bs+at)(dr+q) \quad (8)$$

$$R = u(cq+pd) + (as-bt)(dr+q) + (bs+at)(cr+p) \quad (9)$$

$$a = (x_1 x_2 + y_1 y_2) / (x_2^2 + y_2^2) \quad (10)$$

$$b = (x_2 y_1 - x_1 y_2) / (x_2^2 + y_2^2) \quad (11)$$

$$c = (x_2 x_3 + y_2 y_3) / (x_3^2 + y_3^2) \quad (12)$$

$$d = (x_3 y_2 - x_2 y_3) / (x_3^2 + y_3^2) \quad (13)$$

$$p = \tanh x_2 h_2 (1 + \tanh^2 y_2 h_2) \quad (14)$$

$$q = \tan y_2 h_2 (1 - \tanh^2 x_2 h_2) \quad (15)$$

$$r = 1 + \tanh^2 x_2 h_2 \cdot \tan^2 y_2 h_2 \quad (16)$$

$$s = \tanh x_1 h_1 (1 + \tan^2 y_1 h_1) \quad (17)$$

$$t = \tan y_1 h_1 (1 - \tanh^2 x_1 h_1) \quad (18)$$

$$u = 1 + \tanh^2 x_1 h_1 \cdot \tan^2 y_1 h_1 \quad (19)$$

$$x_m = 2^{-1/2} \{ (k_m^4 + \nu^4)^{1/2} + \nu^2 \}^{1/2} \quad (20)$$

$$y_m = 2^{-1/2} \{ (k_m^4 + \nu^4)^{1/2} - \nu^2 \}^{1/2} \quad (21)$$

$$k_m^2 = 4\pi \omega \sigma_m \quad (22)$$

and $\rho_1 = \sigma_1^{-1}$, the resistivity of the first layer. If we write $|Z(0)|^2 \cdot 2T$ as ρ_a and call this the apparent resistivity of the system, (4) reduces to

$$\rho_a / \rho_1 = \frac{1}{(1 + \nu^4/k_1^4)^{1/2}} \cdot \frac{G^2 + H^2}{Q^2 + R^2} \quad (23)$$

Extensive calculations of ρ_a/ρ_1 and ϕ at various periods for two- and three-layer models were made using (23) and (5) respectively for various values of ν , σ_m , and h_m on IBM 1620 and 7040 computers. For the sake of simplicity the values of ρ_1 and h_1 have been considered as 1 ohm-metre and 1 km respectively in the computation of all master curves given here. The results are plotted as a function of period, T , in Figures 1 to 60*.

Following is an explanation of the different notations used throughout this text as well as in the Figures.

- A represents the value of $\nu = 10^{-1}$ (km⁻¹)
- B represents the value of $\nu = 10^{-2}$ (km⁻¹)
- C represents the value of $\nu = 10^{-3}$ (km⁻¹)
- D represents the value of $\nu = 10^{-4}$ (km⁻¹)
- E represents the value of $\nu = 0$
- μ_1 represents the ratio ρ_2/ρ_1
- μ_2 represents the ratio ρ_3/ρ_1
- λ_1 represents the ratio h_2/h_1
- λ_2 represents the ratio h_3/h_1

The curves are divided into two groups, the two-layer model curves and the three-layer model curves. The two-layer curves were computed for instances where the resistivity of the second layer is higher than that of the first. A decrease in resistivity of the second layer was not considered here in detail because the source effect in such instances for thin top layers becomes negligibly small as can be seen by comparing Figures 3,5,7,9 and 11 with 13. In these instances where ρ_2 is less than ρ_1 and ν very small, the master curves given by Cagniard (1953) and Jackson et al. (1962) can be used. Furthermore master curves for $\nu = 0$ for a low-high resistivity section can be used to interpret a high-low section by means of the dual characteristic of the master curves in such instances (Wait, 1962). According to this dual characteristic the apparent resistivity (ρ_a), phase (ϕ) and other parameters of a low-high-low resistivity section ($\rho_1, \rho_2, \rho_3, h_1, h_2, h_3$) are related to the corresponding quantities of a high-low-high resistivity section ($\rho_1', \rho_2', \rho_3', h_1', h_2', h_3'$) in the following manner:

$$\mu_1' = (\mu_1)^{-1} \quad (24)$$

$$\mu_2' = (\mu_2)^{-1} \quad (25)$$

$$\lambda_1' = (\mu_1)^{-1} \lambda_1 \quad (26)$$

$$\rho_a'/\rho_1' = [\rho_a/\rho_1]^{-1} \quad (27)$$

and

$$\phi' = \frac{\pi}{2} - \phi \quad (28)$$

Hence the curves which are computed for $\nu = 0$ for the interpretation of low-high-low resistivity sections can also be used for the interpretation of high-low-high resistivity sections using (27) and (28) when ν is very small. However, such a dual characteristic does not hold true when ν is finite.

A set of two-layer curves for various values of h_1 are plotted in Figures 1 and 2. Though the curves in Figures 1 and 2 are given for various values of h_1 , they can also be considered for various values of ν because the quantities $x_1 \cdot h_1$ and $y_1 h_1$ (equations 20, 21) are dimensionless, and their values will be unchanged if k_1 and ν are changed by a factor of $1/L$ and h_1 by a factor of L . Hence the curve corresponding to $h_1 = 10$ in Figure 1 is exactly the same as the curve $\rho_2/\rho_1 = 100$ in Figure 7 except for a horizontal displacement of 10^2 sec. In this manner Figures 1 and 2 can be used to obtain values of h_1 and ν for the field curve in instances where no reasonable fit could be obtained with the other master curves. The method of application of these curves is discussed later.

A set of three-layer master curves for low-high-low (Figures 15 to 48), low-high-high (Figures 49, 50), high-low-high, and high-low-low resistivity sections (Figures 51 to 60) are computed for various values of ν . The apparent resistivity and phase values for low-high-low resistivity sections are given here for $\rho_2 = 100, 200, 500$ ohm-metres and $\rho_3 = 1, 10, 20, 10^{-1}, 10^{-2}$ ohm-metres in different combinations. Again the values of ρ_1 and h_1 were kept constant, assigning them values of 1 ohm-metre and 1 km respectively for all the models. It can be seen from Figures 15 to 50 that as the values of ρ_3 increase from 1 to 10^3 ohm-metres the curves for various values of λ_1 begin to merge into each other and closely resemble two-layer curves. This suggests that the resolving power of the magnetotelluric method decreases as the resistivity of the third layer increases in low-high-high sections. Similarly in the case of low-high-low sections the difference between the curves, for the same value of λ_1 and ν , but different μ_2 , becomes less as the value of ρ_3 decreases from .1 to .01. It can also be seen that for small values of ν of λ_1 the shape of the curves is largely influenced by μ_2 while for large values of λ_1 this is not so.

*Type of graph paper used; K+E Logarithmic, 3x3 cycles, #467402.

K+E Semilogarithmic 7 cycles x 60 Divisions #358-96.

In Figures 51 to 60 a set of master curves are plotted for high-low-low as well as high-low-high sections for various values of ν and μ_2 . A comparison between the curves, for the same values of μ_2 but different ν , shows that they do not differ from each other appreciably. This shows that for such sections the effect of the source is very small except when $\nu = 10^{-1} \text{ km}^{-1}$, an improbable value. A comparison of Figures 51 to 60 shows that as the value of λ_1 increases from 5 to 100 curves for various values of μ_2 tend to merge into each other. Figures 59 and 61 show that when $\lambda_1 = 100$ the shape of the curve remains the same even though μ_2 is changed from 10^{-3} to 10^3 . This demonstrates that the resolving power of the magnetotelluric method decreases as the thickness of the middle increases in both high-low-high or high-low-low sections. Figure 59 is exactly the same as the curve for $\mu_1 = .01$ in Figure 13. Such a characteristic can also be shown theoretically (Wait 1962).

Application of the Curves

The method of interpretation of magnetotelluric data given by Cagniard (1953) involves matching a field curve with a set of master curves drawn for simple layered earth models. The application of master curves to the interpretation of the magnetotelluric data is based on the law of "similitude" which states that the impedance value at a period T for a geologic section whose parameters are ρ and h will be the same at a period $T.m$ for another geologic section whose parameters are $\rho.n$ and $h.l$ provided the following condition is satisfied:

$$L^2 = m.n. \quad (29)$$

Since the master curves are plotted as ρ_a/ρ_1 against T on log-versus-log paper and the field curve is plotted as ρ_a against T on similar paper, a vertical shift of the field curve over the master curve with which the match is obtained will give the value of n if ρ_1 is considered to be unity for the master curve, and the horizontal shift will give the value of m . Hence, L can easily be calculated using (29). Phase values are generally used to check the above interpretation. A match between the field-phase curve and the master-phase curve, corresponding to the master apparent resistivity curve which gave a best fit to the field curve, is then tried. If a match between the two, after a horizontal shift equal to m is obtained, the resistivity distribution first obtained is justified.

The method of interpretation described above remains basically the same when the dimensions of the source are taken into consideration. The only difference is that the apparent resistivity and phase-field curves are matched with a set of master curves which are drawn for various values of ν . If a match between the apparent resistivity field curve and one of the master curves is obtained, the value of ν for the field curve, ν^* , (symbols with an asterisk signify the field values) can be calculated, using the value of ν for the master curve with which the match is obtained and the relation $\nu^* = \nu/L$. The phase curve can then be used, in the same manner as described above in order to check the interpretation. Knowing ρ_1^* and h_1^* the parameters of the other layers can easily be determined as the models are computed for various values of the ratios ρ_2/ρ_1 , h_2/h_1 , ρ_3/ρ_1 , h_3/h_1 and so on. For the sake of simplicity the values of ρ_1 and h_1 have been taken as 1 ohm-metre and 1 km respectively in the computation of all master curves. Thus, when a match between the experimental and one of the master curves is obtained, one simply reads the value of ρ_a on the field curve corresponding to the line $\rho_a/\rho_1 = 1$ of the master curve and the value of T on the field curve corresponding to the line $T = 1$ of the master curve. This will give us the value of ρ_1^* while h_1^* can be calculated using (29).

One other quantity which can be used to check the above interpretation is the H_z/H_x ratio. Considering P and dP/dx to be independent of T , the H_z/H_x ratio for a three-layer resistivity model can be written in the form

$$\frac{H_z}{H_x} = \left(\frac{P}{dP/dx} \right) \frac{\nu^2}{\theta_1} \coth \left[\theta_1 h_1 + \coth^{-1} \left\{ \frac{\theta_1}{\theta_2} \coth \left(\theta_2 h_2 + \coth^{-1} \frac{\theta_2}{\theta_3} \right) \right\} \right] \quad (30)$$

(Srivastava 1965), where P is a function of x , y , and ν which satisfies the equation

$$\frac{\partial^2 P}{\partial x^2} + \frac{\partial^2 P}{\partial y^2} + \nu^2 P = 0 \quad (31)$$

Equations 1 and 30 are similar. Substituting (30) into (1) we get

$$Z(0) = \frac{i\omega}{\nu^2} \cdot \frac{1}{P} \cdot \frac{dP}{dx} \cdot \frac{H_z}{H_x} \quad (32)$$

Taking the amplitude and phase of (32) we obtain,

$$\left| \frac{H_z}{H_x} \right|^2 = \frac{\nu^4}{8\pi^2} \cdot \left| \frac{P}{dP/dx} \right|^2 \cdot (T \cdot \rho_a) \quad (33)$$

$$\text{and } \psi = \phi - 90^\circ + \xi \quad (34)$$

Where ψ is the phase angle between H_z and H_x , ξ is the phase angle between P and dP/dx and ϕ is given by (5). Using (28) and (29) $|H_z/H_x|^2$ and ψ can easily be computed for various values of T from the master curves which gave best fits to the apparent resistivity and phase-angle curves. The values of $|H_z^*/H_x^*|^2$ and ψ^* are then calculated from the field data. The two sets of values of $|H_z/H_x|^2$ and ψ , one computed from the master curves and the other from the field data, are plotted separately on a log-vs-log and linear-vs-log scale respectively as a function of T . If satisfactory matches between $|H_z/H_x|^2$ curves and ψ curves are obtained, except for the vertical displacements of one curve over the other (due to $\frac{\nu^4}{8\pi^2} \cdot \left| \frac{P}{dP/dx} \right|^2$ and ξ terms in (33) and (34)), the resistivity distribution estimated from the apparent resistivity curves can be considered to be adequate.

Another way of looking at this problem is to plot $|H_z^*/H_x^*|^2 \cdot \rho_a^*$ (field data) on a linear scale as a function of T . Equation 33 shows that such a plot should give a straight line passing through the origin with a slope of $\frac{\nu^4}{8\pi^2} \cdot \left| \frac{P}{dP/dx} \right|^2$. The slope of this straight line should then be the same as the vertical displacement obtained during the matching of the $|H_z/H_x|^2$ curves.

In instances where the two $|H_z/H_x|^2$ curves, observed and calculated, differ from each other significantly an accurate resistivity distribution can not be obtained by the method given here. Such differences could arise if P and dP/dx depend on T or if structural inhomogeneities are present which invalidate the assumption of a horizontally layered model.

- a) dependence of P and dP/dx on T .
- b) presence of an inhomogeneity.

Acknowledgments

The author is grateful to K. Shimizu of the Computing Centre, Department of Mines and Technical Surveys, Ottawa, and the Computing Centres of the University of Alberta and the University of British Columbia for helping with the machine programming involved in this paper. Appreciation is expressed to the National Research Council and the Defence Research Board of Canada for financial support through a Post Doctoral Fellowship held at the Dominion Observatory, Ottawa, and to Dr. E.R. Niblett for reviewing the manuscript.

References

- Cagniard, L. 1953:
Basic theory of the magnetotelluric method of geophysical prospecting. *Geophysics*, 18, 605.
- Price, A. T. 1962:
The theory of magnetotelluric methods when the source field is considered. *J. Geophys. Res.*, 67, 1907.
- Srivastava, S. P. 1965:
Method of interpretation of magnetotelluric data when source field is considered. *J. Geophys. Res.*, 67, 945.
- Wait, J. R. 1954:
On the relation between telluric currents and the earth's magnetic field. *Geophysics*, 19, 281.
- 1962:
Theory of magnetotelluric fields. *J. Res.*, 66D, 509.

List of Figures

- Fig. 1,3,5,7,9,11,13 - Plot of apparent resistivity divided by the resistivity of the top layer versus period for two-layer resistivity models.
- Fig. 2,4,6,8,10,12,14 - Plot of phase value between electric and magnetic variations versus period for two-layer resistivity models.
- Fig. 15,17,19,21,23, - Plot of apparent resistivity divided by the resistivity of the top layer versus period for three-layer resistivity models.
25,27,29,31,33,
35,37,39,41,43,
45,47,49,51,53,
55,57,59.
- Fig. 16,18,20,22,24, - Plot of phase value between electric and magnetic variations versus period for three-layer resistivity models.
26,28,30,32,34,
36,38,40,42,44,
46,48,50,52,54,
56,58,60.

Description of the Figures

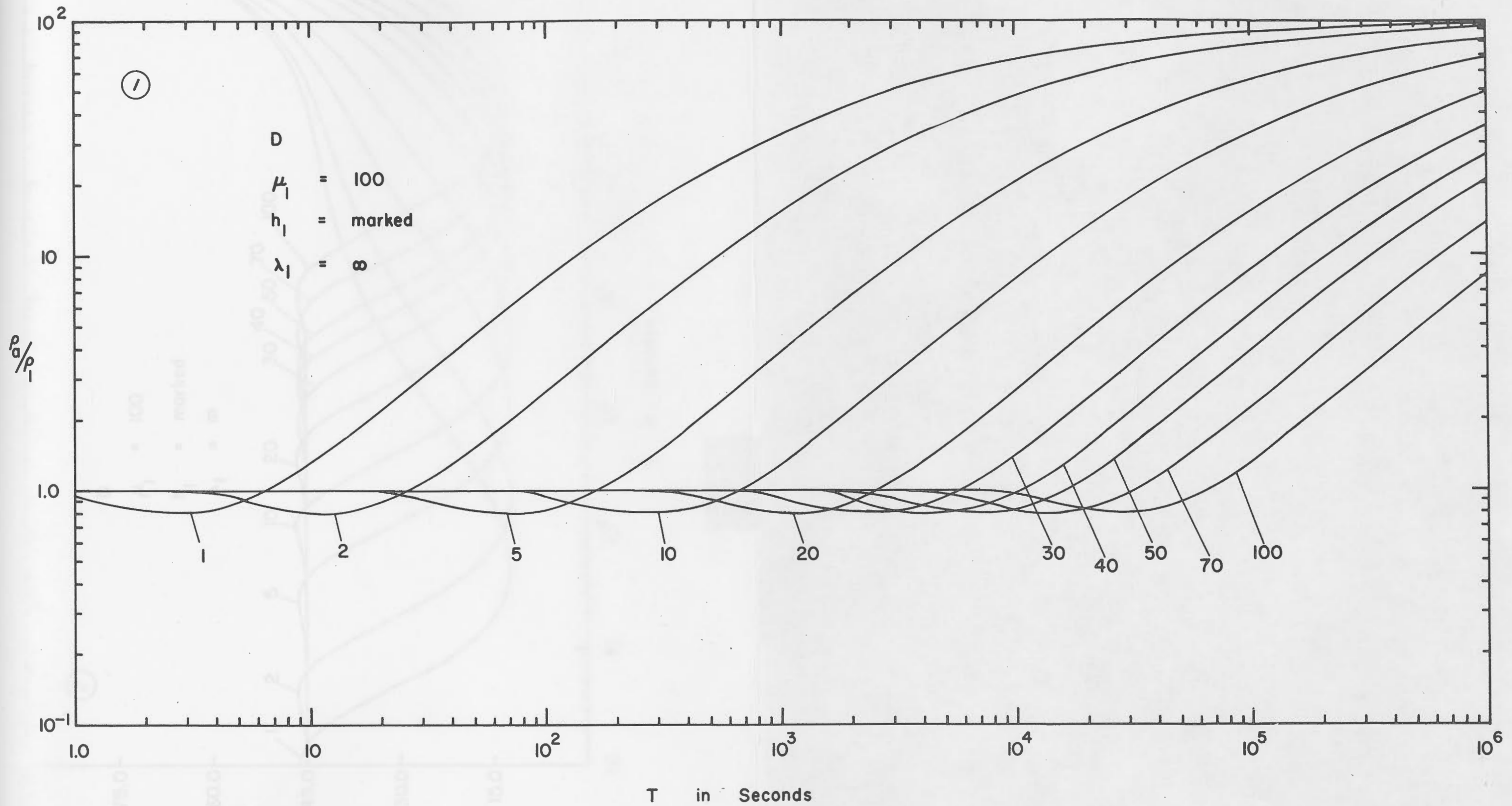
Plot

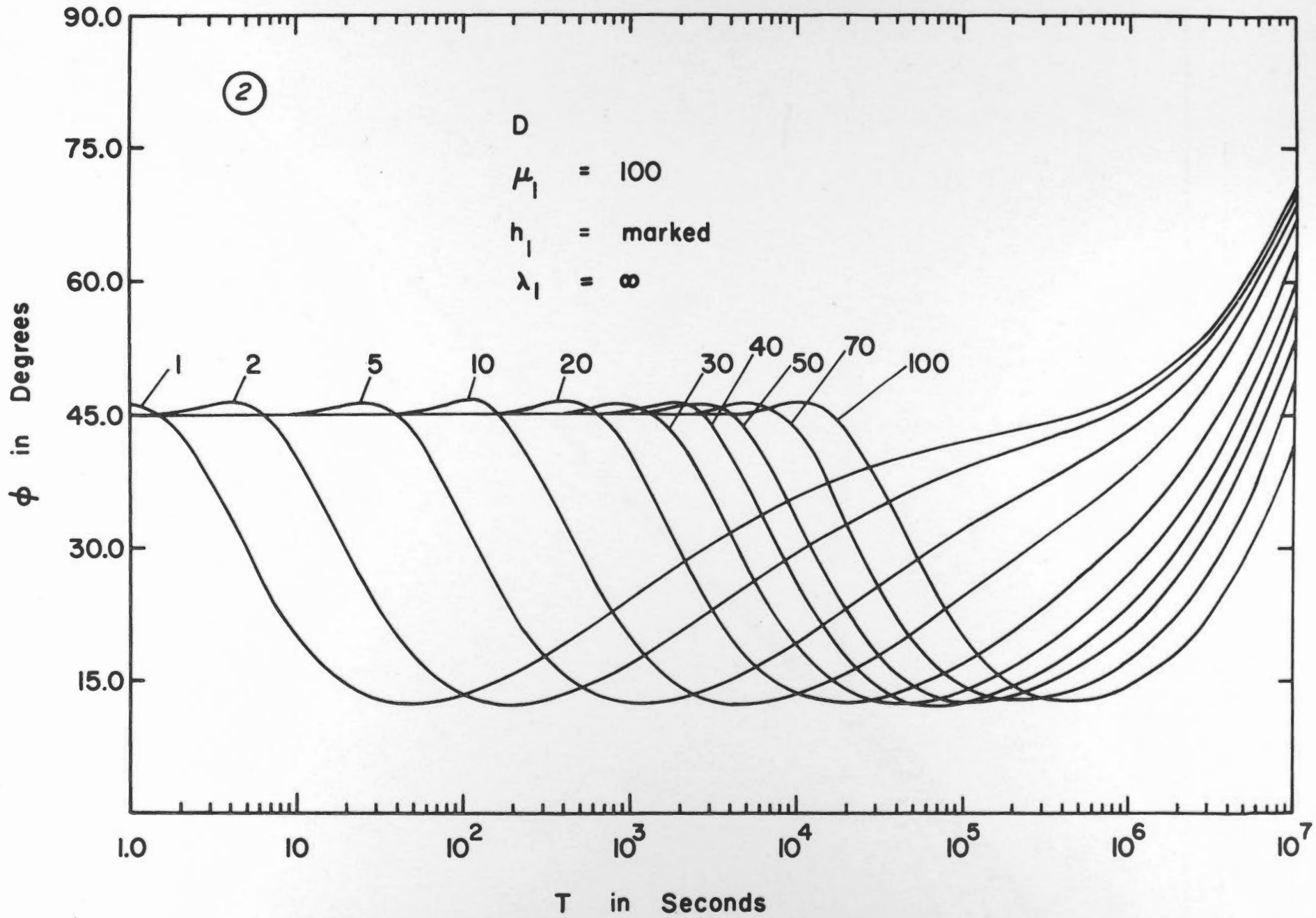
Fig.	Plot	vs	T
1	ρ_a		
2	θ		
3	ρ_a		
4	θ		
5	ρ_a		
6	θ		
7	ρ_a		
8	θ		
9	ρ_a		
10	θ		
11	ρ_a		
12	θ		
13	ρ_a		
14	θ		
15	ρ_a		
16	θ		
17	ρ_a		
18	θ		
19	ρ_a		
20	θ		
21	ρ_a		
22	θ		
23	ρ_a		
24	θ		
25	ρ_a		
26	θ		
27	ρ_a		
28	θ		
29	ρ_a		
30	θ		
31	ρ_a		
32	θ		
33	ρ_a		
34	θ		
35	ρ_a		
36	θ		
37	ρ_a		
38	θ		
39	ρ_a		
40	θ		
41	ρ_a		
42	θ		
43	ρ_a		
44	θ		
45	ρ_a		

Parameters

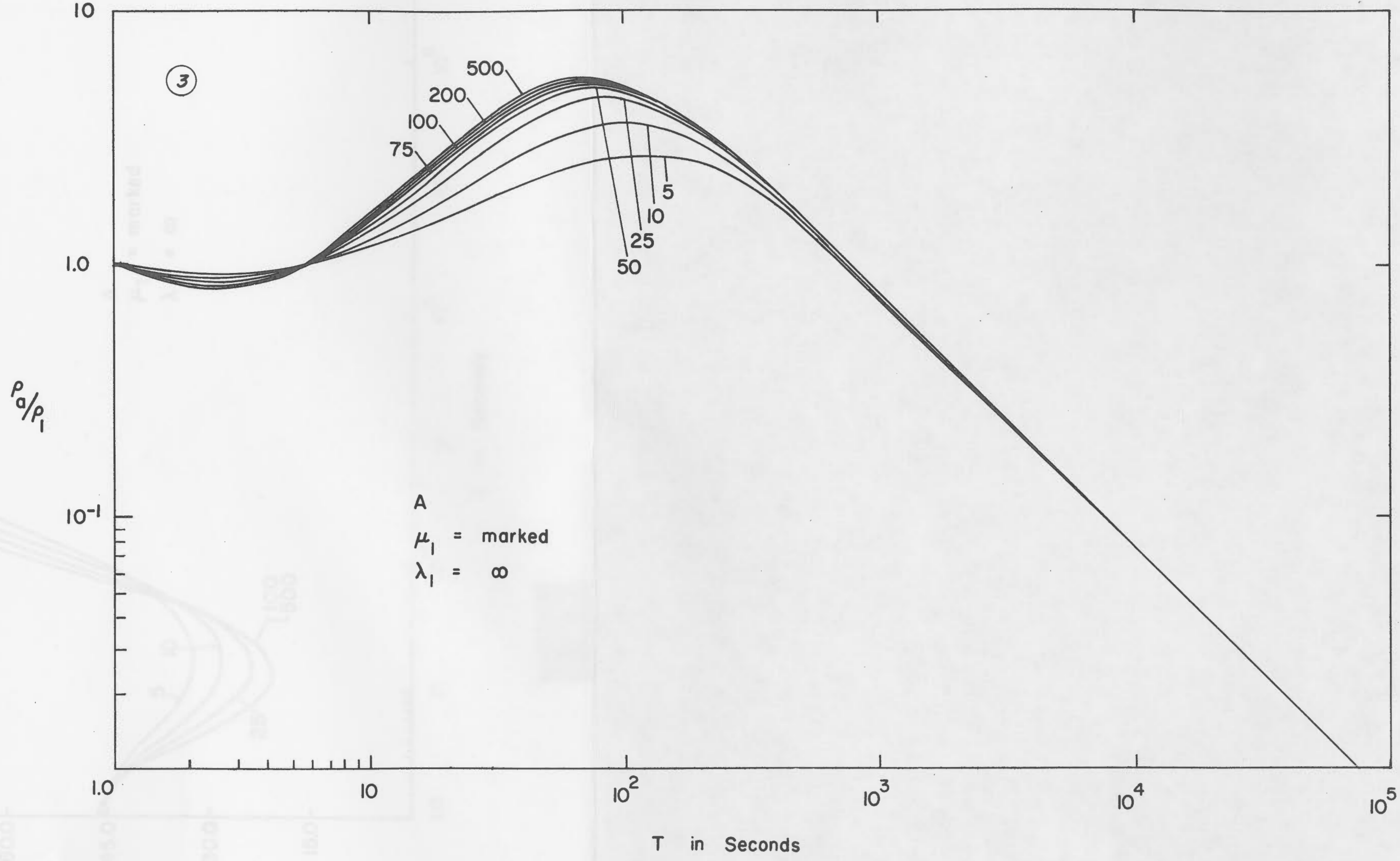
D, $\mu_1 = 100$, $h_1 =$ marked, $\lambda_1 = \infty$
D, $\mu_1 = 100$, $h_1 =$ " , $\lambda_1 = \infty$
A, $\mu_1 =$ marked, $\lambda_1 = \infty$
A, $\mu_1 =$ marked, $\lambda_1 = \infty$
B, $\mu_1 =$ marked, $\lambda_1 = \infty$
B, $\mu_1 =$ marked, $\lambda_1 = \infty$
C, $\mu_1 =$ marked, $\lambda_1 = \infty$
C, $\mu_1 =$ marked, $\lambda_1 = \infty$
D, $\mu_1 =$ marked, $\lambda_1 = \infty$
D, $\mu_1 =$ marked, $\lambda_1 = \infty$
E, $\mu_1 =$ marked, $\lambda_1 = \infty$
E, $\mu_1 =$ marked, $\lambda_1 = \infty$
A,B,C,D,E, $\mu_1 = .01, .2, \lambda_1 = \infty$
A,B,C,D,E, " " " " "
A, $\mu_1 = 100$, $\mu_2 = 1.0$, $\lambda_1 =$ marked $\lambda_2 = \infty$
" " " " " " " "
B, " " " " " " " "
B, " " " " " " " "
C, " " " " " " " "
C, " " " " " " " "
D,E, " " " " " " " "
D,E, " " " " " " " "
A, $\mu_1 = 100$, $\mu_2 = 10$, $\lambda_1 =$ marked, $\lambda_2 = \infty$
A, " " " " " " " "
B, $\mu_1 = 100$, $\mu_2 = 10$, $\lambda_1 =$ marked, $\lambda_2 = \infty$
B " " " " " " " "
C " " " " " " " "
C " " " " " " " "
D,E, " " " " " " " "
D,E, " " " " " " " "
A, $\mu_1 = 200$, $\mu_2 = 20$, $\lambda_1 =$ marked $\lambda_2 = \infty$
A, " " " " " " " "
B, " " " " " " " "
B, " " " " " " " "
C, " " " " " " " "
C, " " " " " " " "
D,E, " " " " " " " "
D,E, " " " " " " " "
A, $\mu_1 = 500$, $\mu_2 = 1$, $\lambda_1 =$ marked $\lambda_2 = \infty$
" " " " " " " "
B, " " " " " " " "
B, " " " " " " " "
C,D,E, " " " " " " " "
C,D,E, " " " " " " " "
A,B,C,D,E, $\mu_1 = 100$, $\mu_2 = .1$, $\lambda_1 = 5$, $10, 25, 50, 100$, $\lambda_2 = \infty$

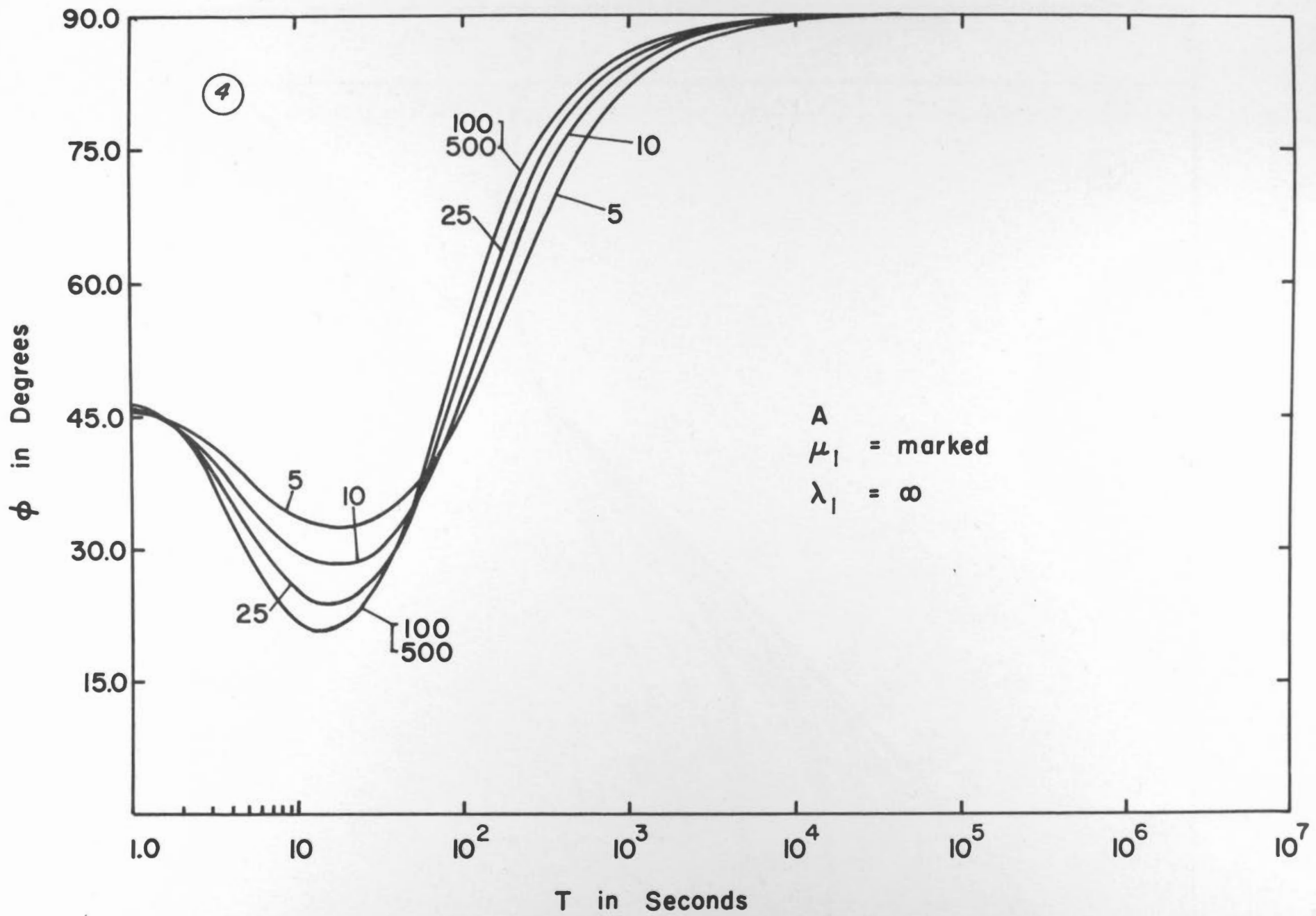
Plot			Parameters
" 46	θ	" "	" " " " " " " " " " " " " " " " " "
" 47	ρ_a	" "	A,B,C,D,E, $\mu_1 = 100$, $\mu_2 = .01$, $\lambda_1 = 5$, 10,25,50,100, $\lambda_2 = \infty$
" 48	θ	" "	" " " " " " " " " " " " " " " " " "
" 49	ρ_a	" "	A,B,C,D,E, $\mu_1 = 100$, $\mu_2 = 1000$, $\lambda_1 = 5, 10, 25, 50, 100$, $\lambda_2 = \infty$
" 50	θ	" "	" " " " " " " " " " " " " " " " " "
" 51	ρ_a	" "	A,B,C,D,E, $\mu_1 = .01$, $\mu_2 = 10^{-3}, 10^{-1}$, 1,10,10 ² ,10 ³ , $\lambda_1 = 5$, $\lambda_2 = \infty$
" 52	θ	" "	" " " " " " " " " " " " " " " " " "
" 53	ρ_a	" "	A,B,C,D,E, $\mu_1 = .01$, $\mu_2 = 10^{-3}, 10^{-1}$, 1,10,10 ² ,10 ³ , $\lambda_1 = 10$, $\lambda_2 = \infty$
" 54	θ	" "	" " " " " " " " " " " " " " " " " "
" 55	ρ_a	" "	A,B,C,D,E, $\mu_1 = .01$, $\mu_2 = 10^{-3}, 10^{-1}$, 1,10,10 ² ,10 ³ , $\lambda_1 = 25$, $\lambda_2 = \infty$
" 56	θ	" "	" " " " " " " " " " " " " " " " " "
" 57	ρ_a	" "	A,B,C,D,E, $\mu_1 = .01$, $\mu_2 = 10^{-3}, 10^{-1}$, 1,10,10 ² ,10 ³ , $\lambda_1 = 50$, $\lambda_2 = \infty$
" 58	θ	" "	" " " " " " " " " " " " " " " " " "
" 59	ρ_a	" "	A,B,C,D,E, $\mu_1 = .01$, $\mu_2 = 10^{-3}, 10^{-1}$, 1,10,10 ² ,10 ³ , $\lambda_1 = 100$, $\lambda_2 = \infty$
" 60	θ	" "	" " " " " " " " " " " " " " " " " "

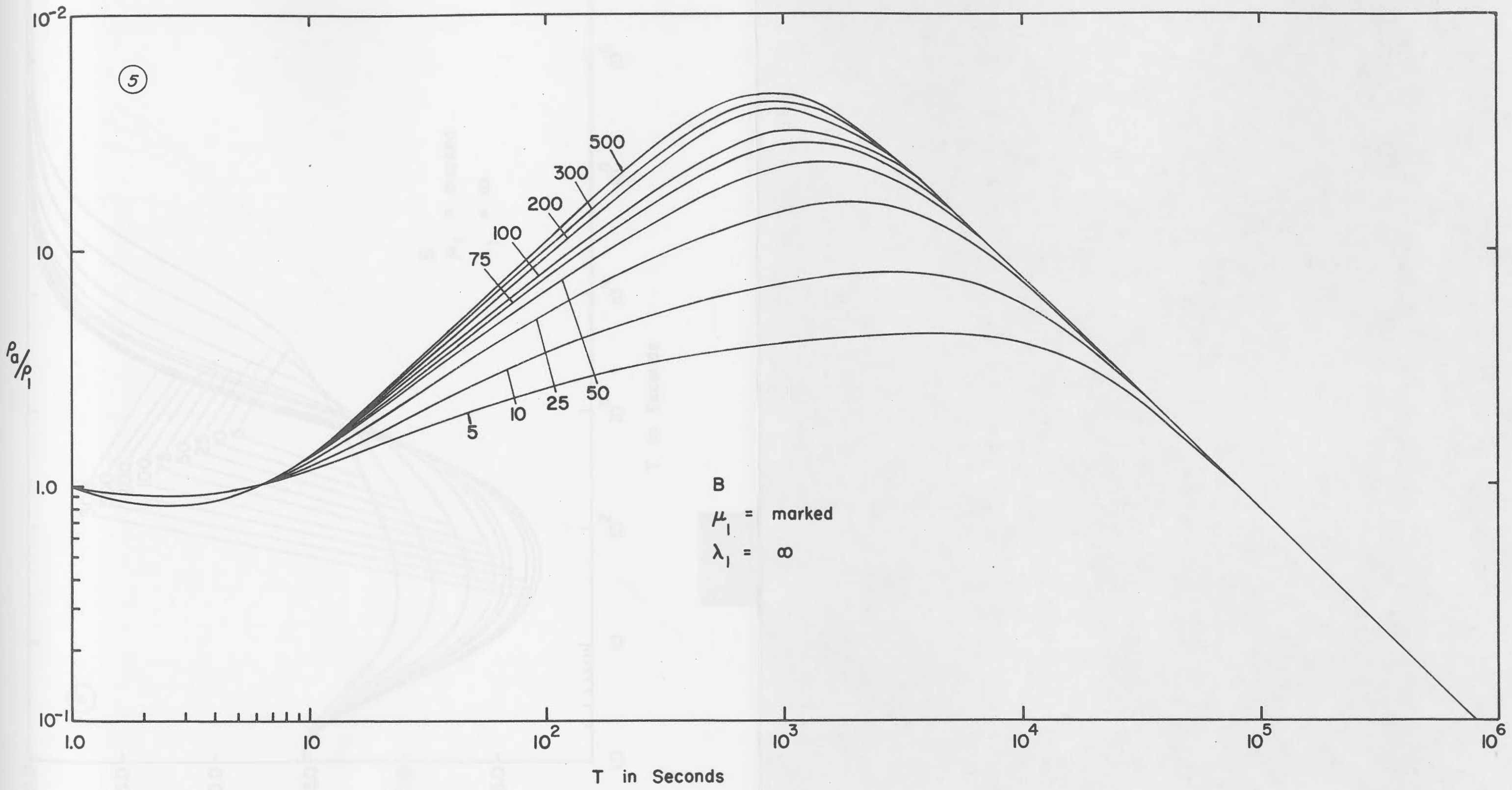


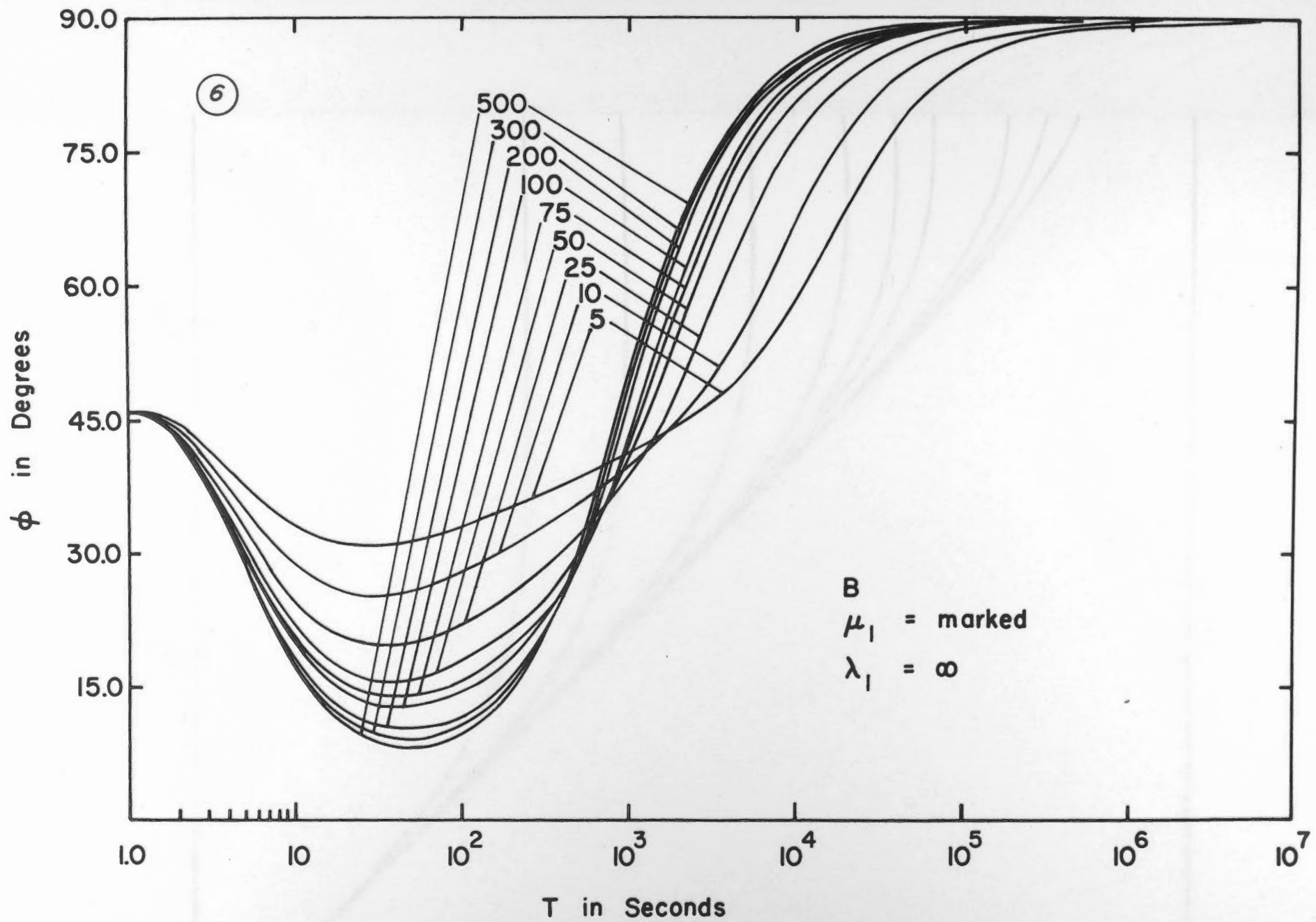


3



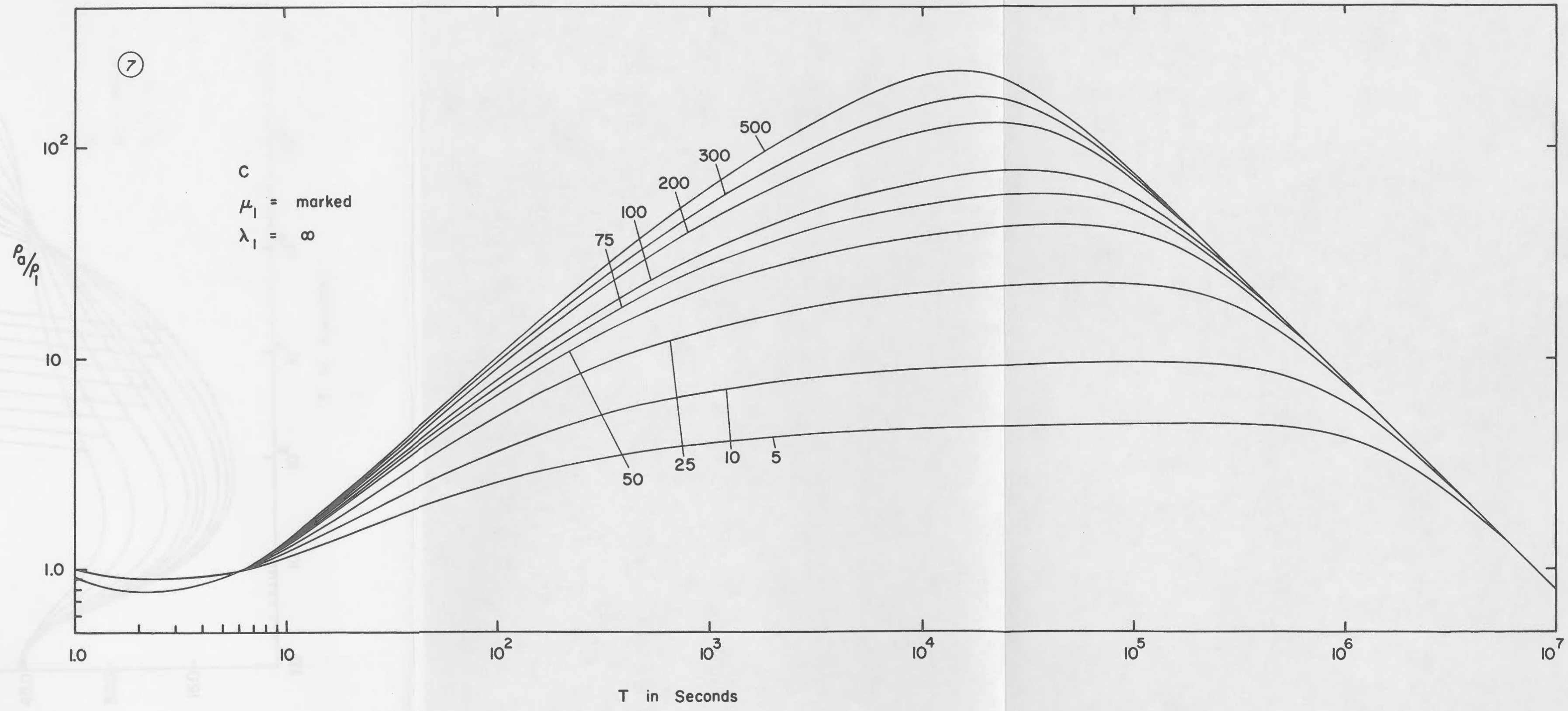


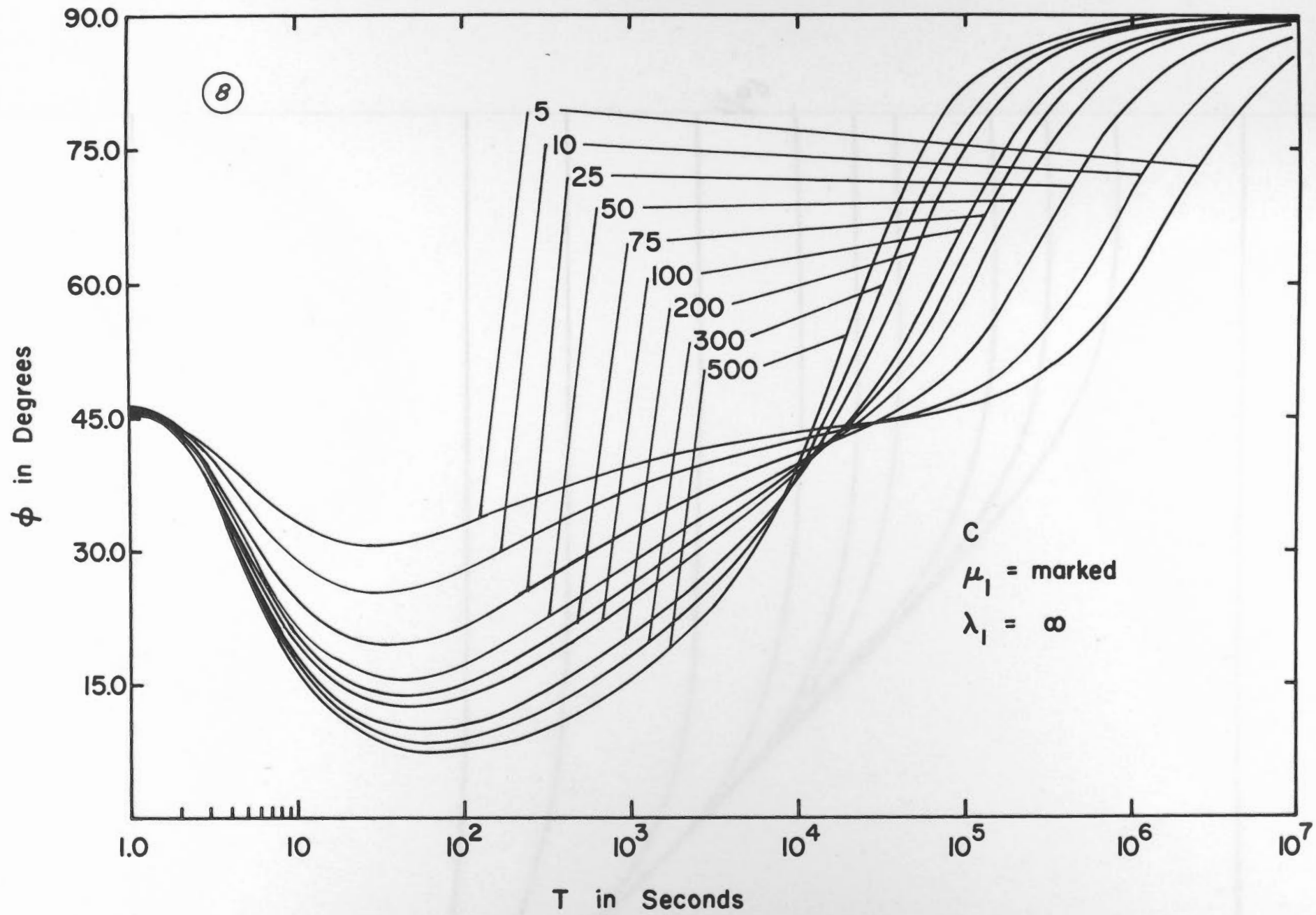


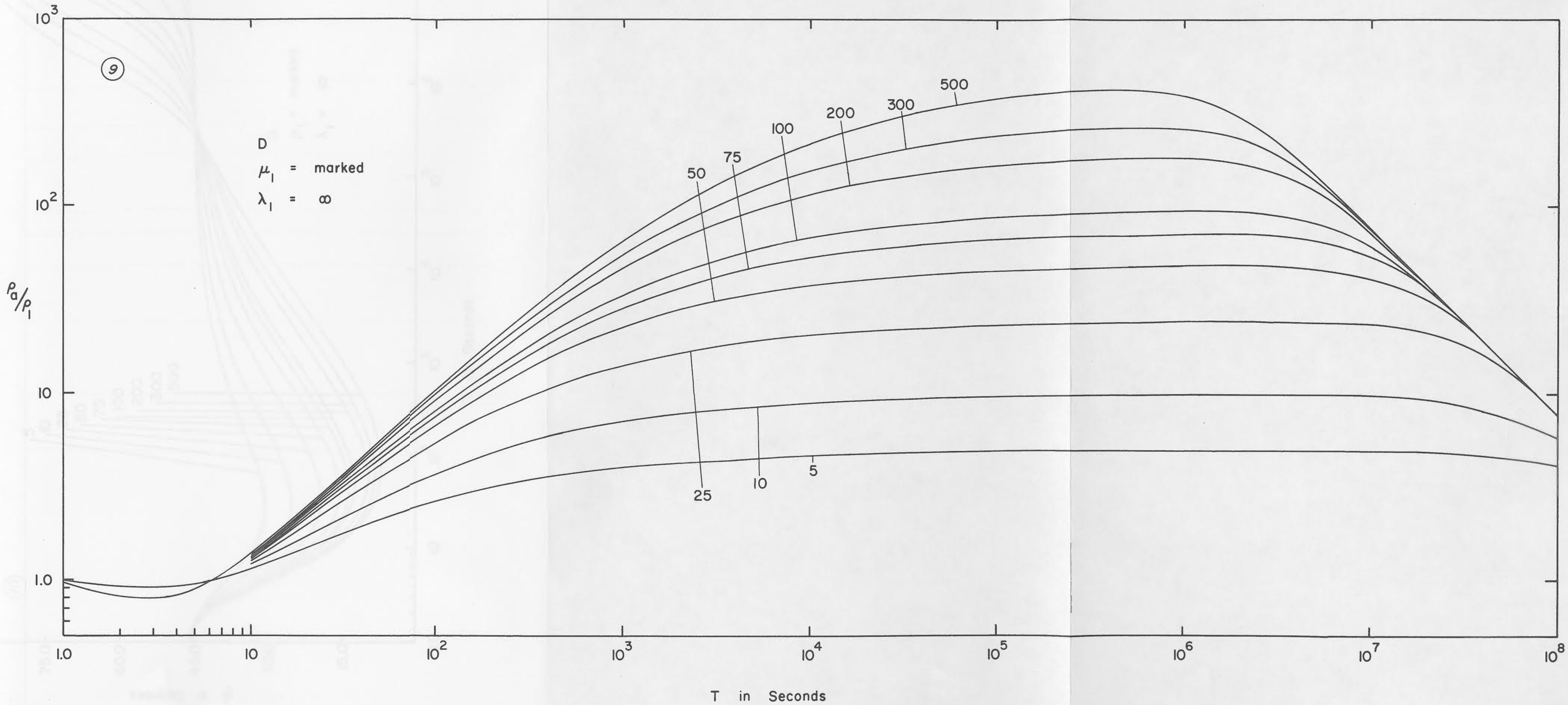


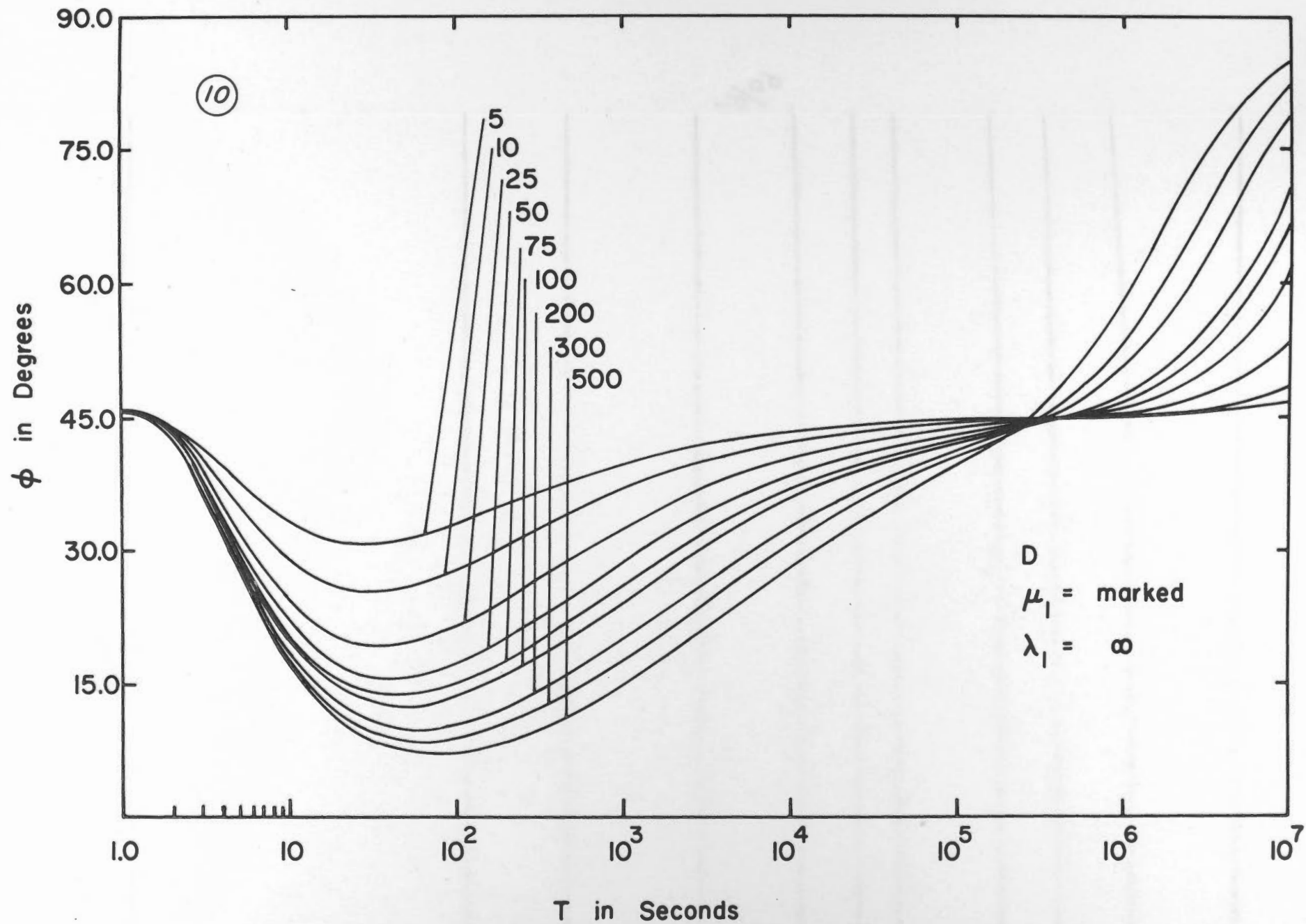
7

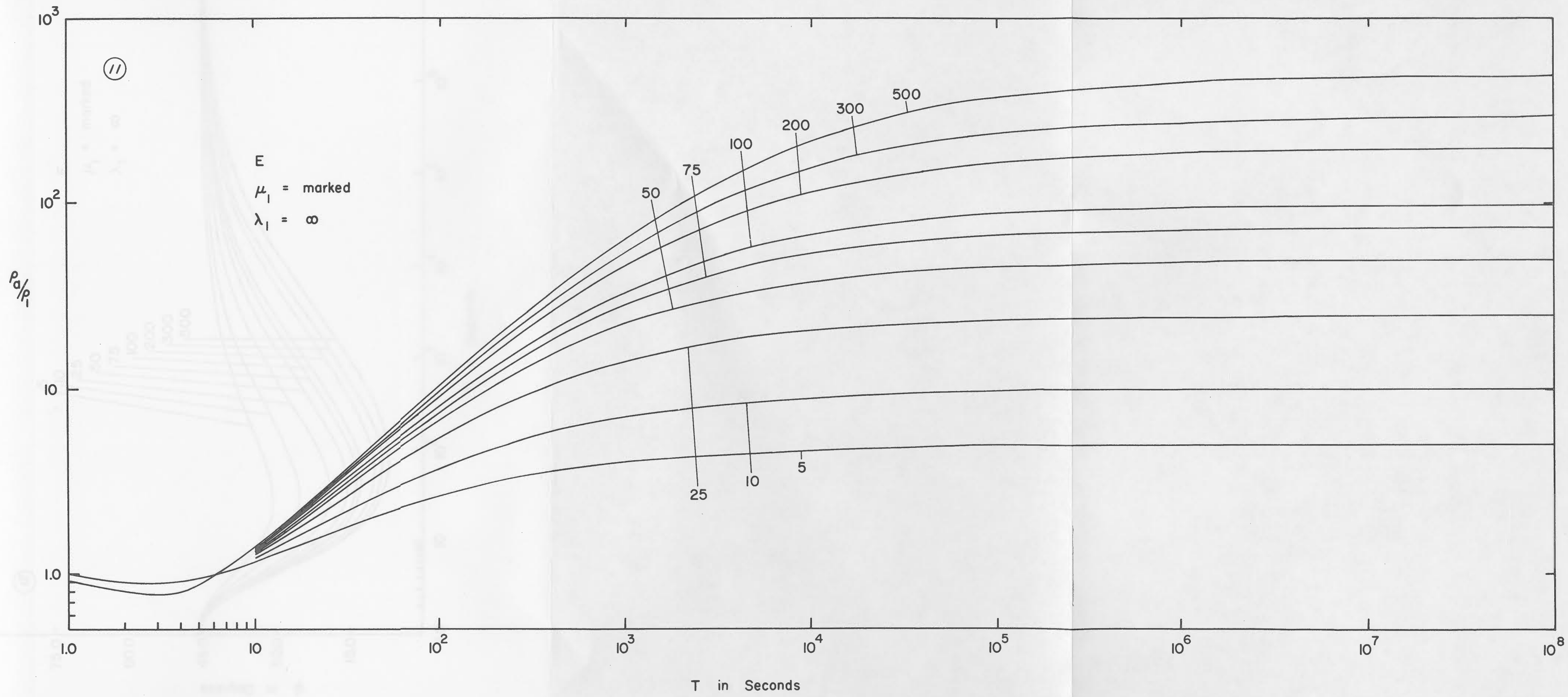
C
 $\mu_1 = \text{marked}$
 $\lambda_1 = \infty$

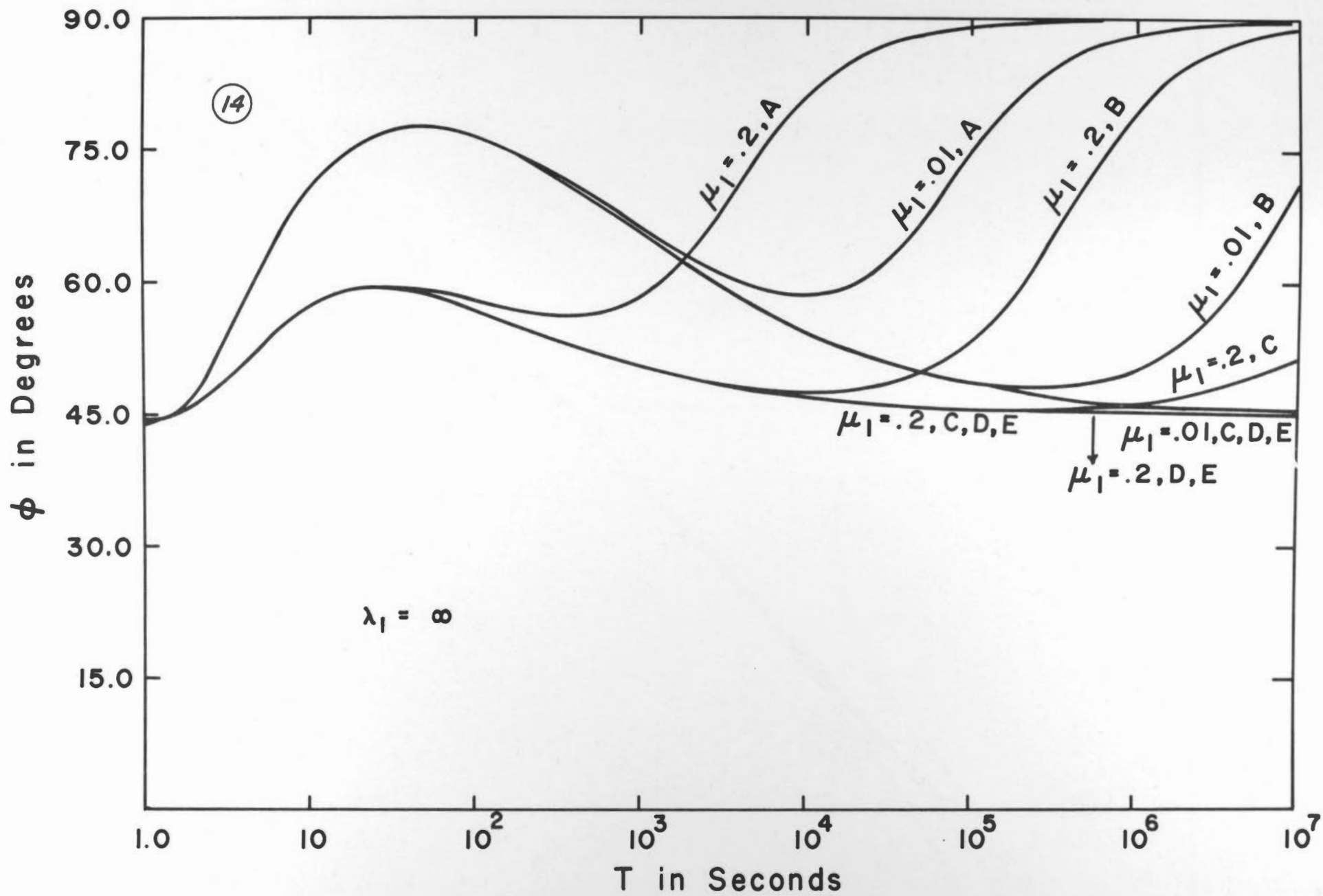


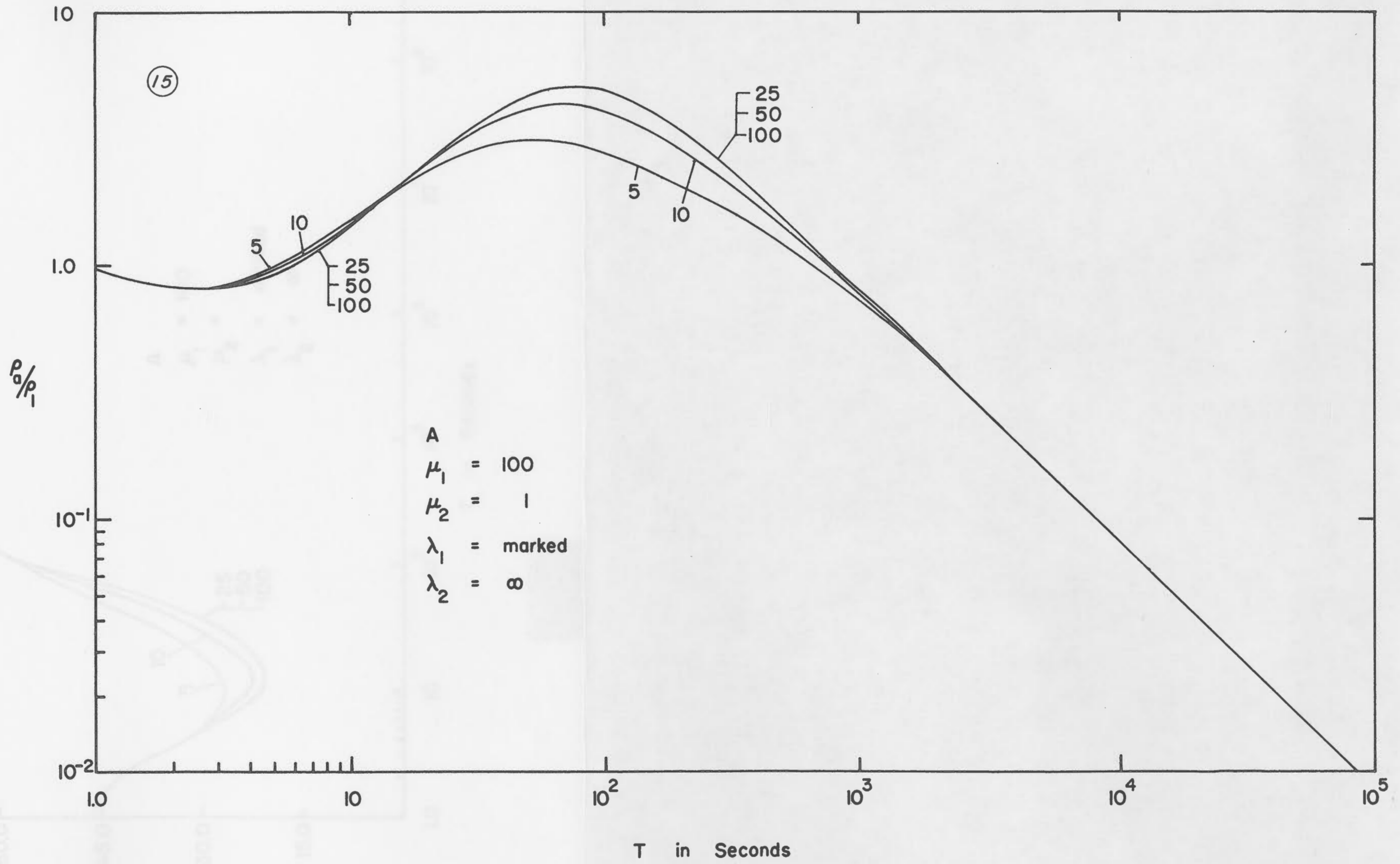


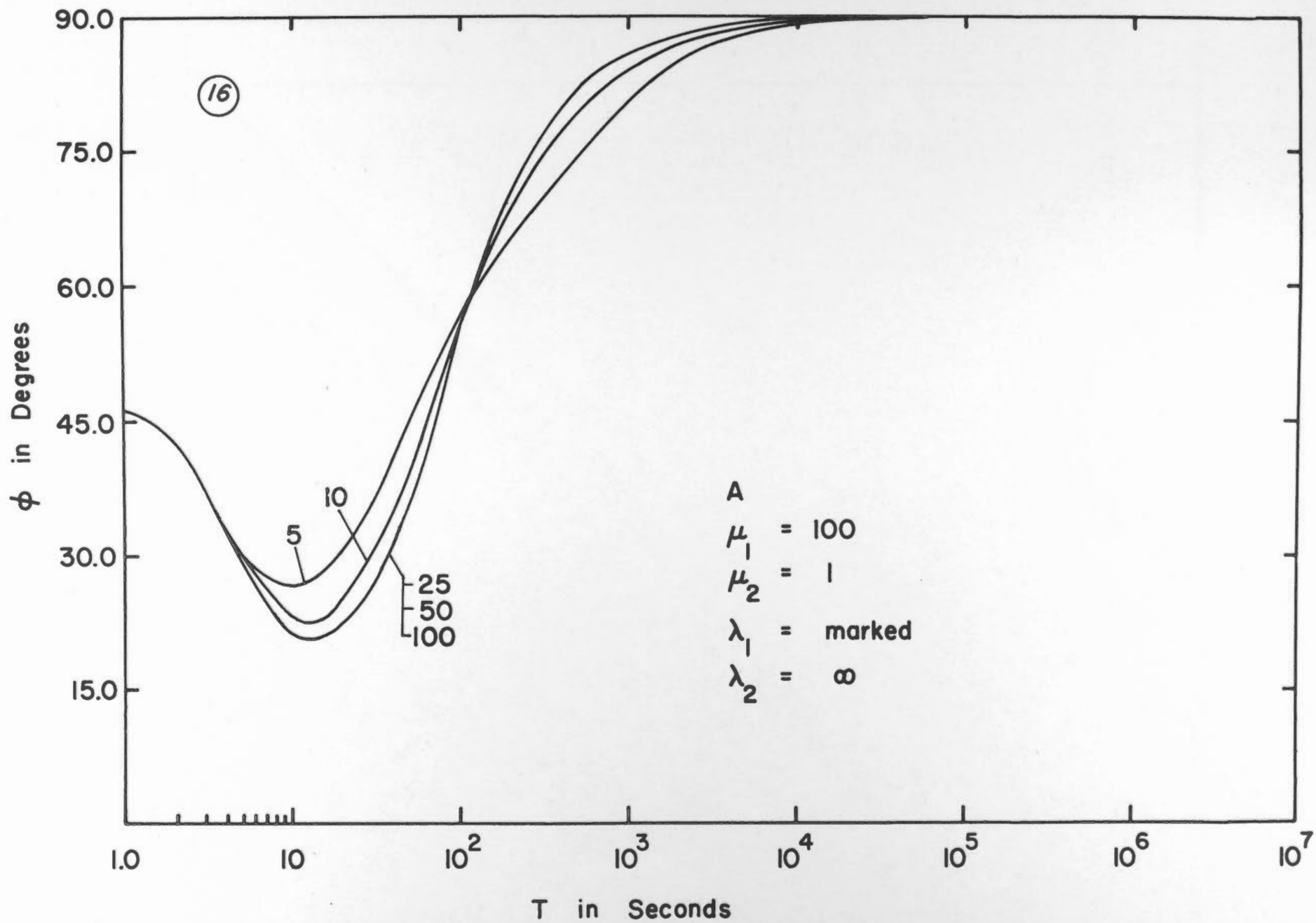




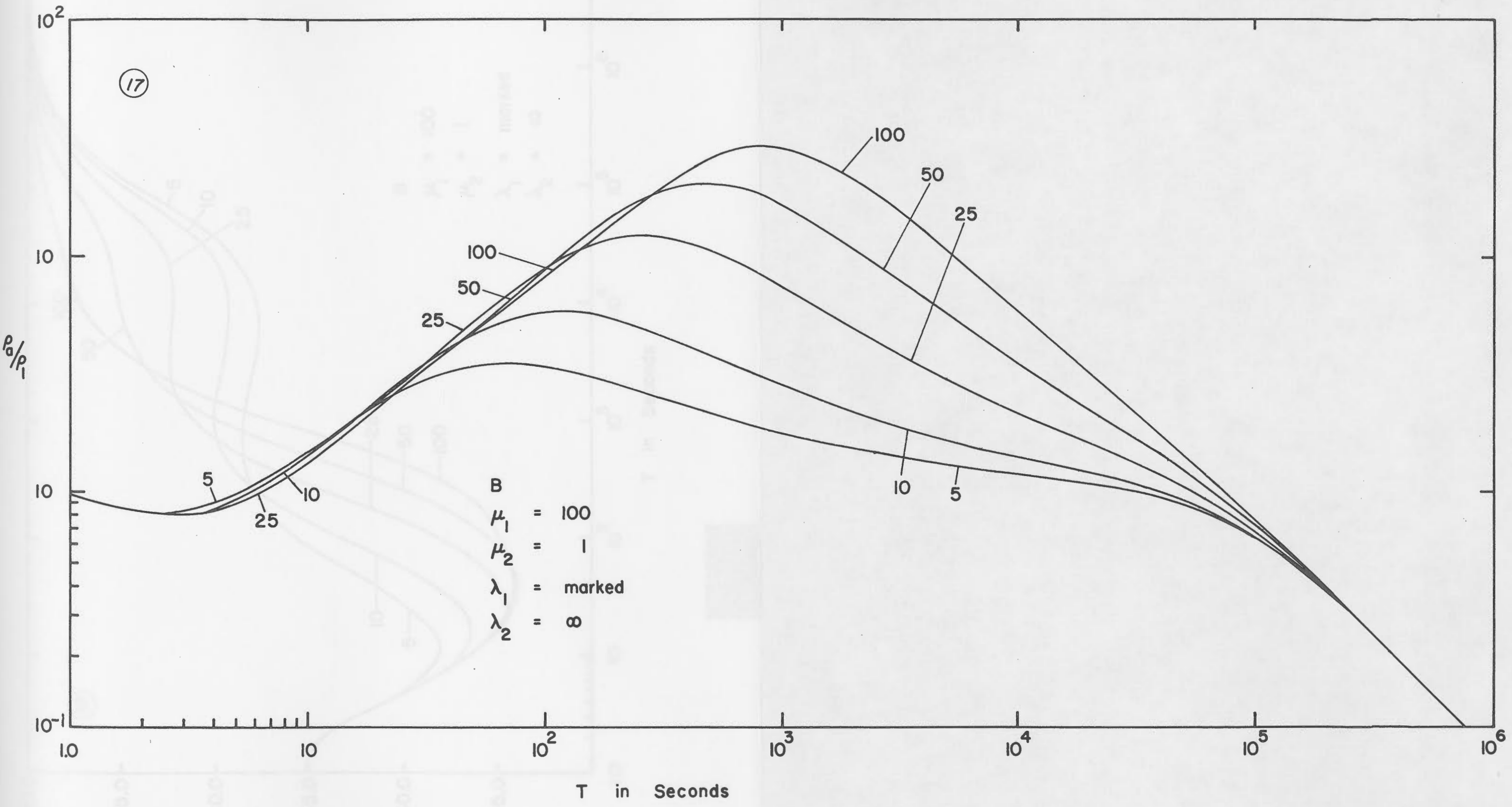


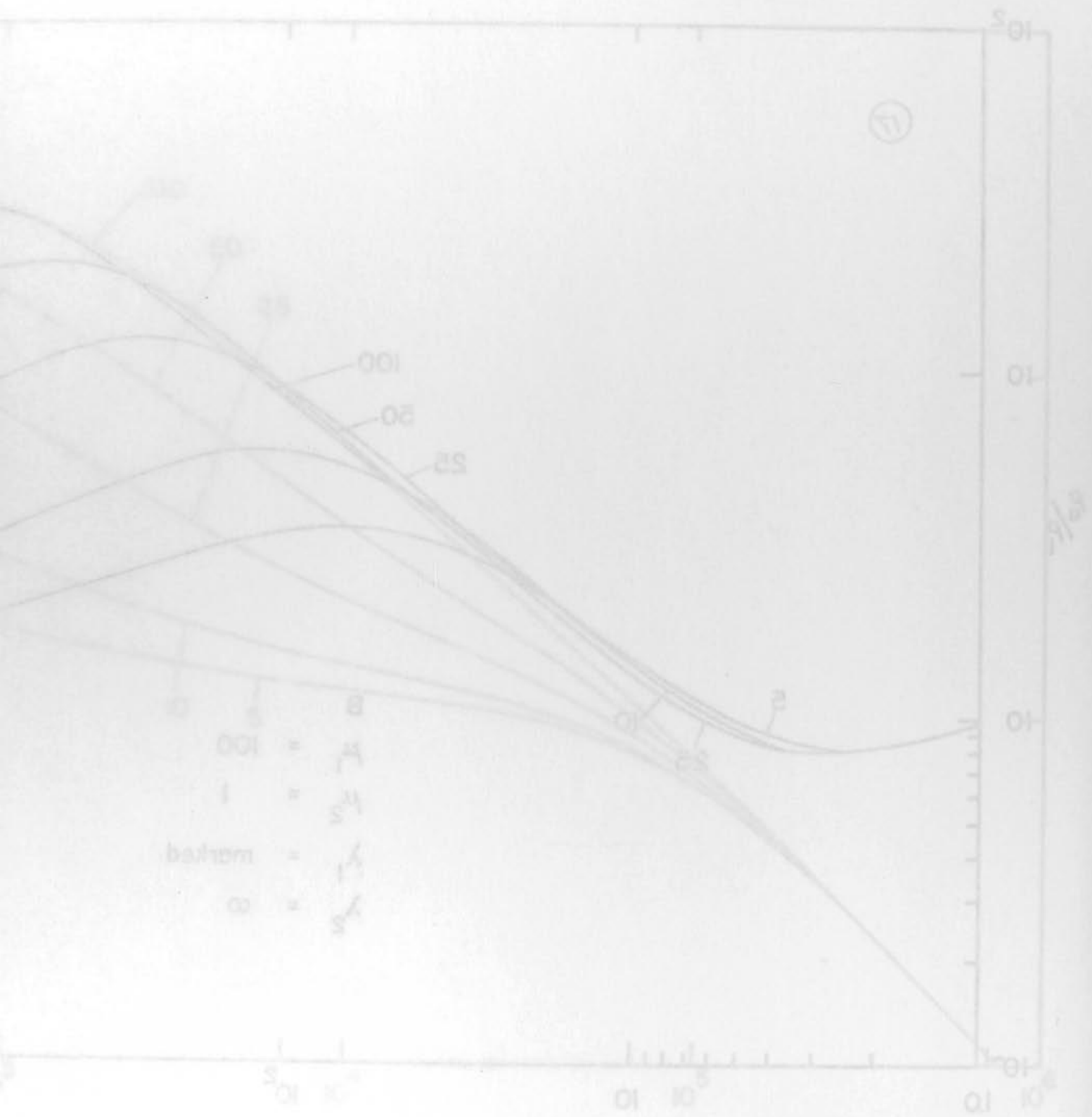


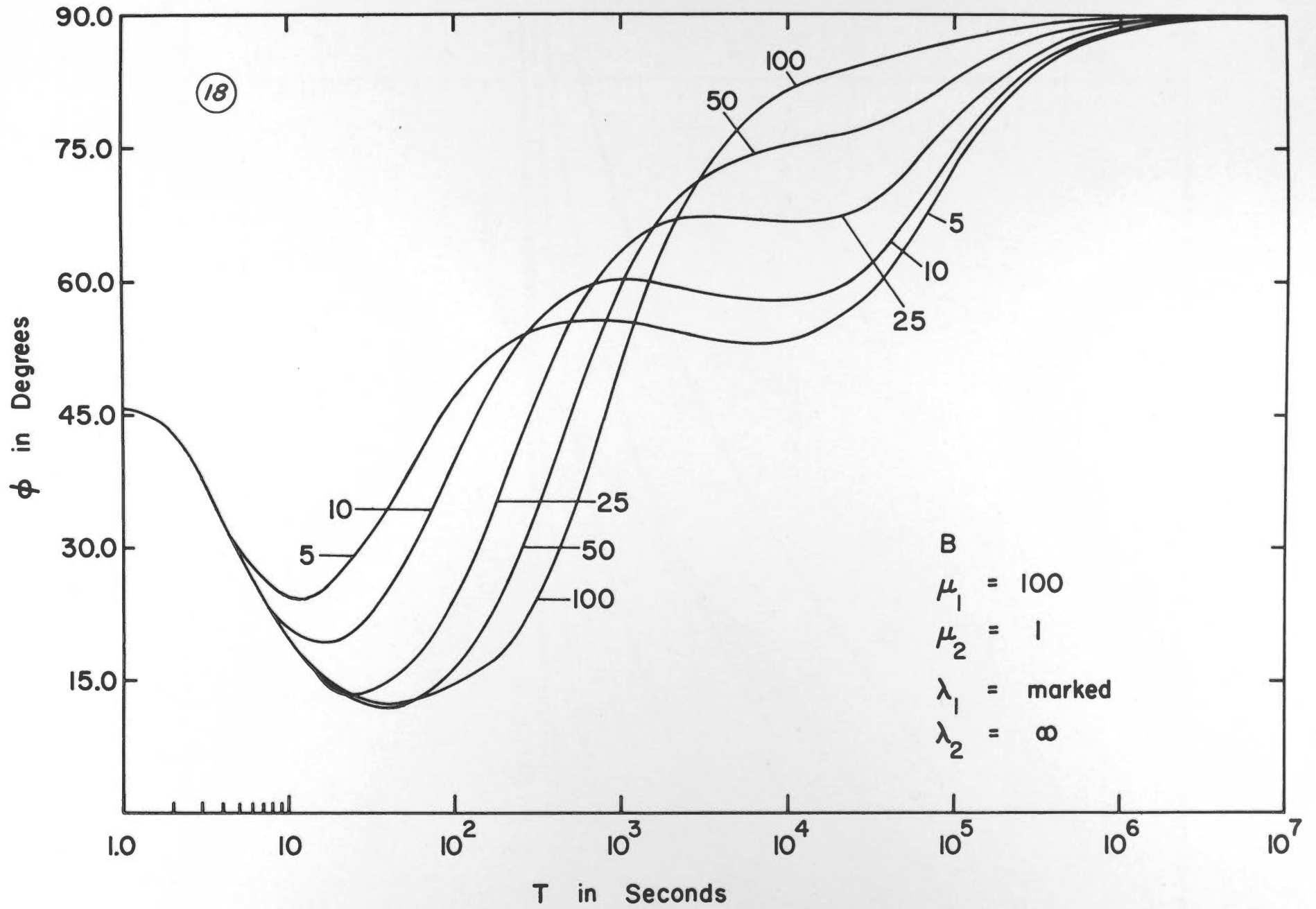




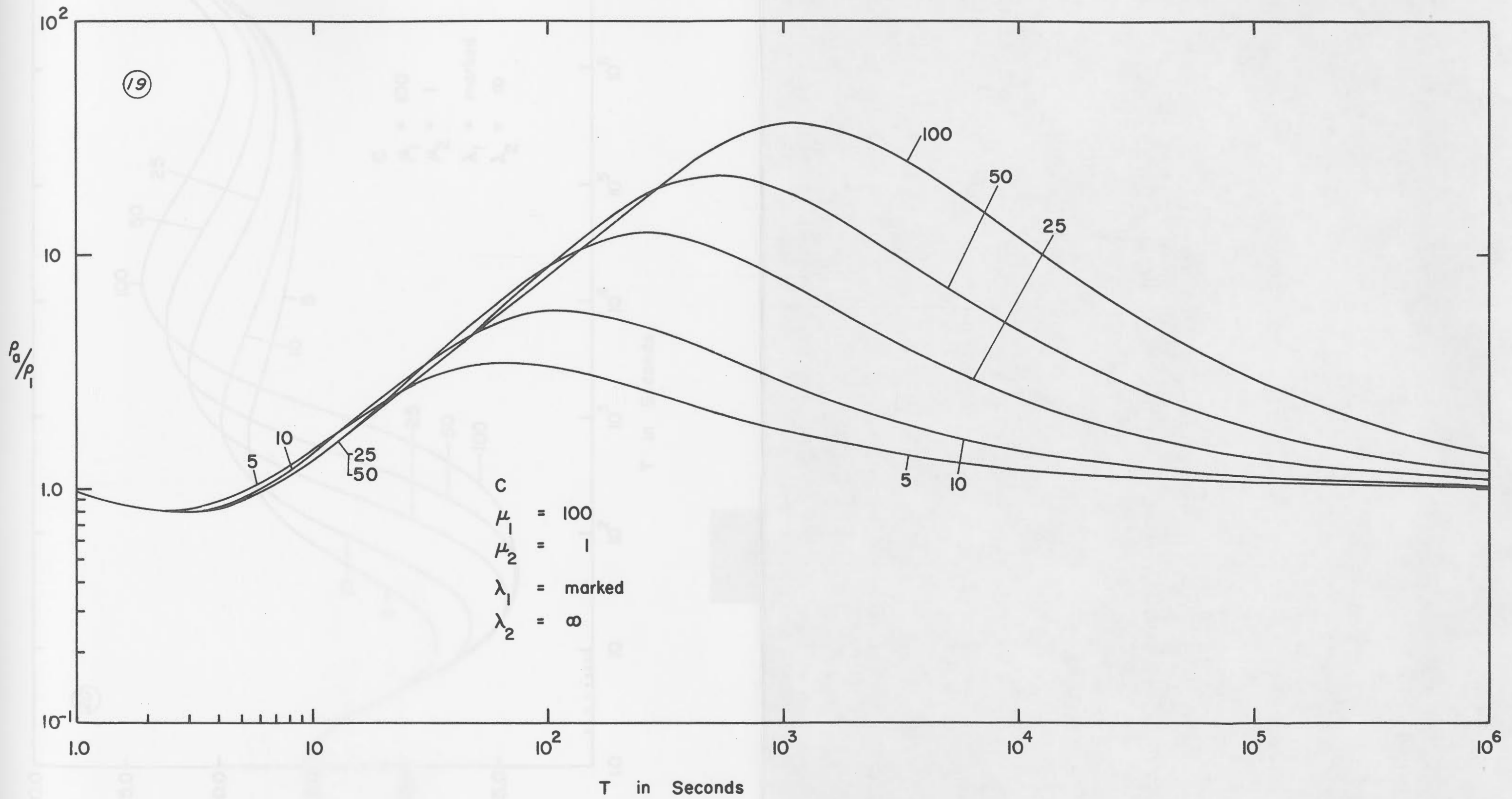
17

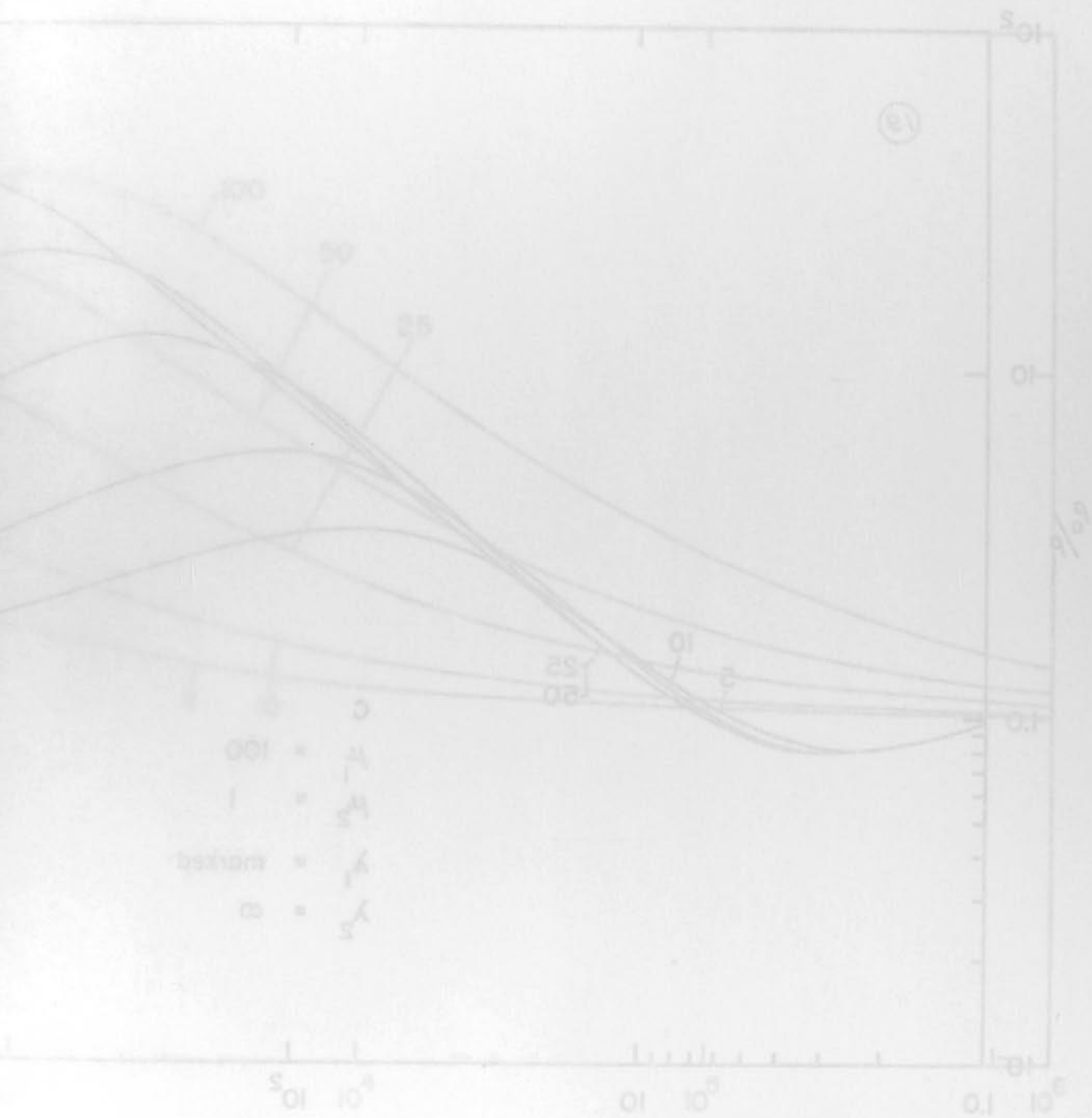


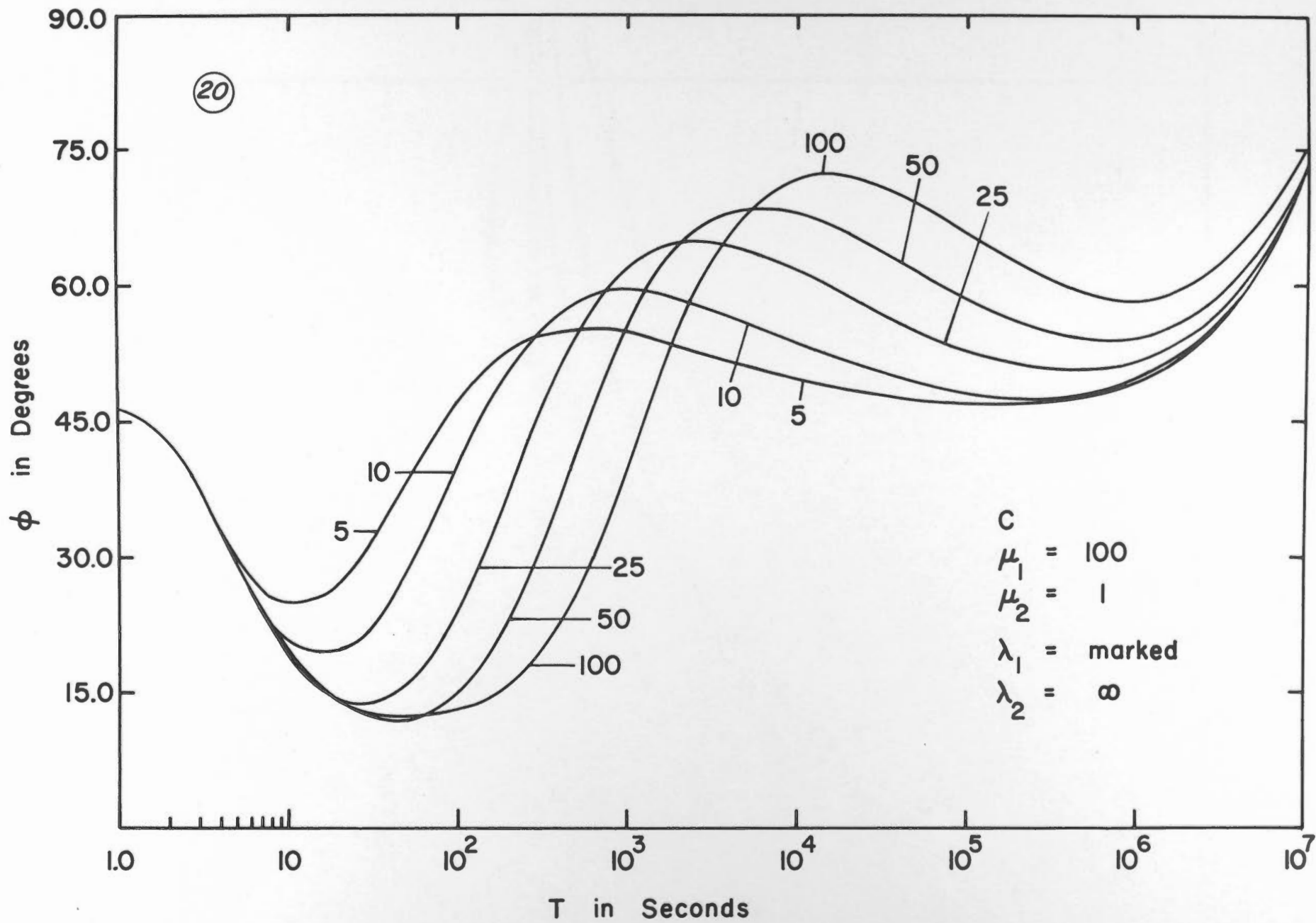




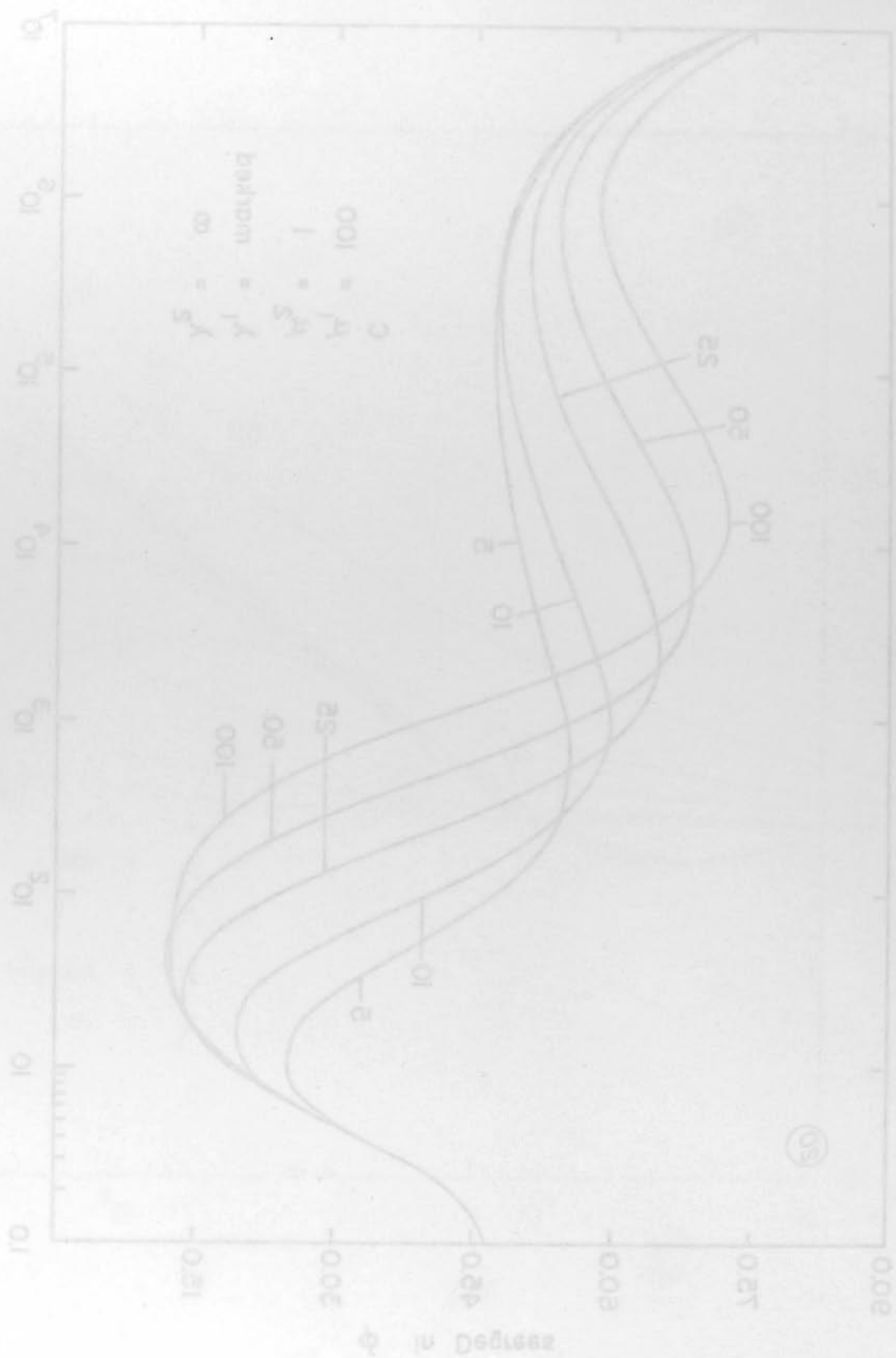


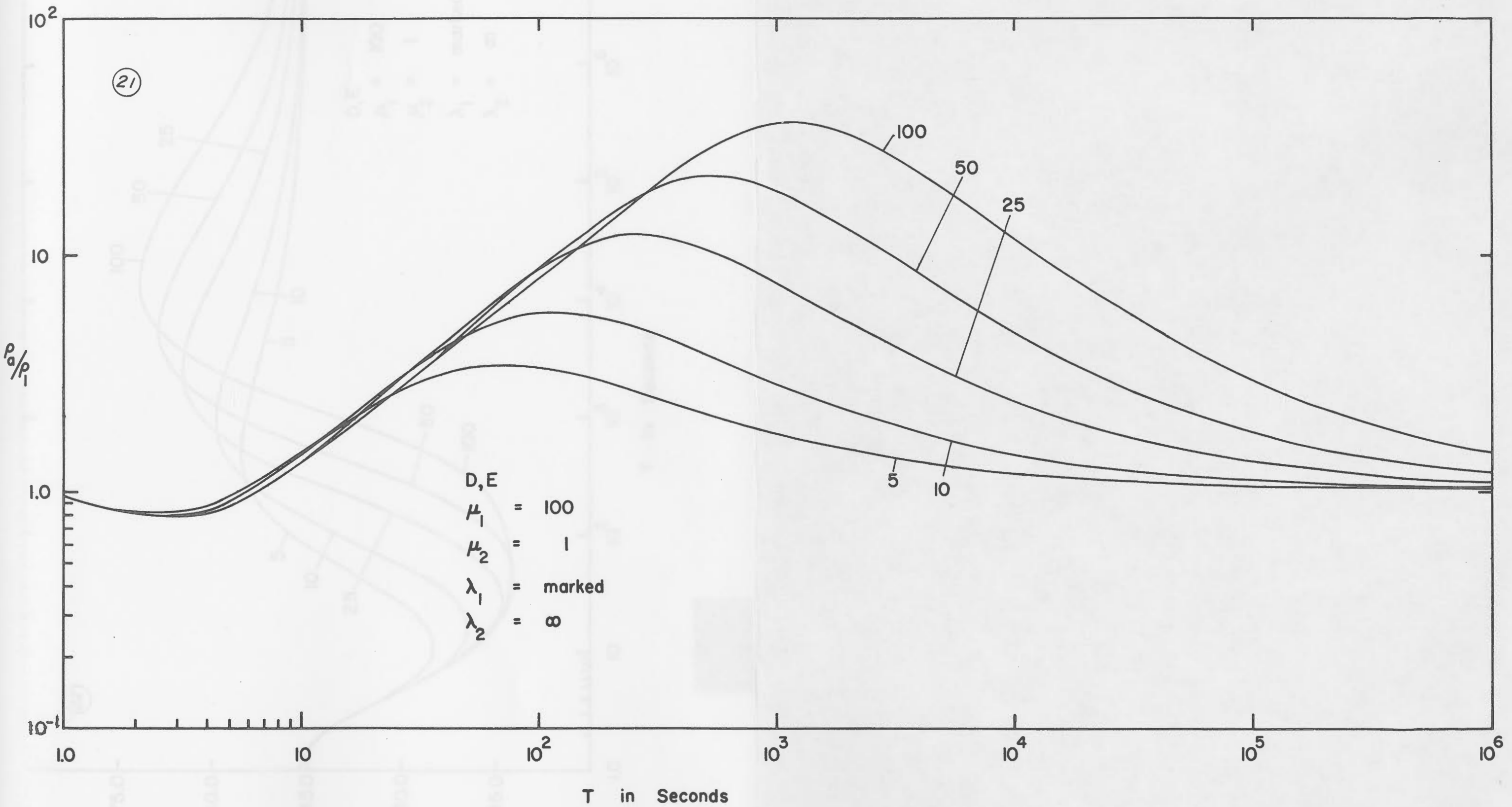


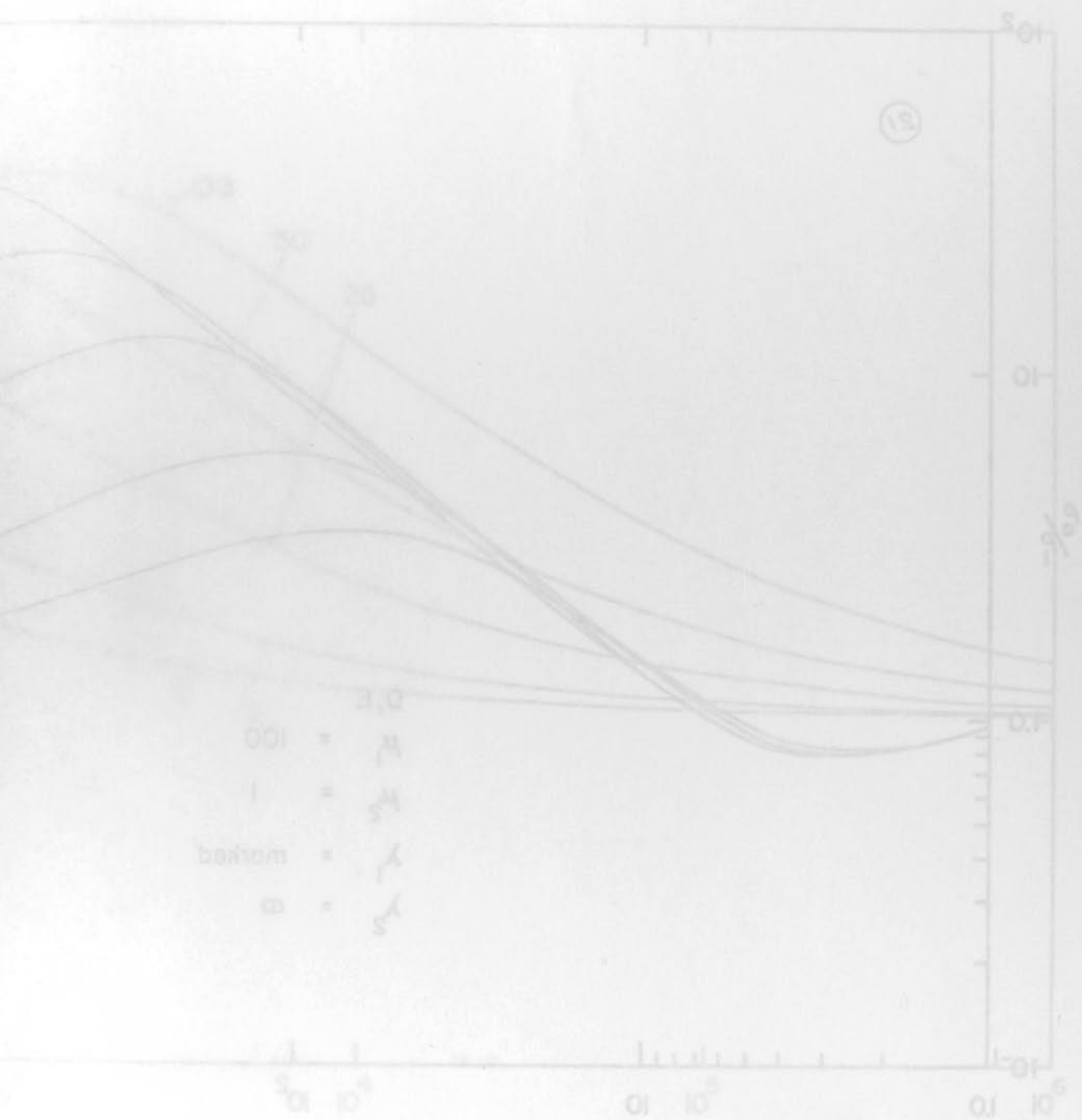




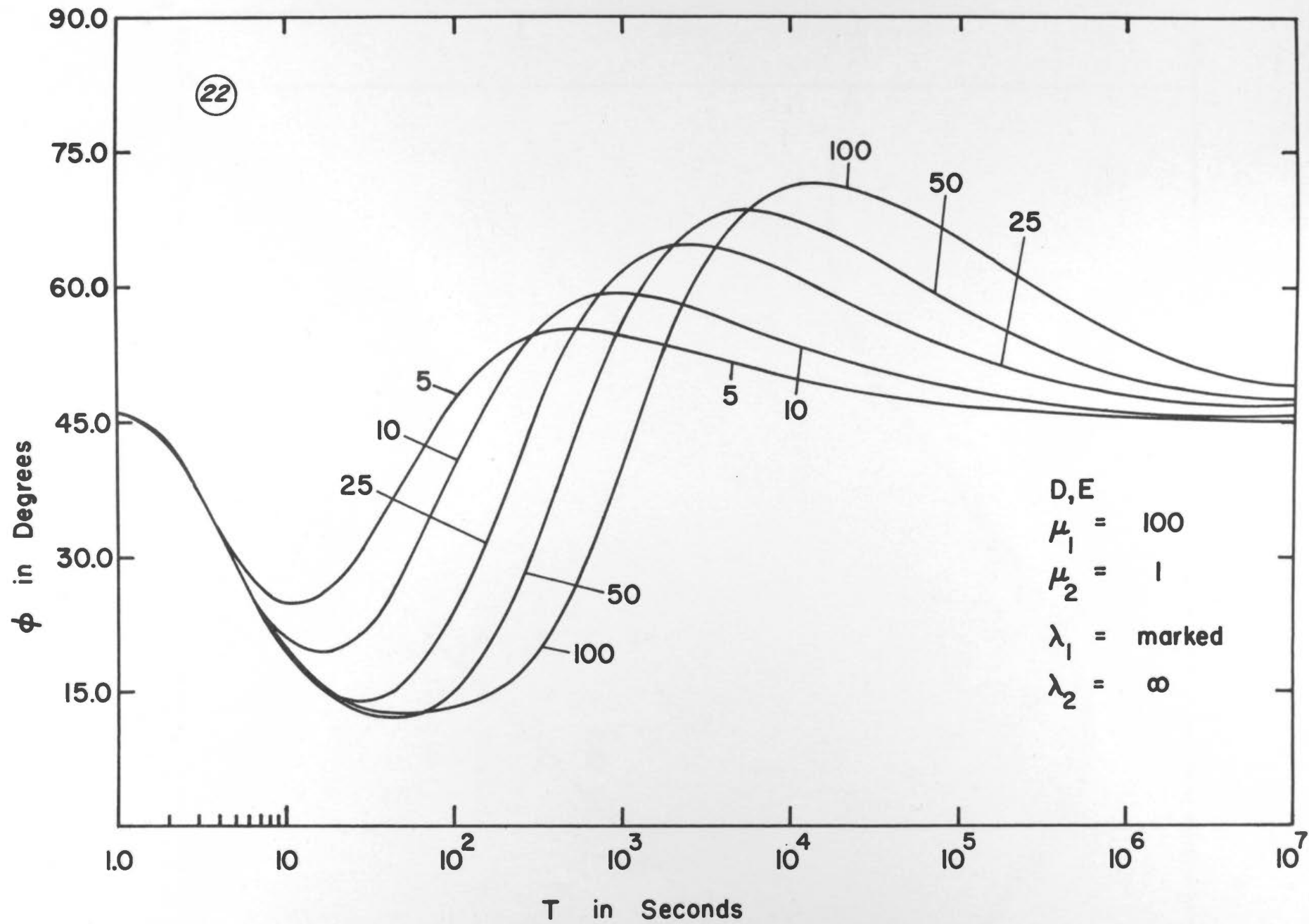
T in Seconds





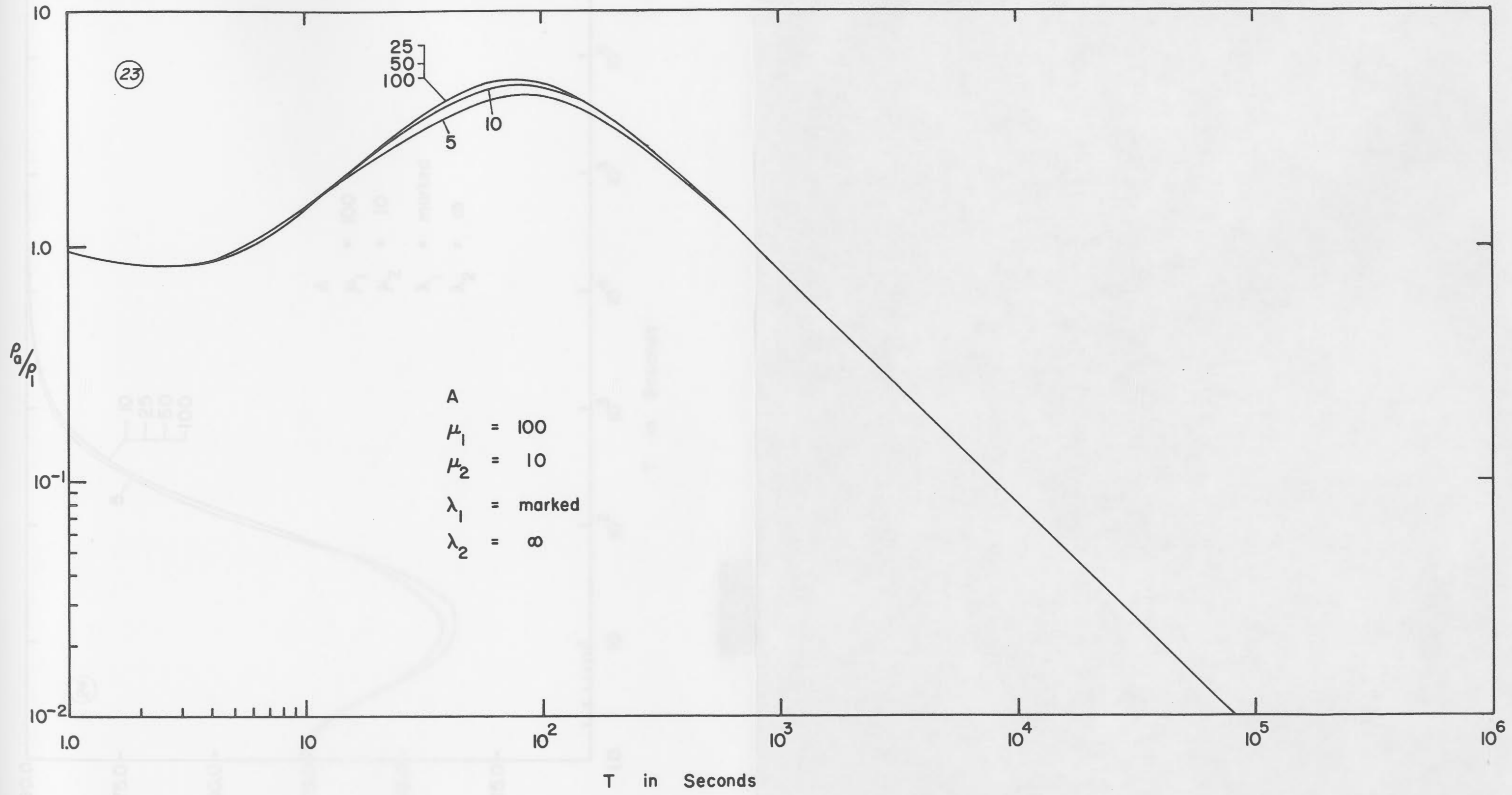


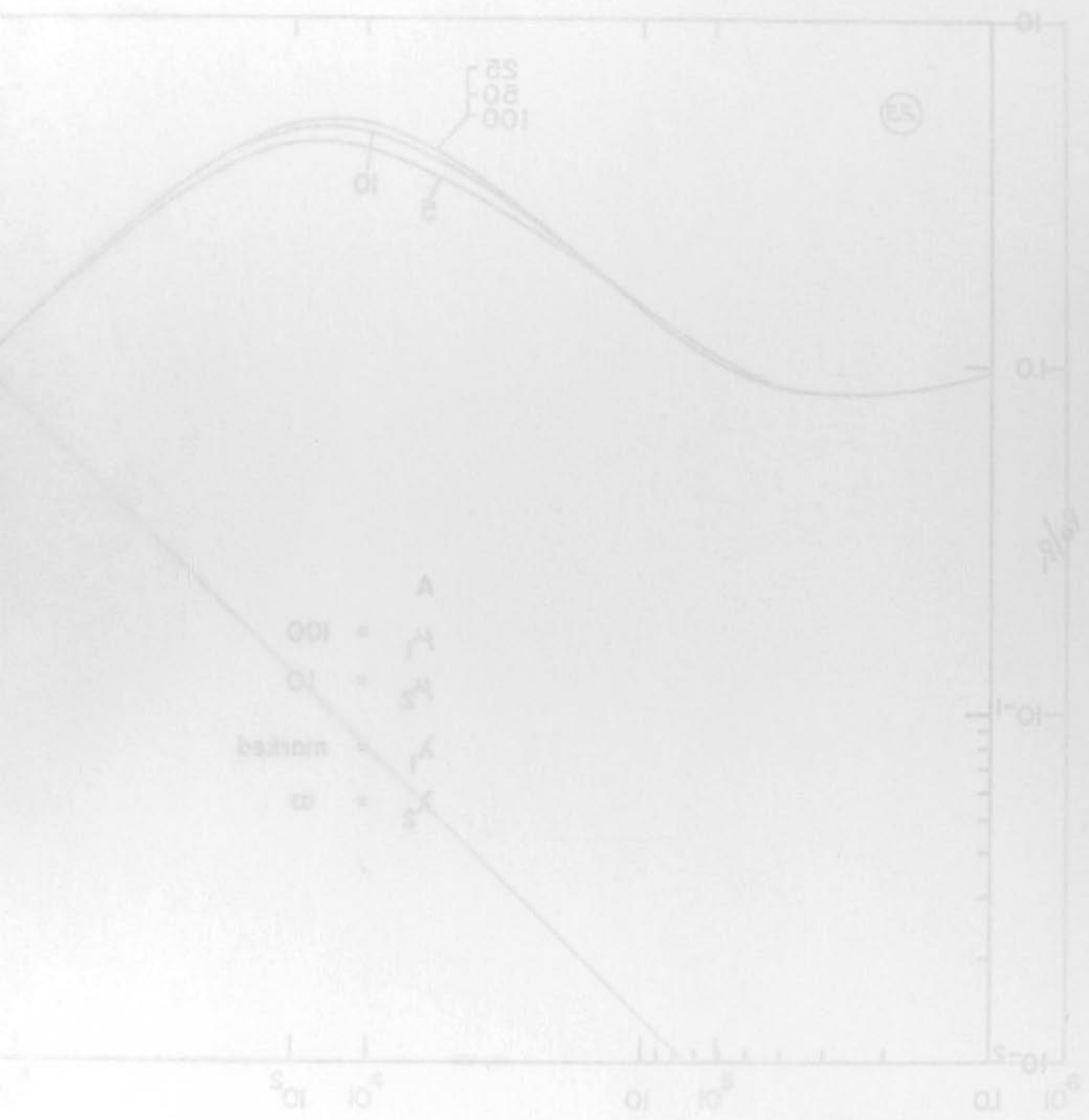
T in ...



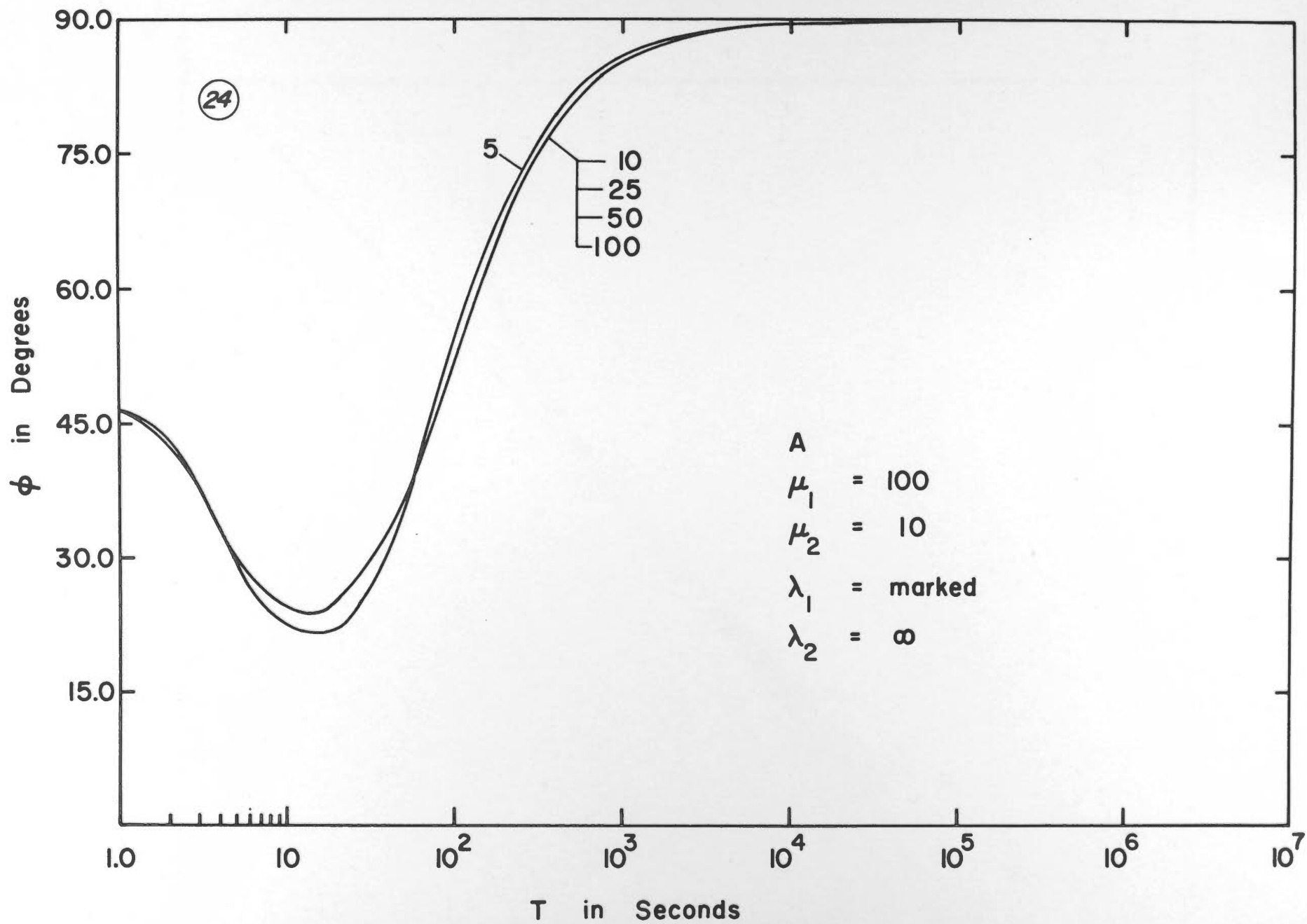
Δ in Decoups



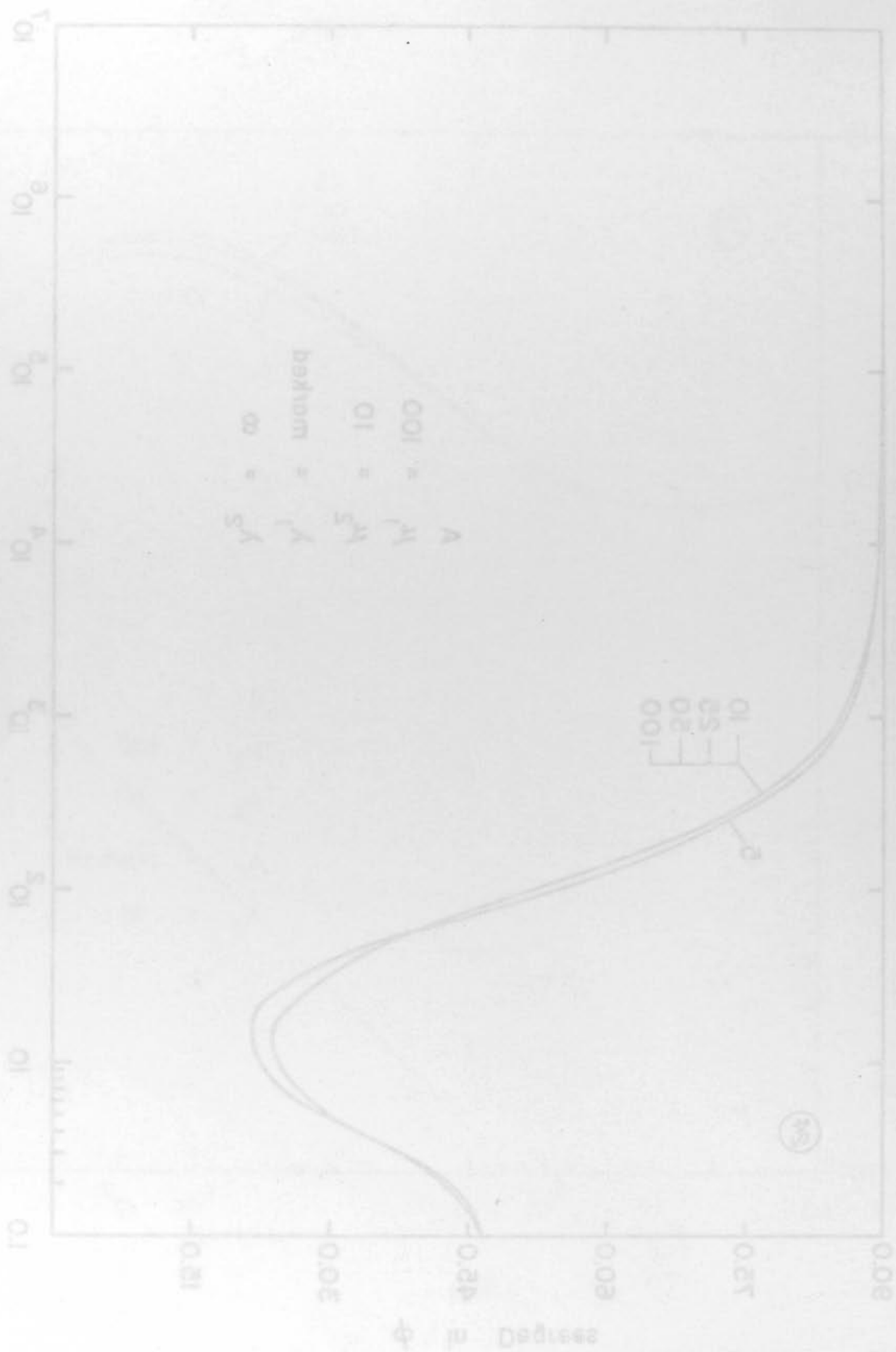


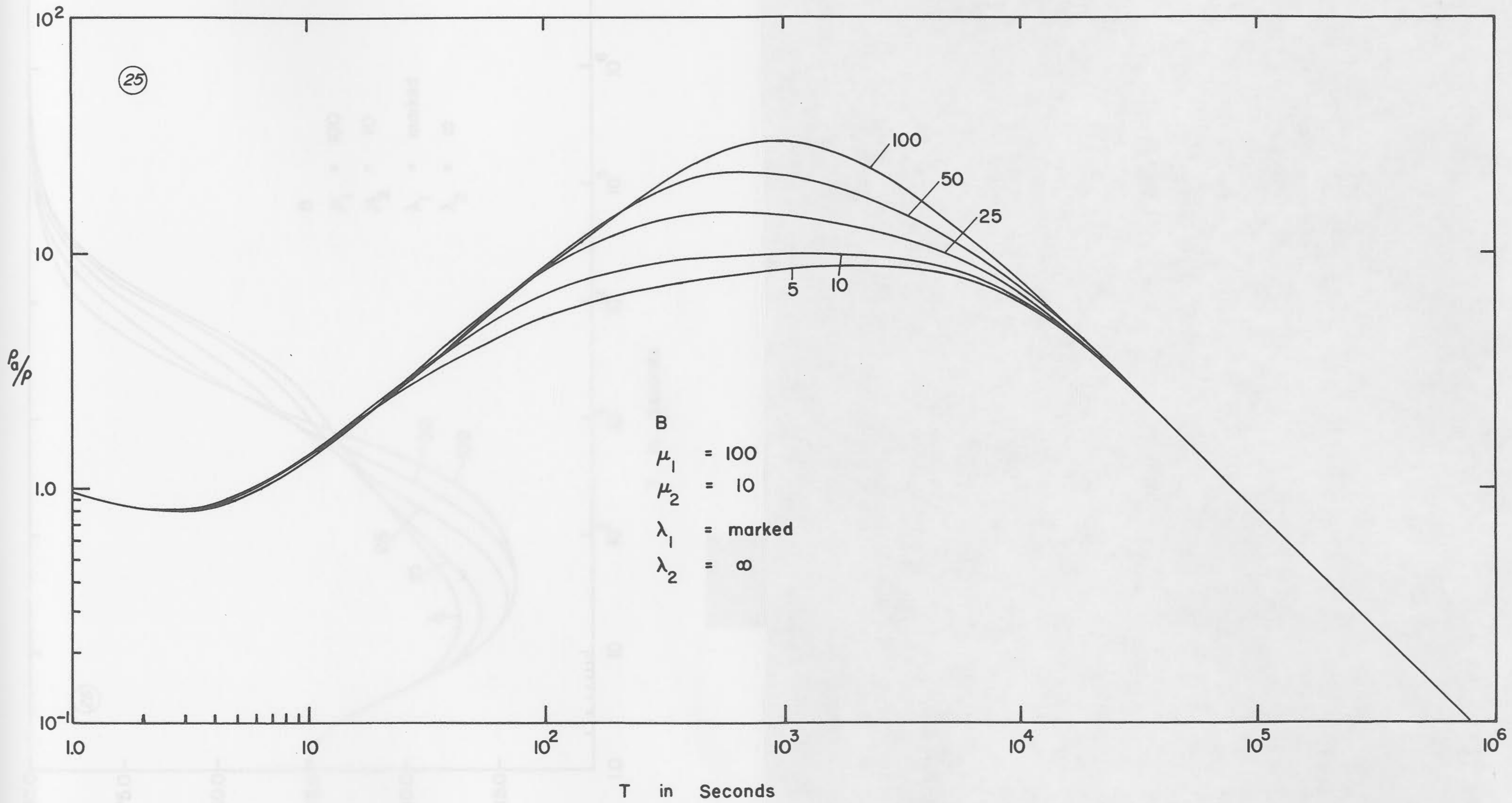


T in 200



T in Seconds





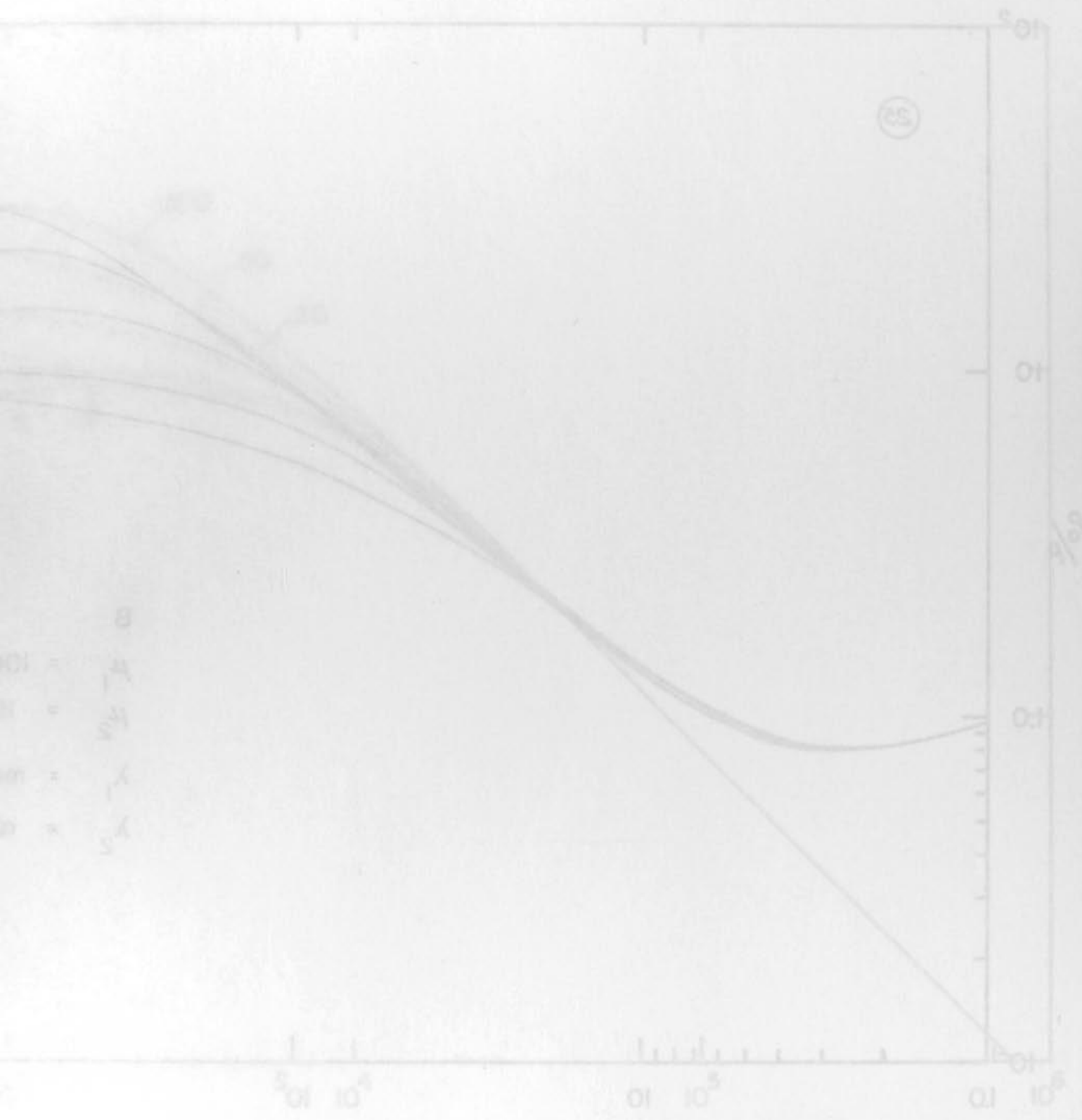
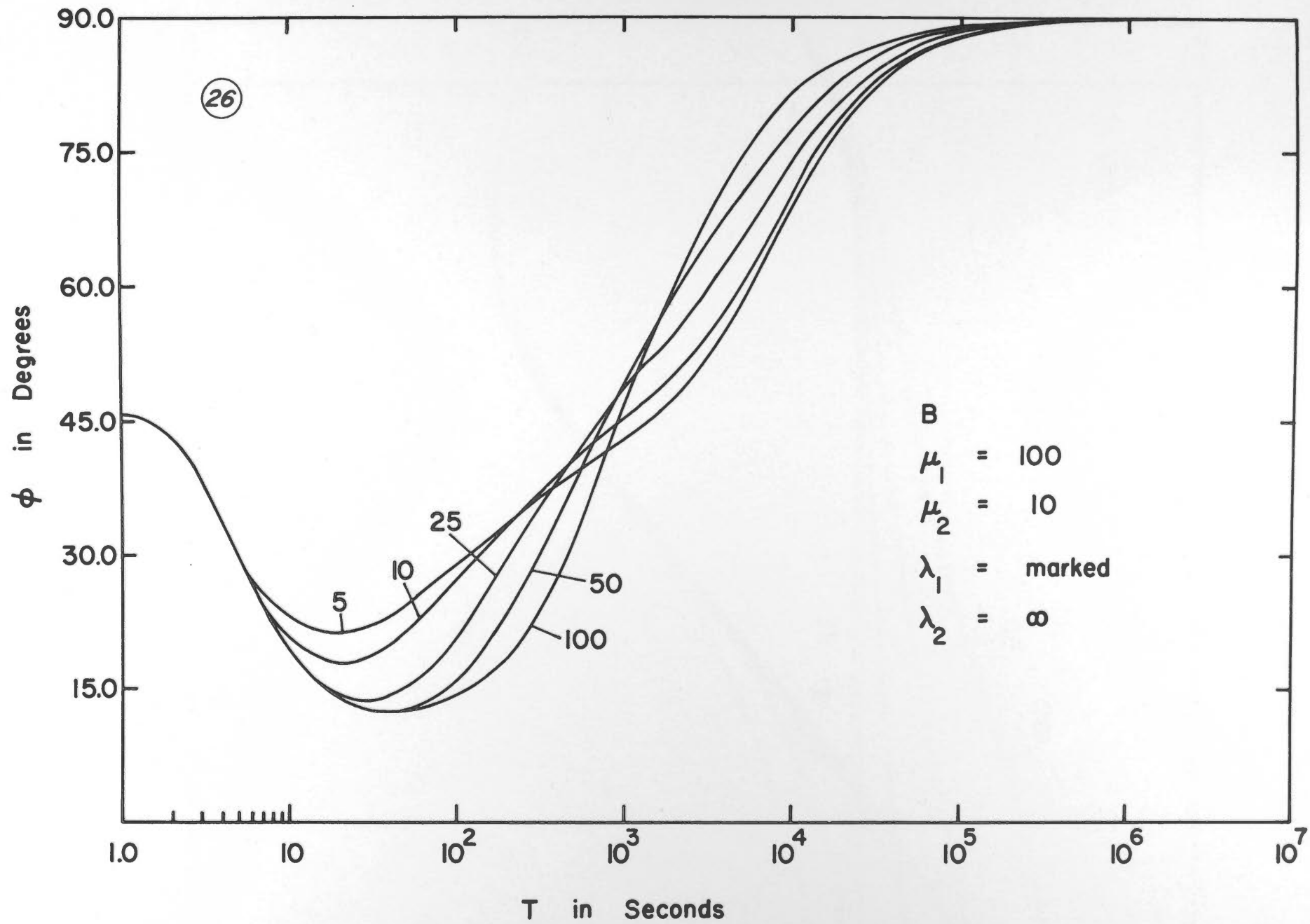
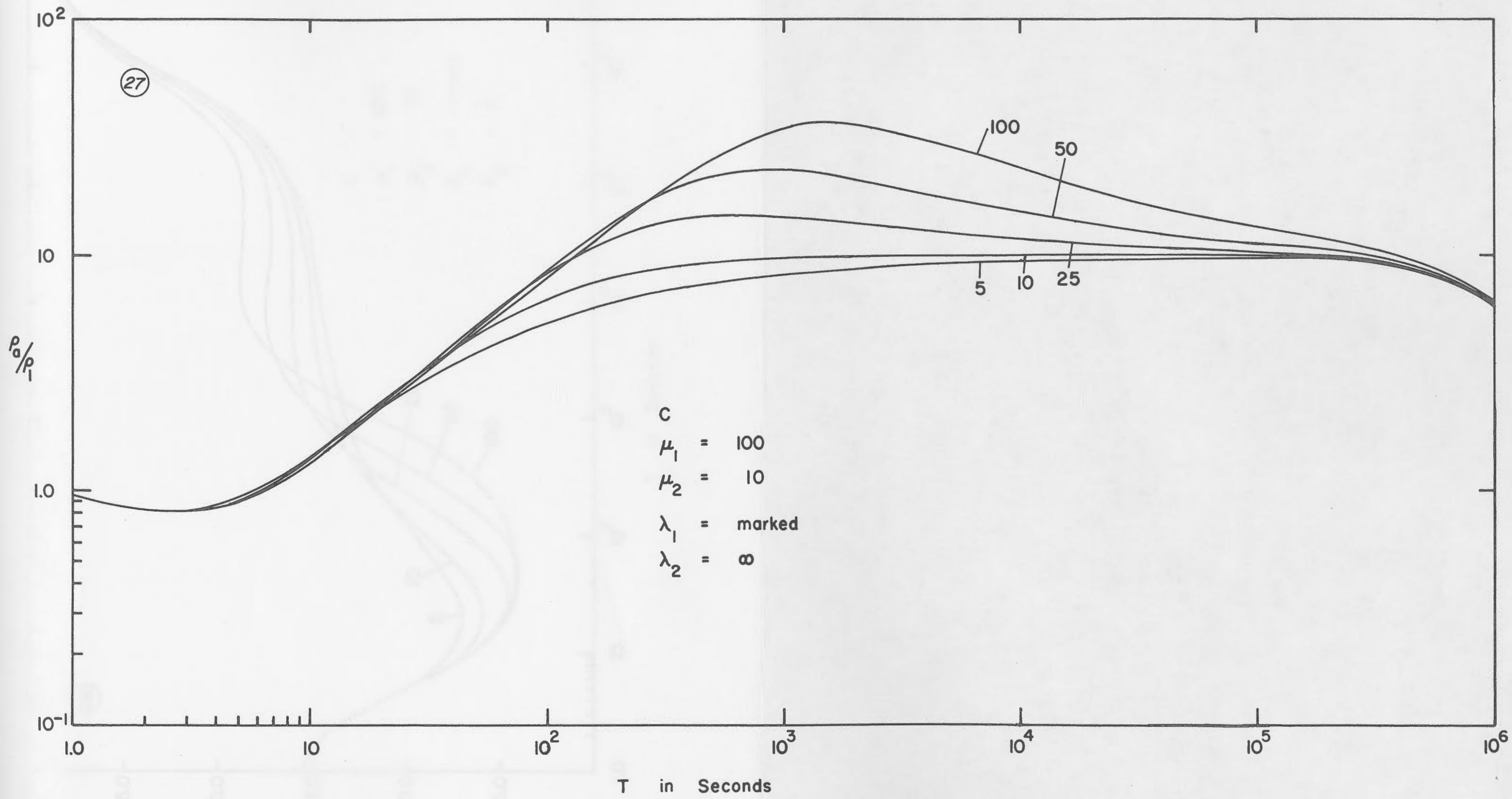


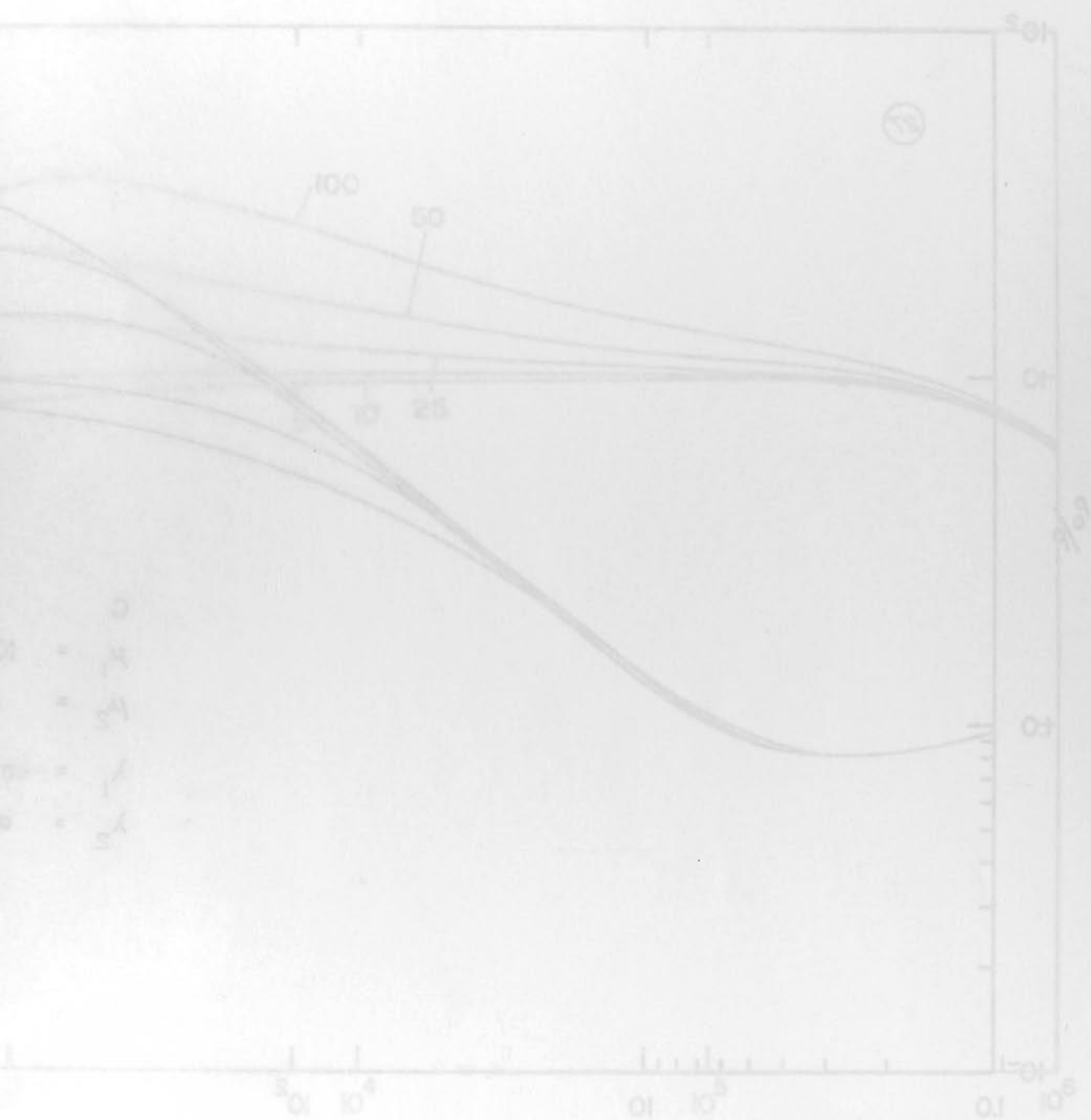
Figure 11

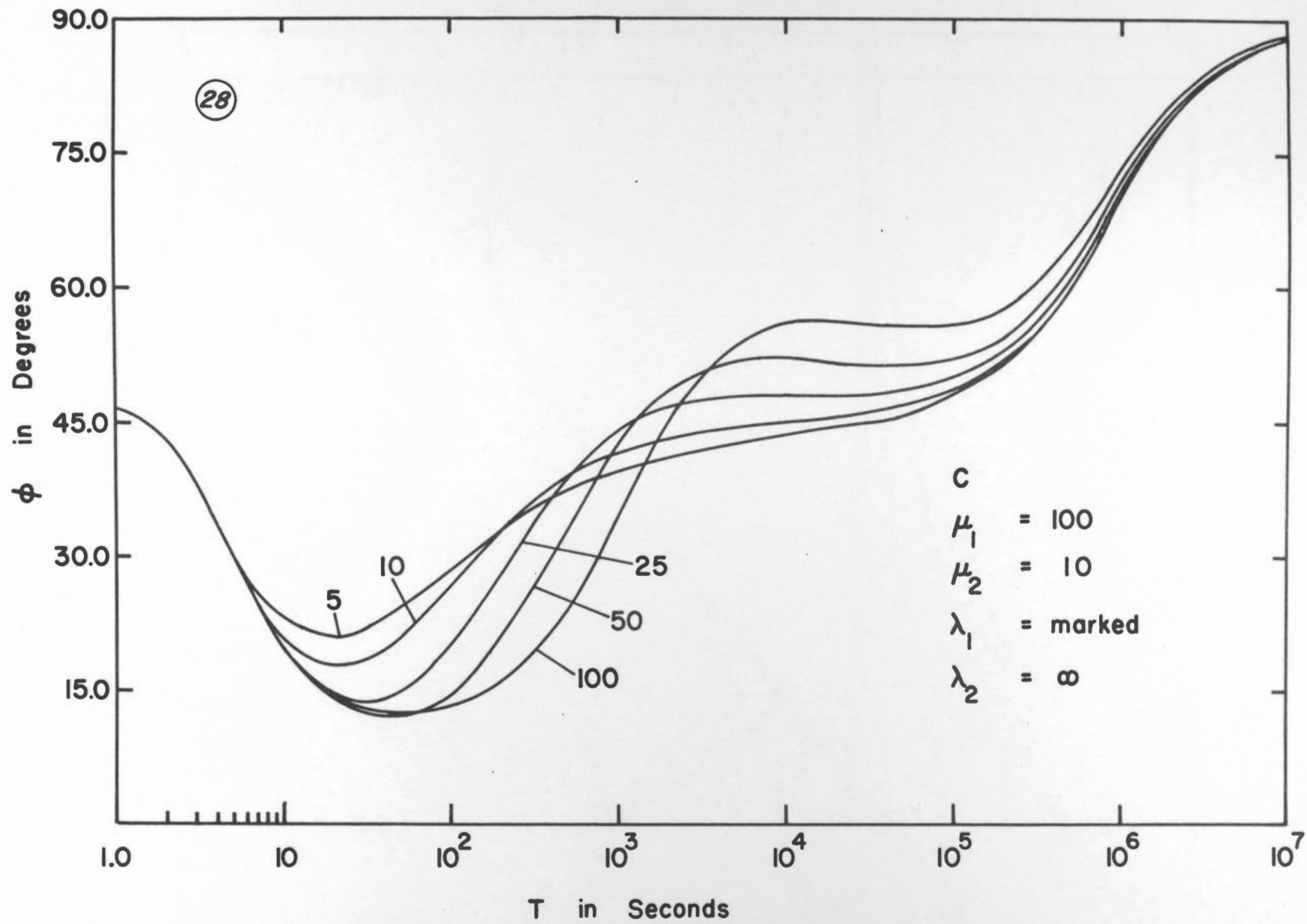


1 in 260000

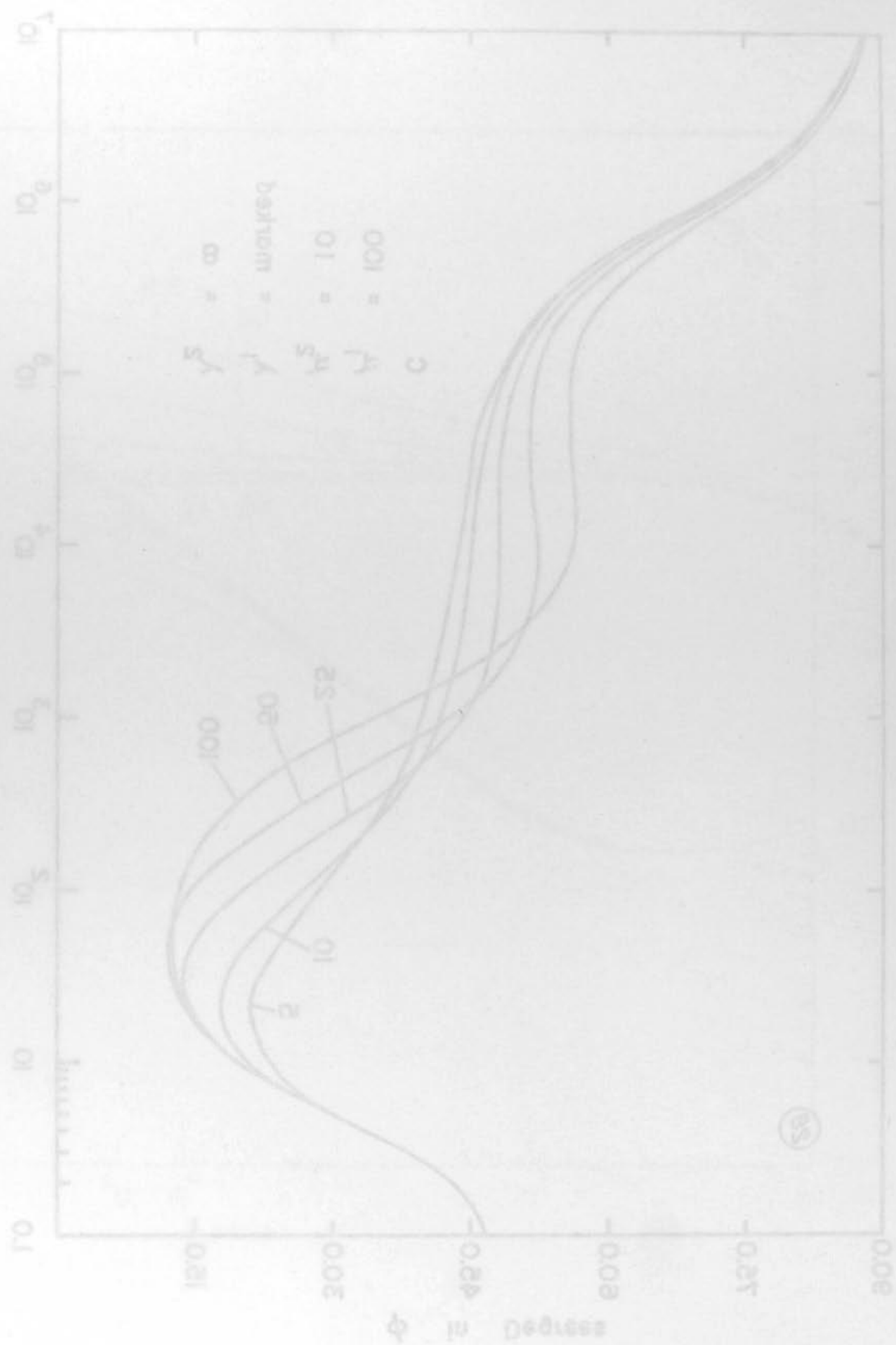


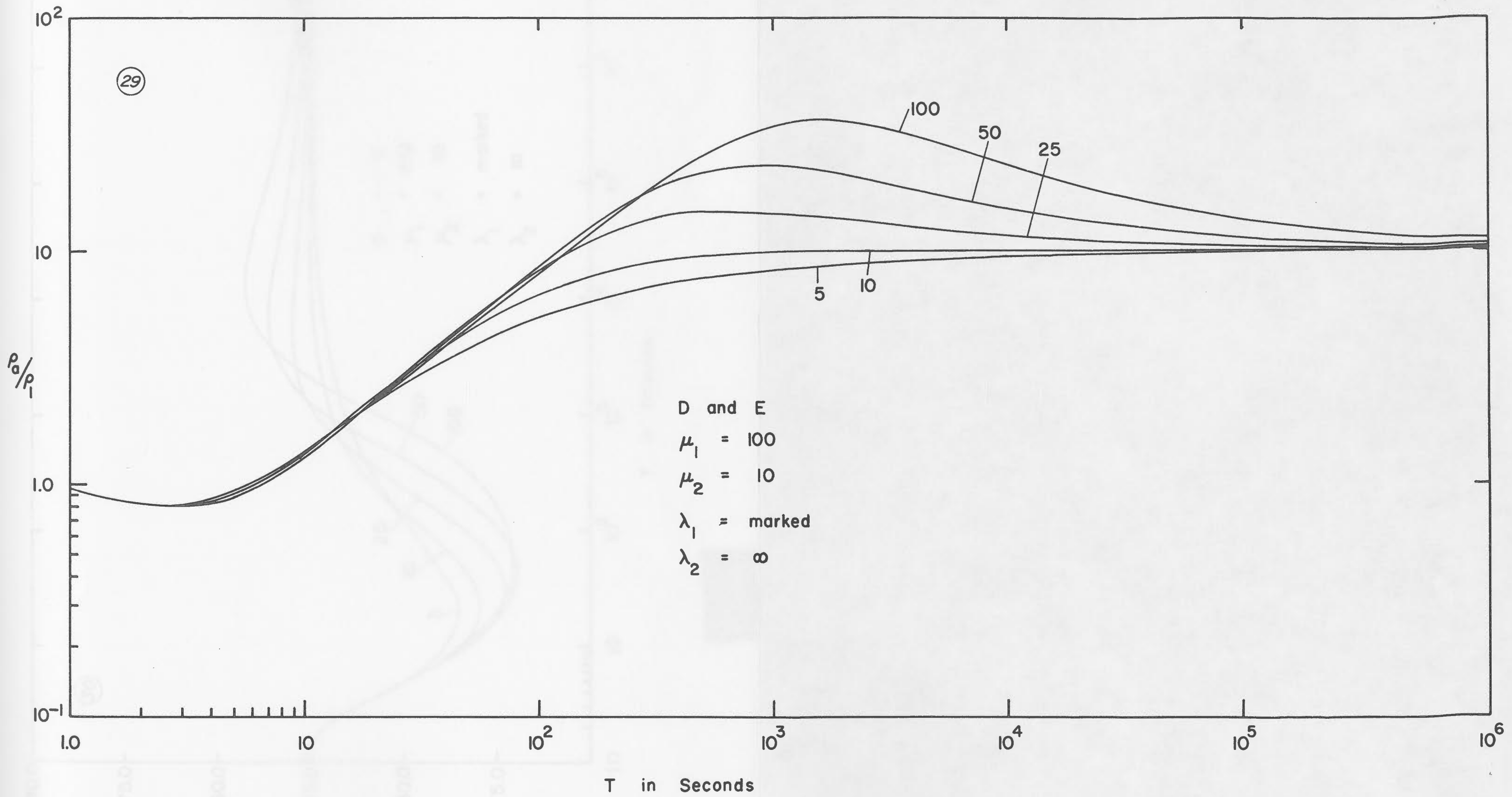


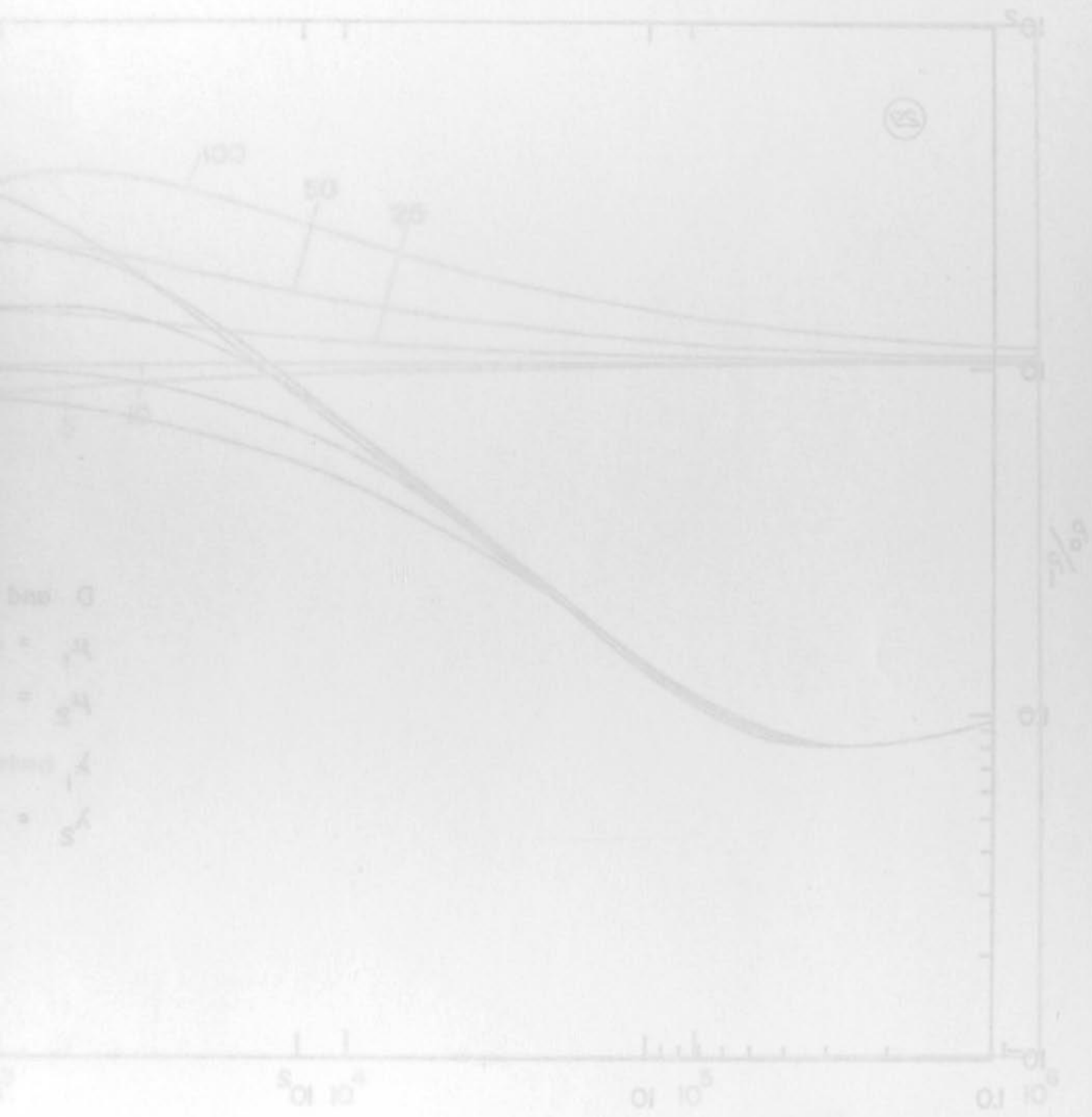




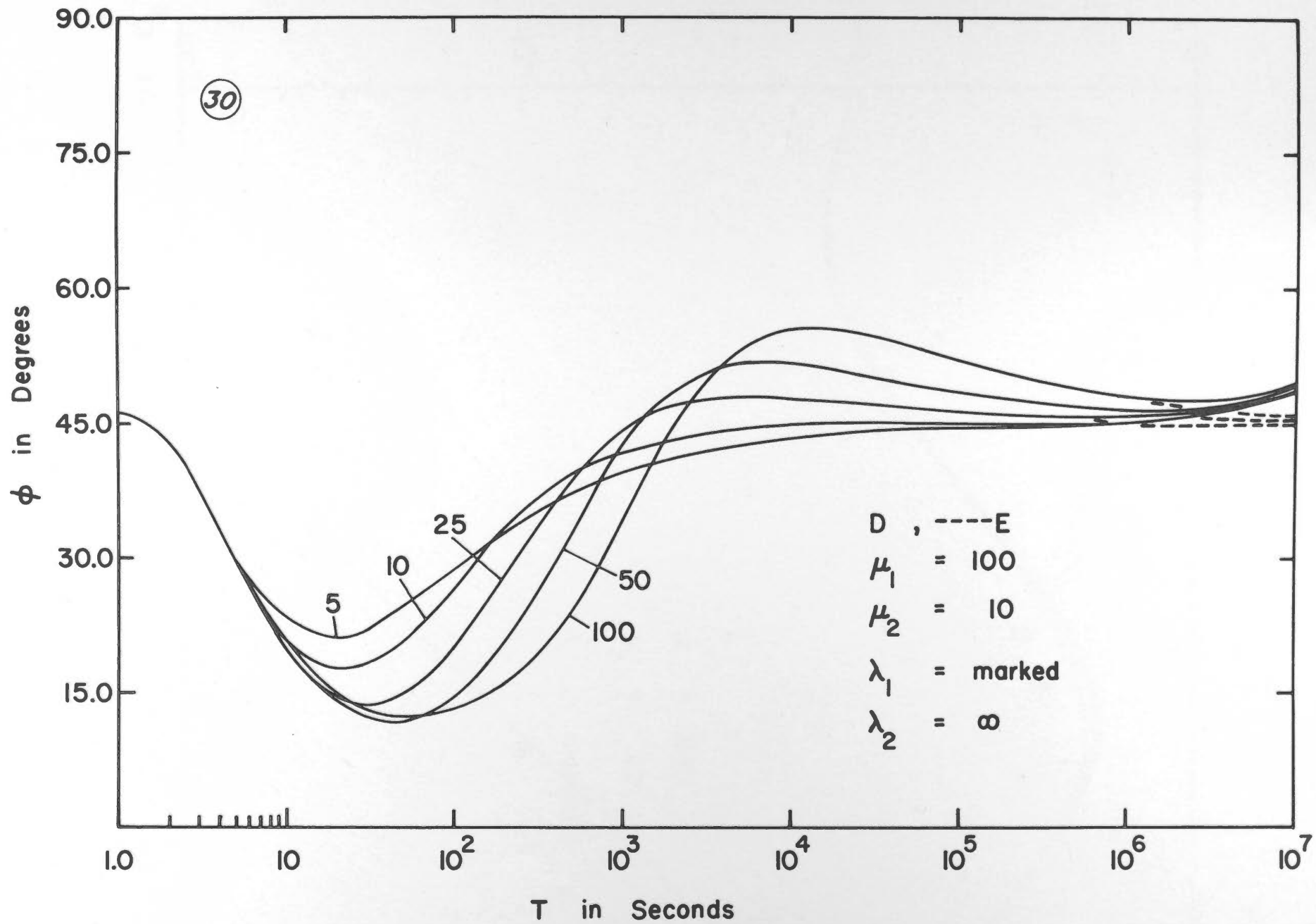
J. W. Saccouga



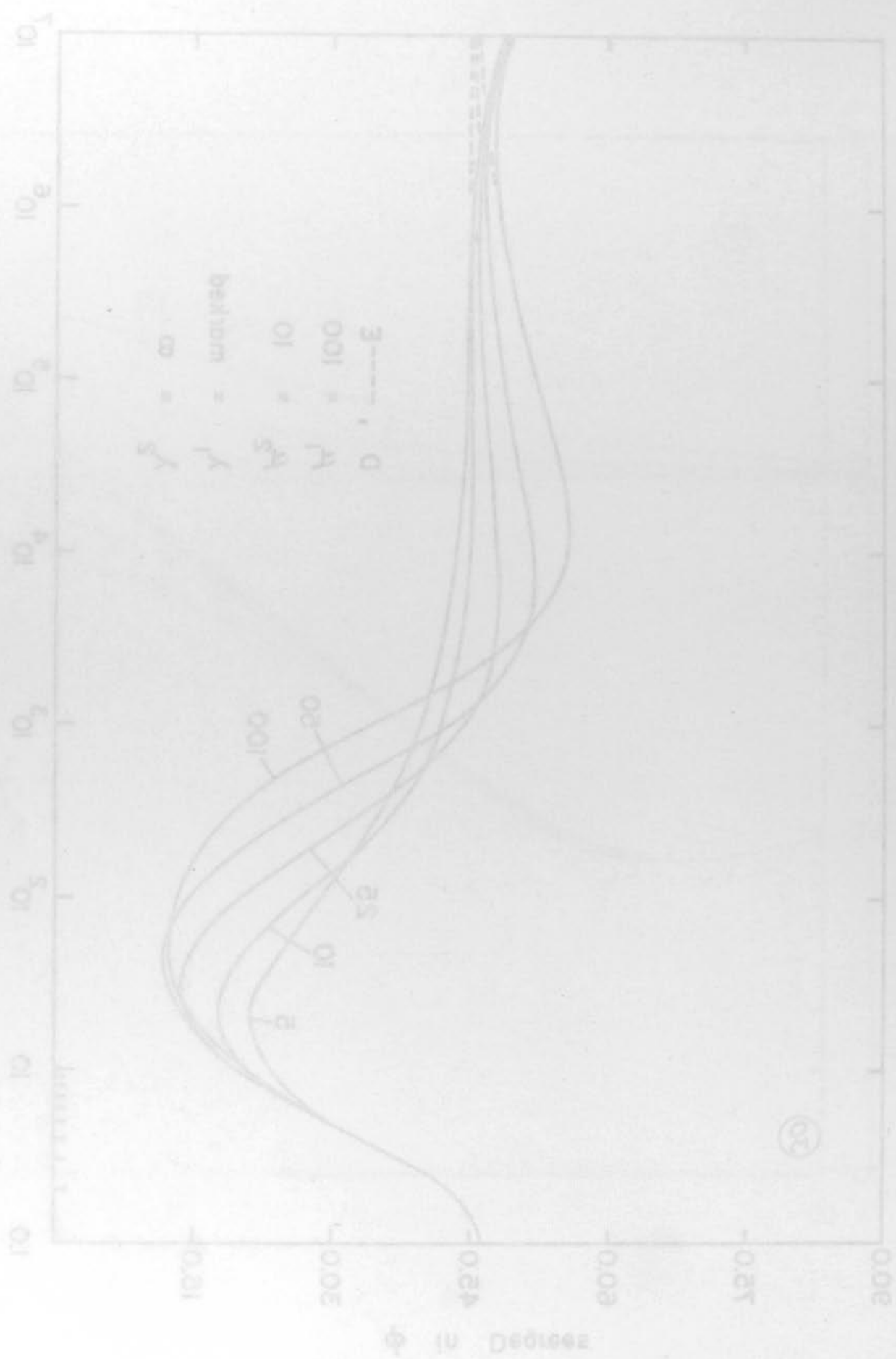


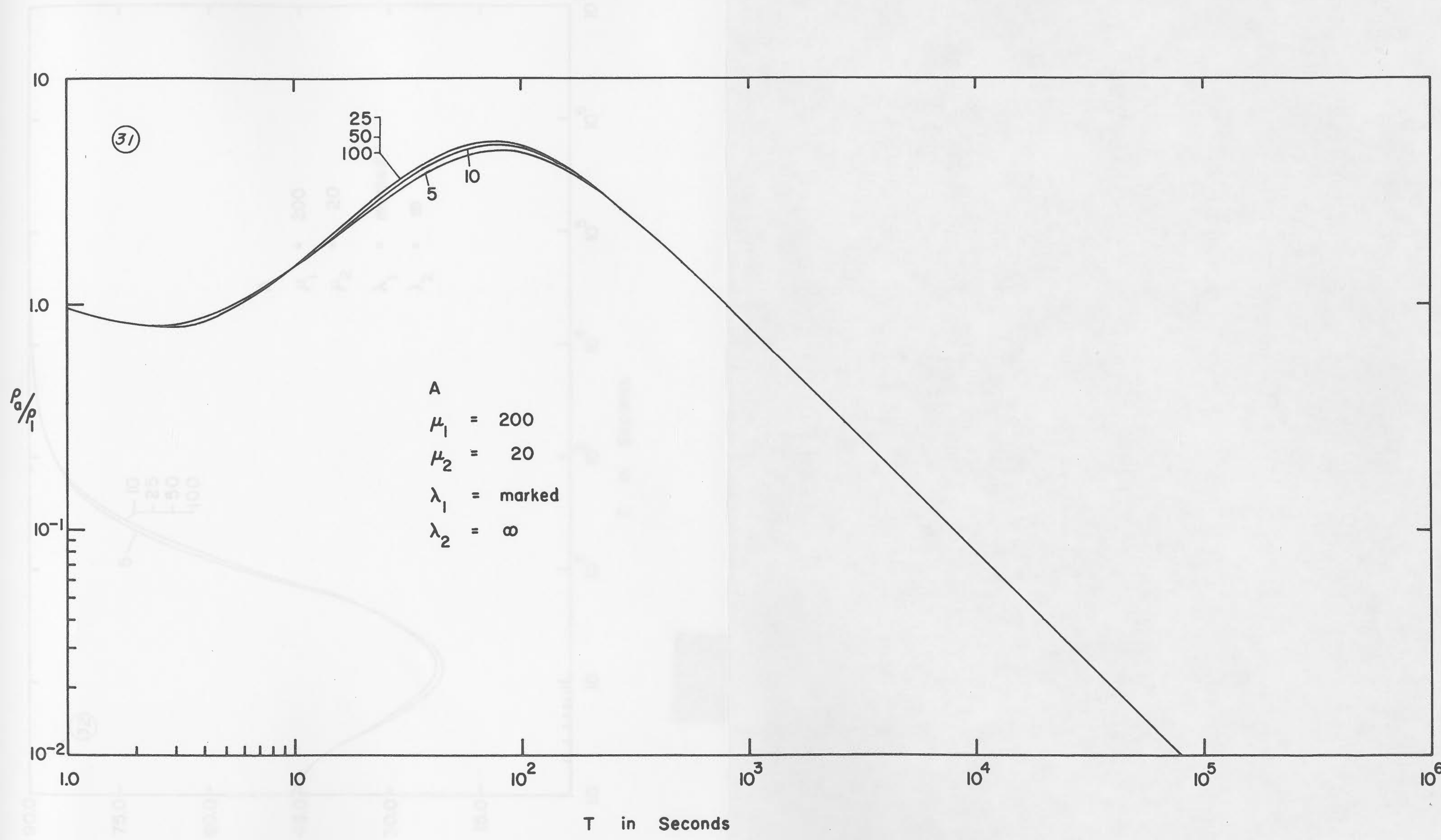


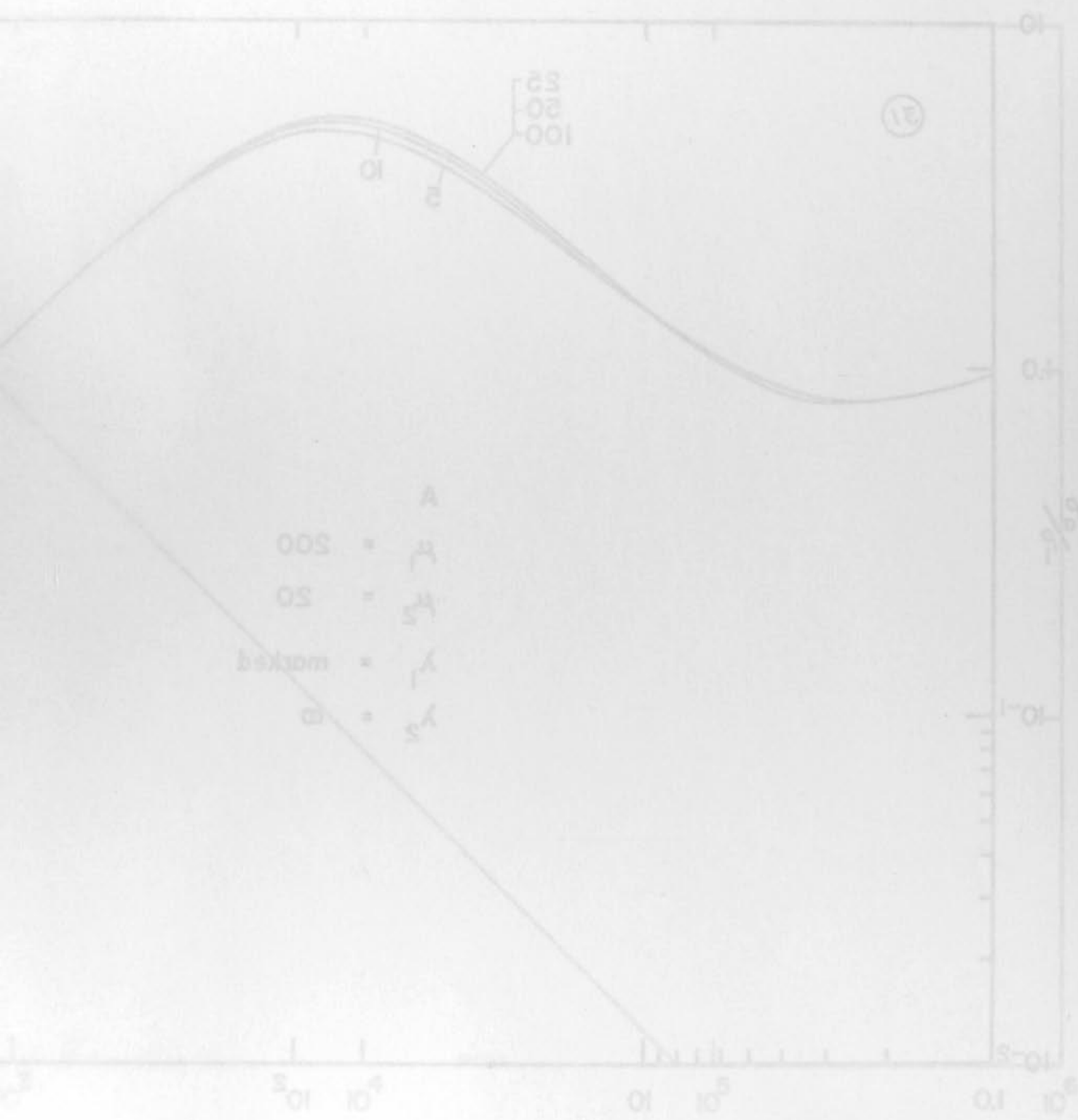
T in Seconds



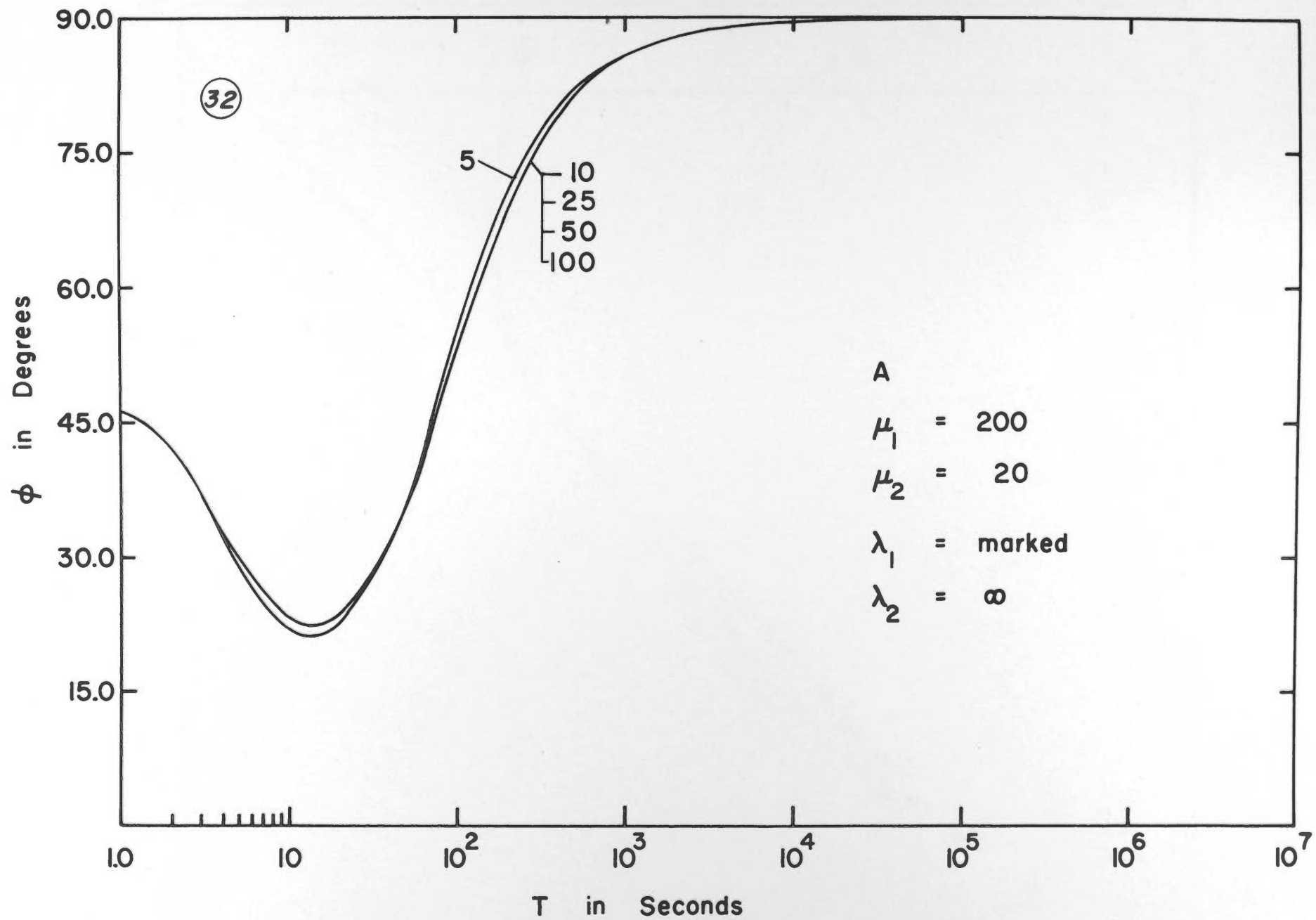
abscissa in T



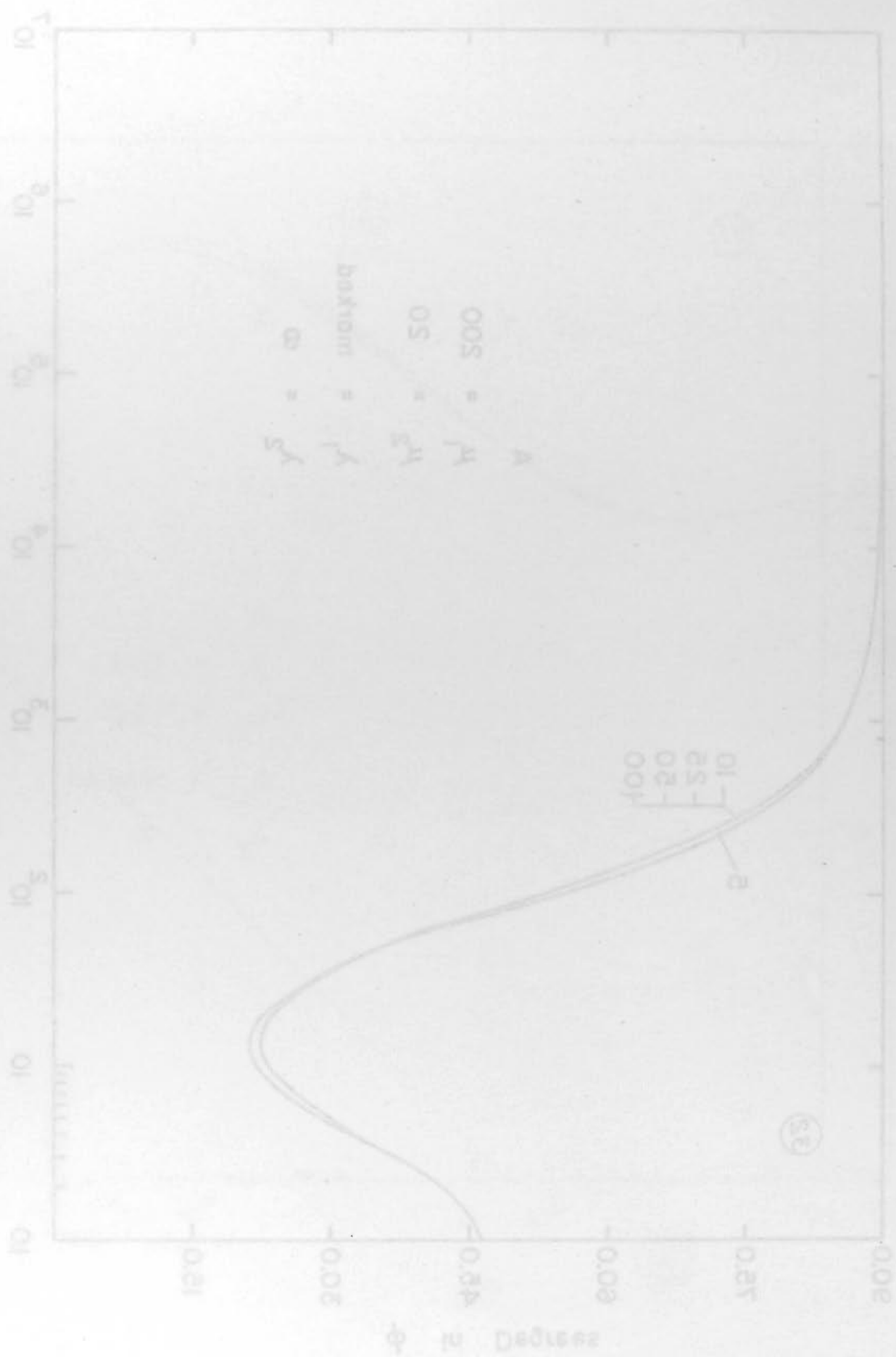


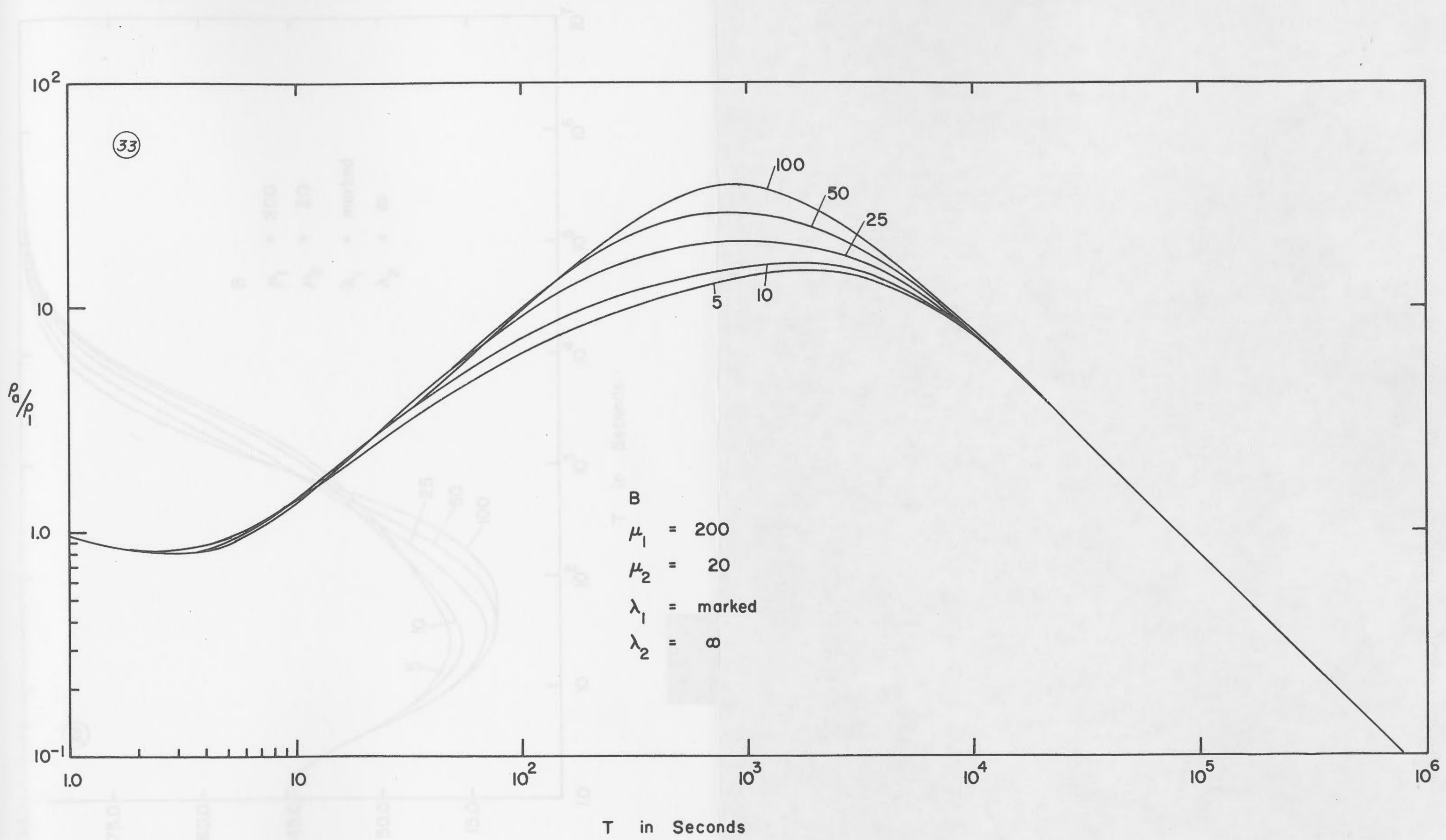


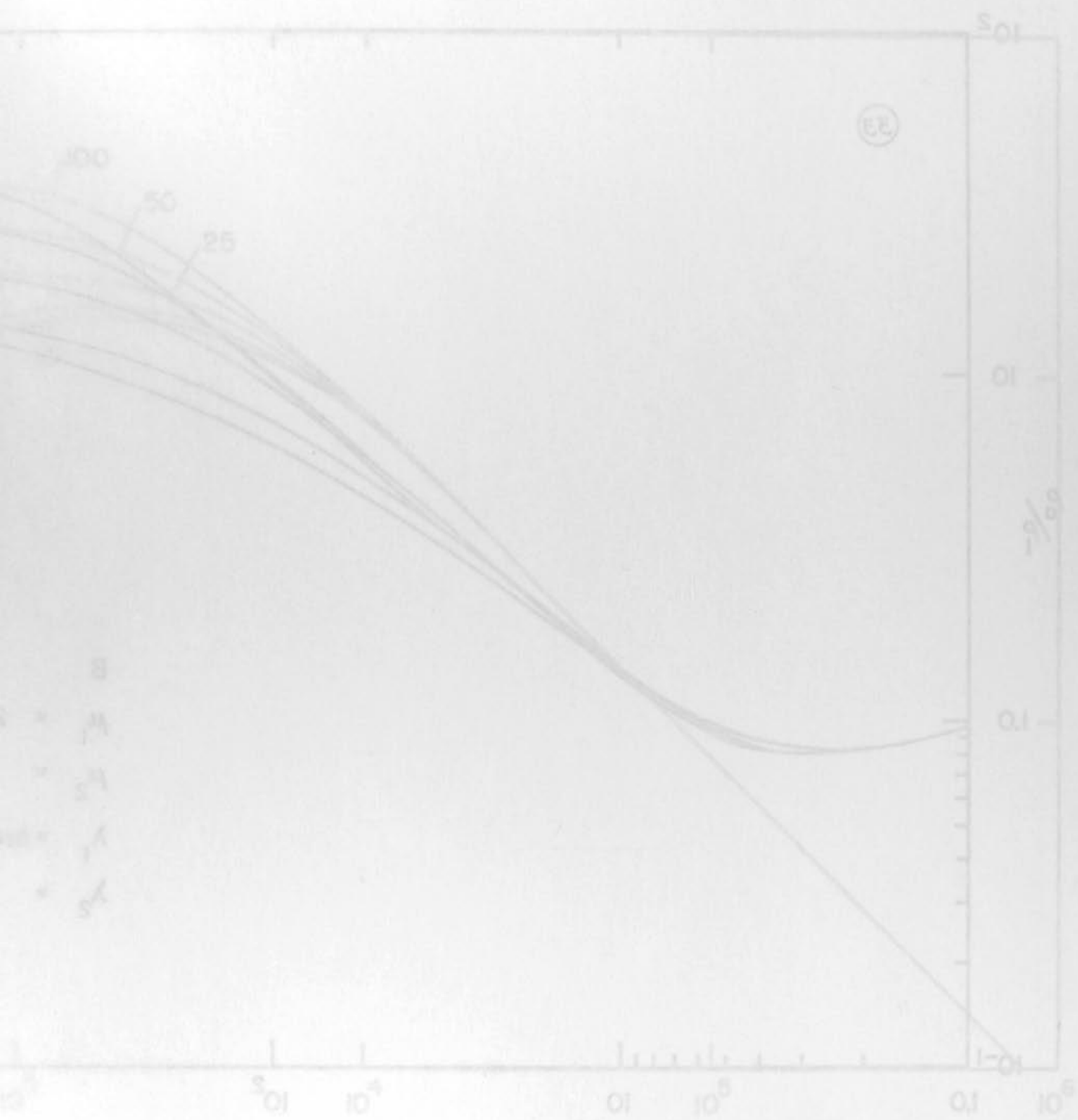
T in Sec



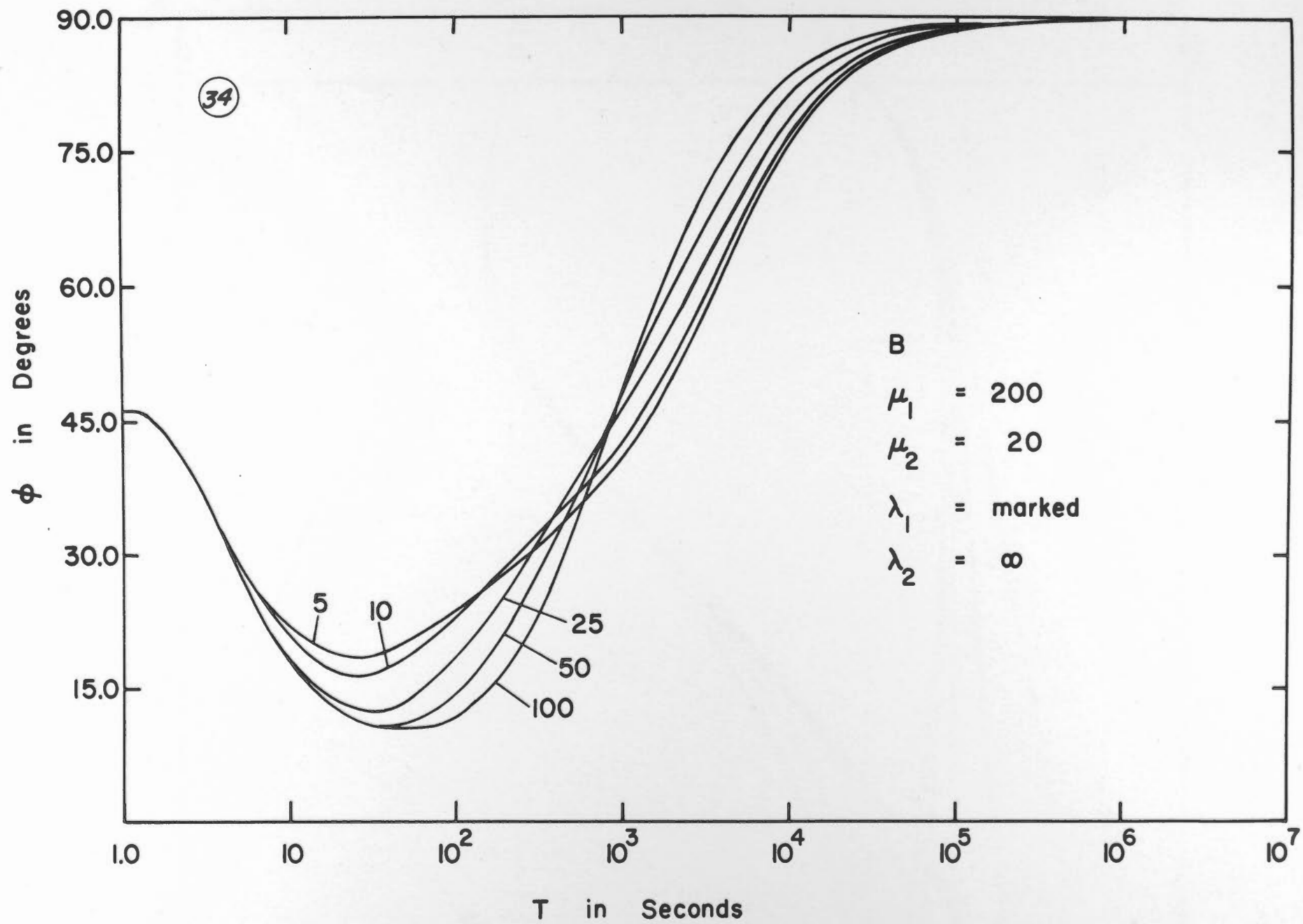
T in Seconds

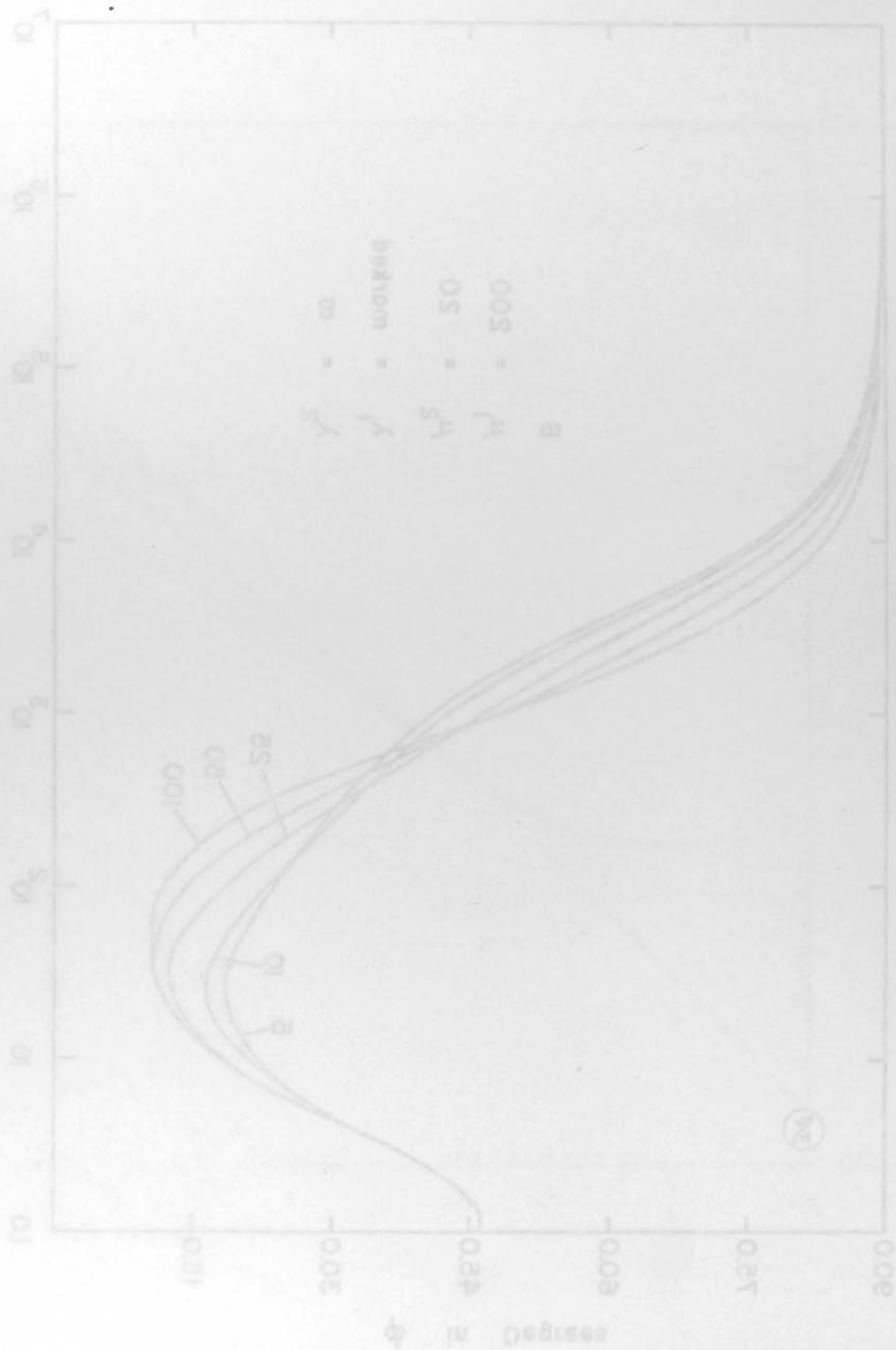


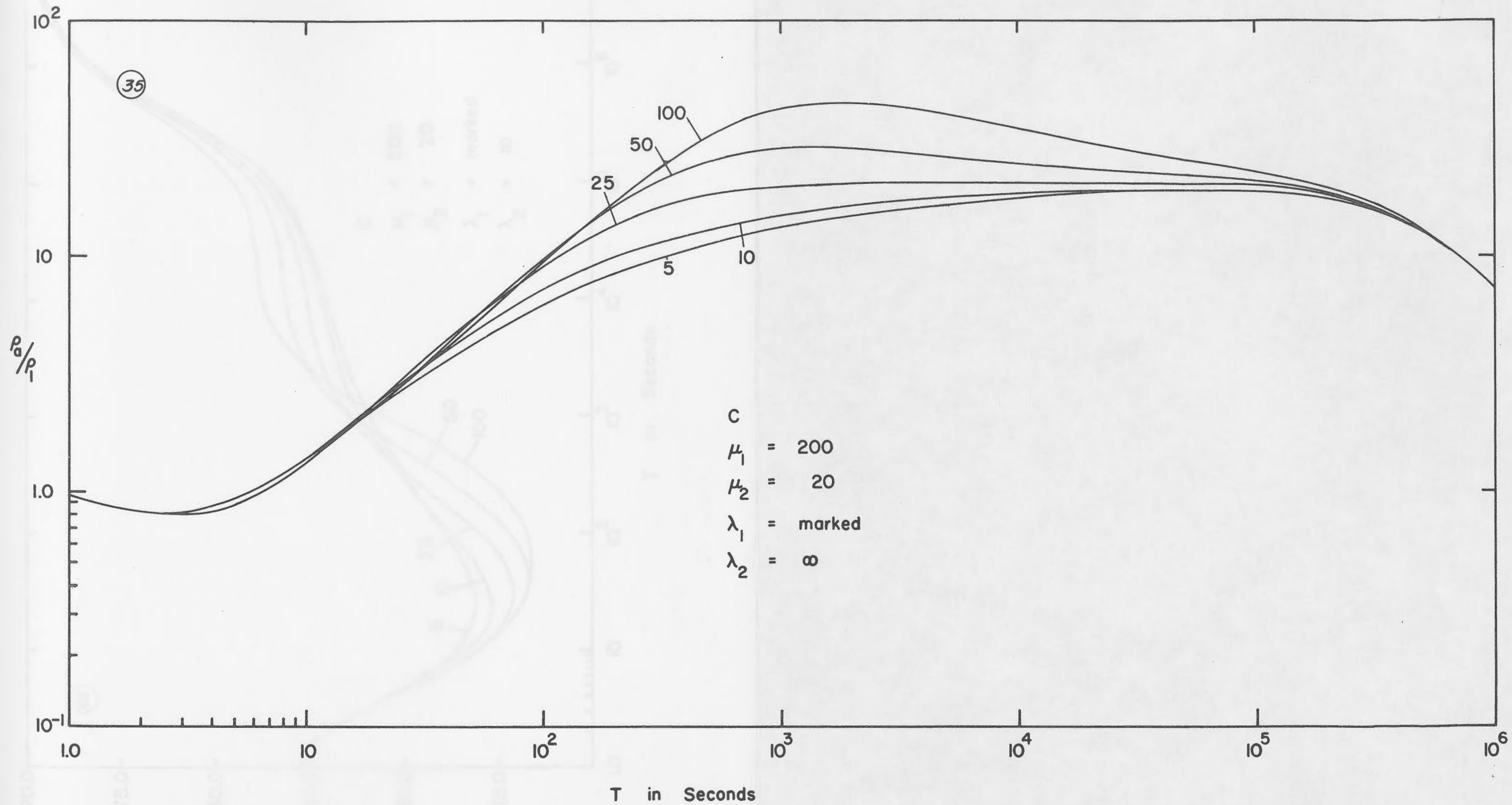


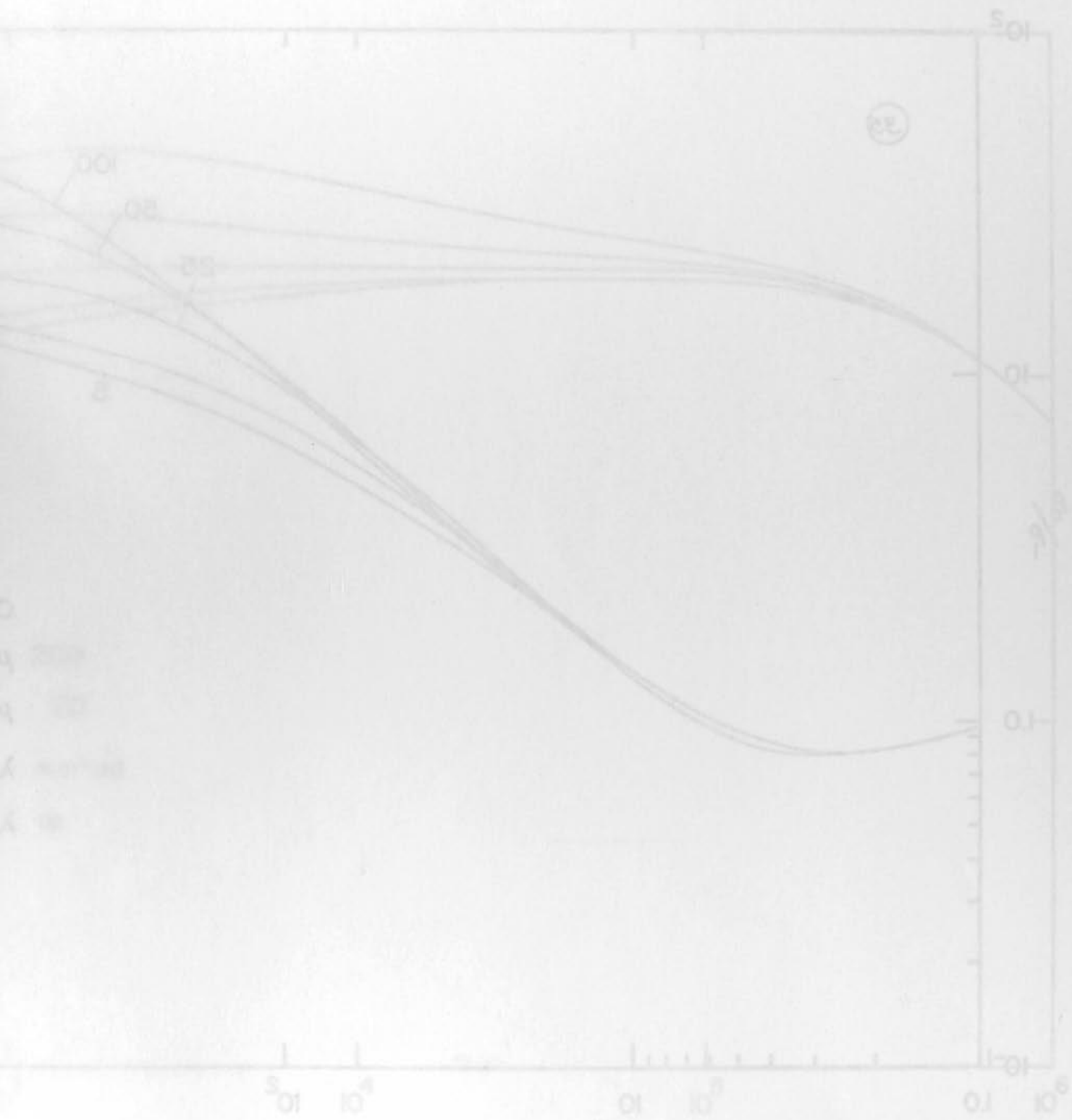


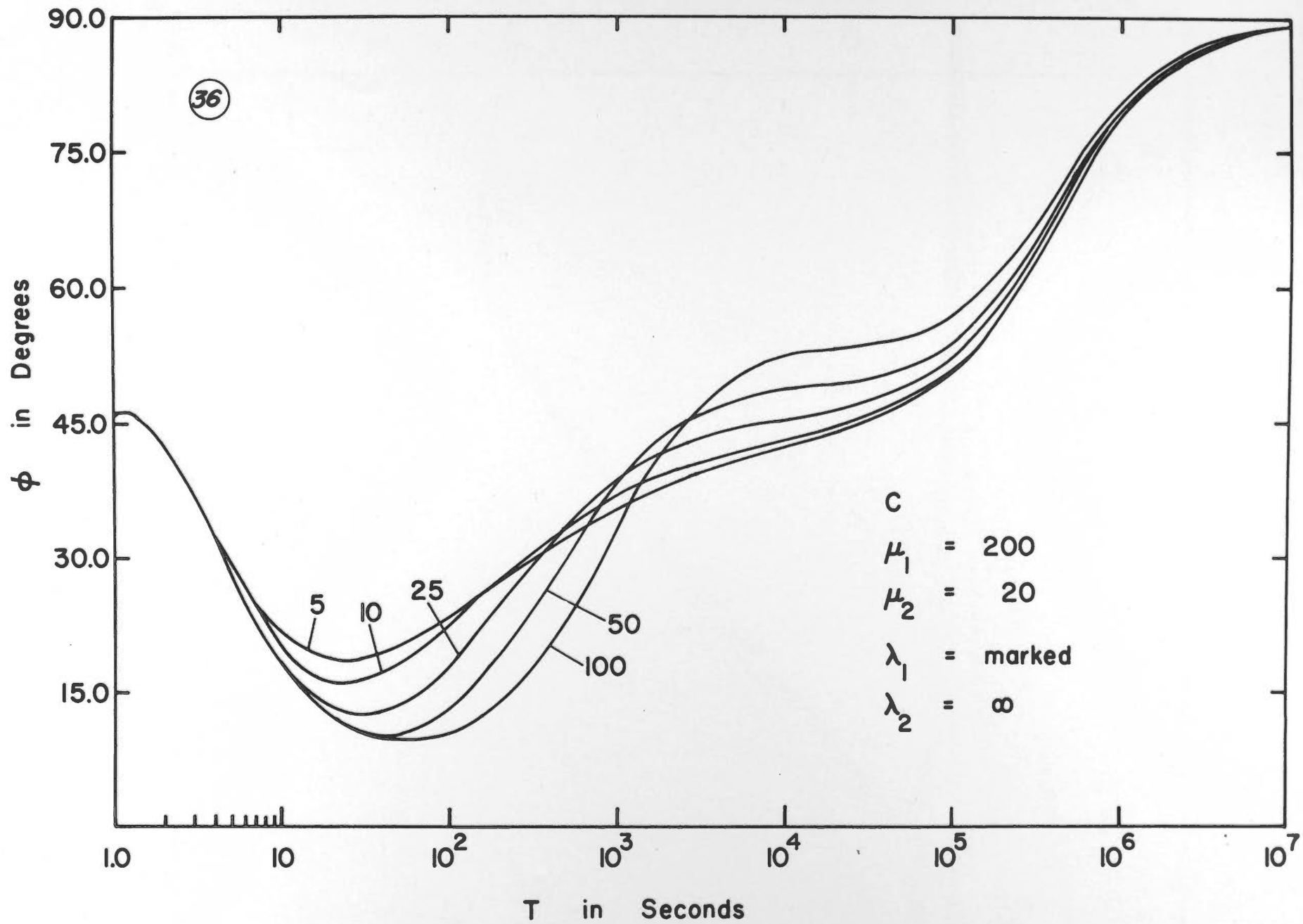
T in Sec

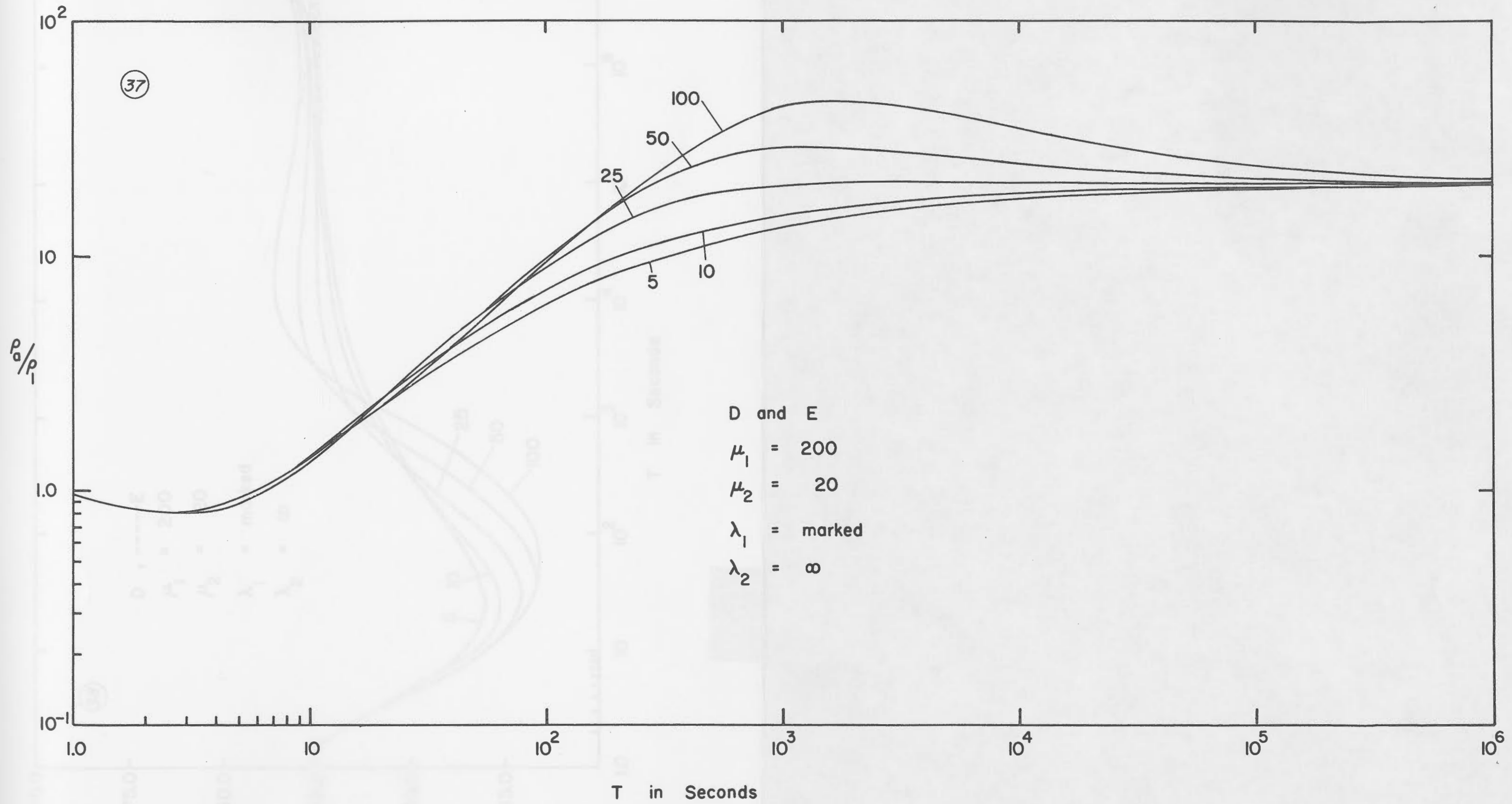


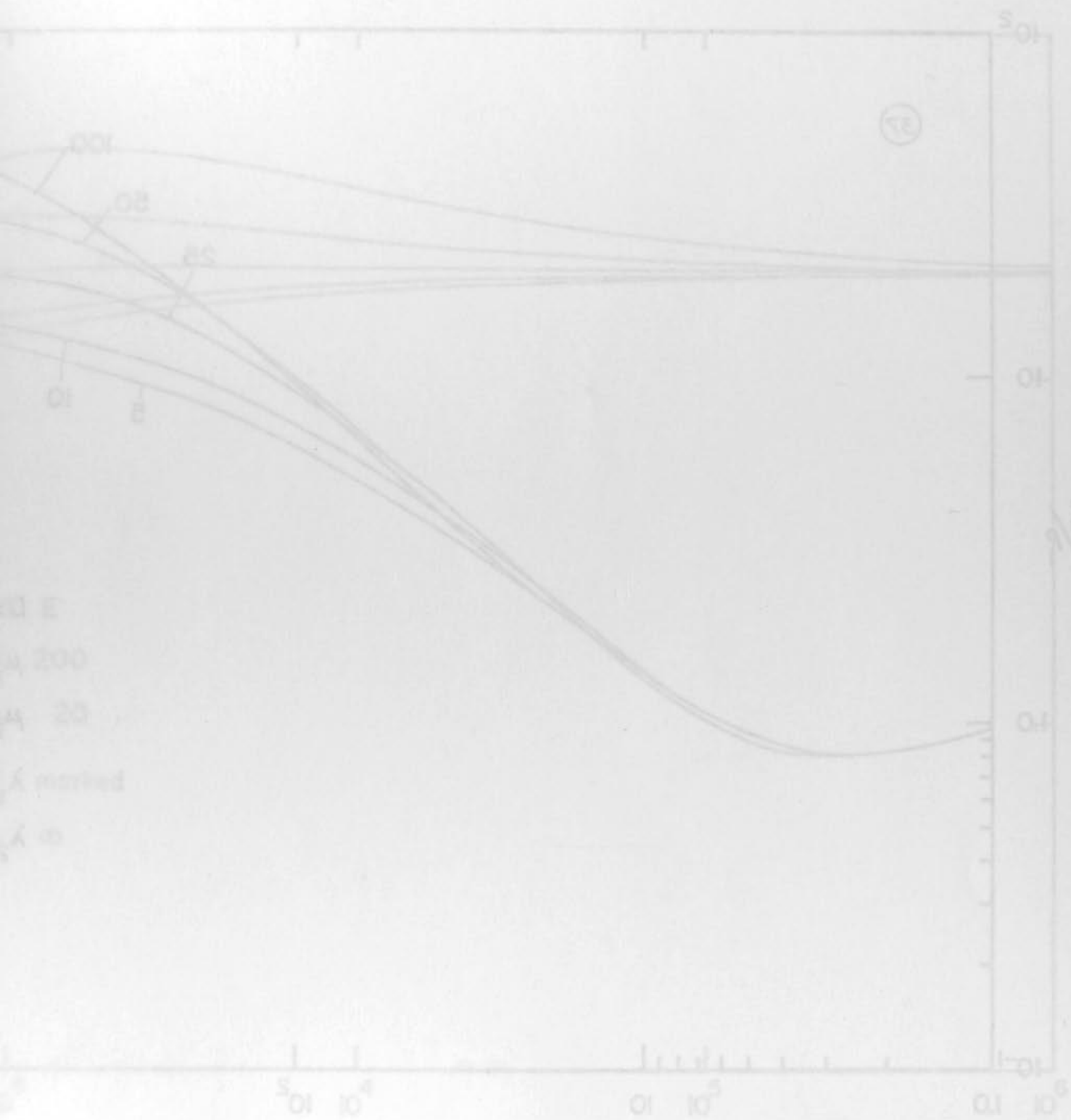






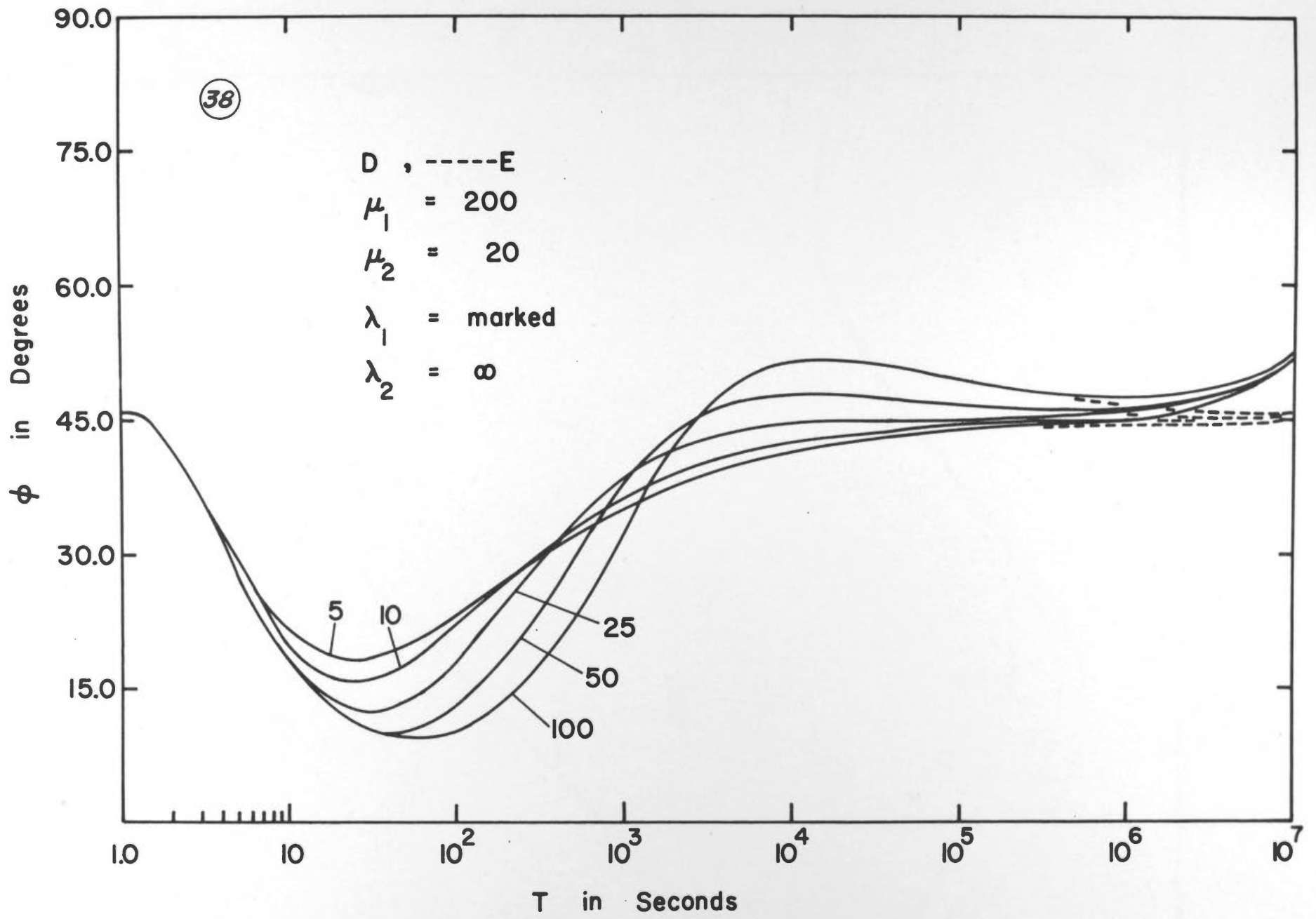




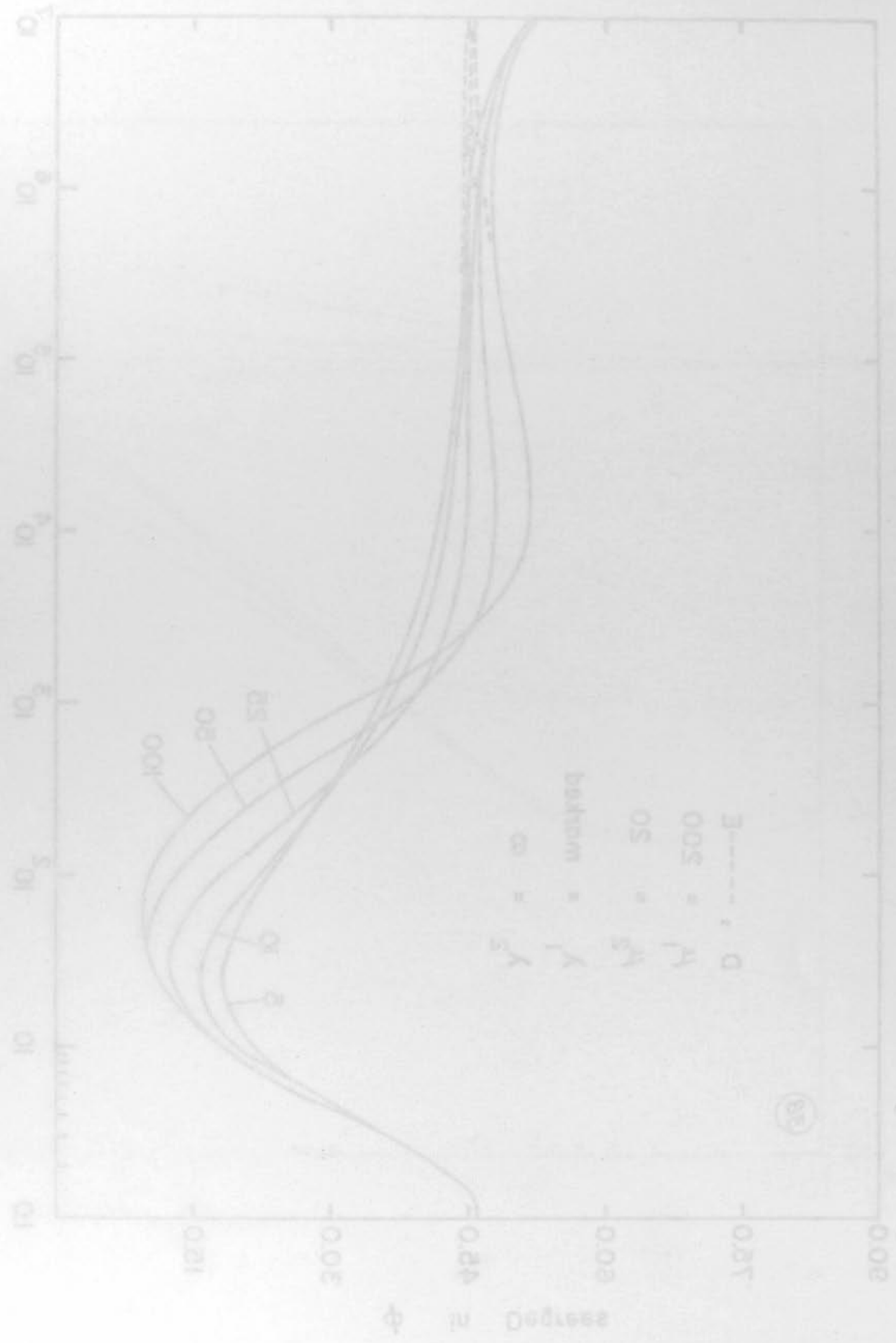


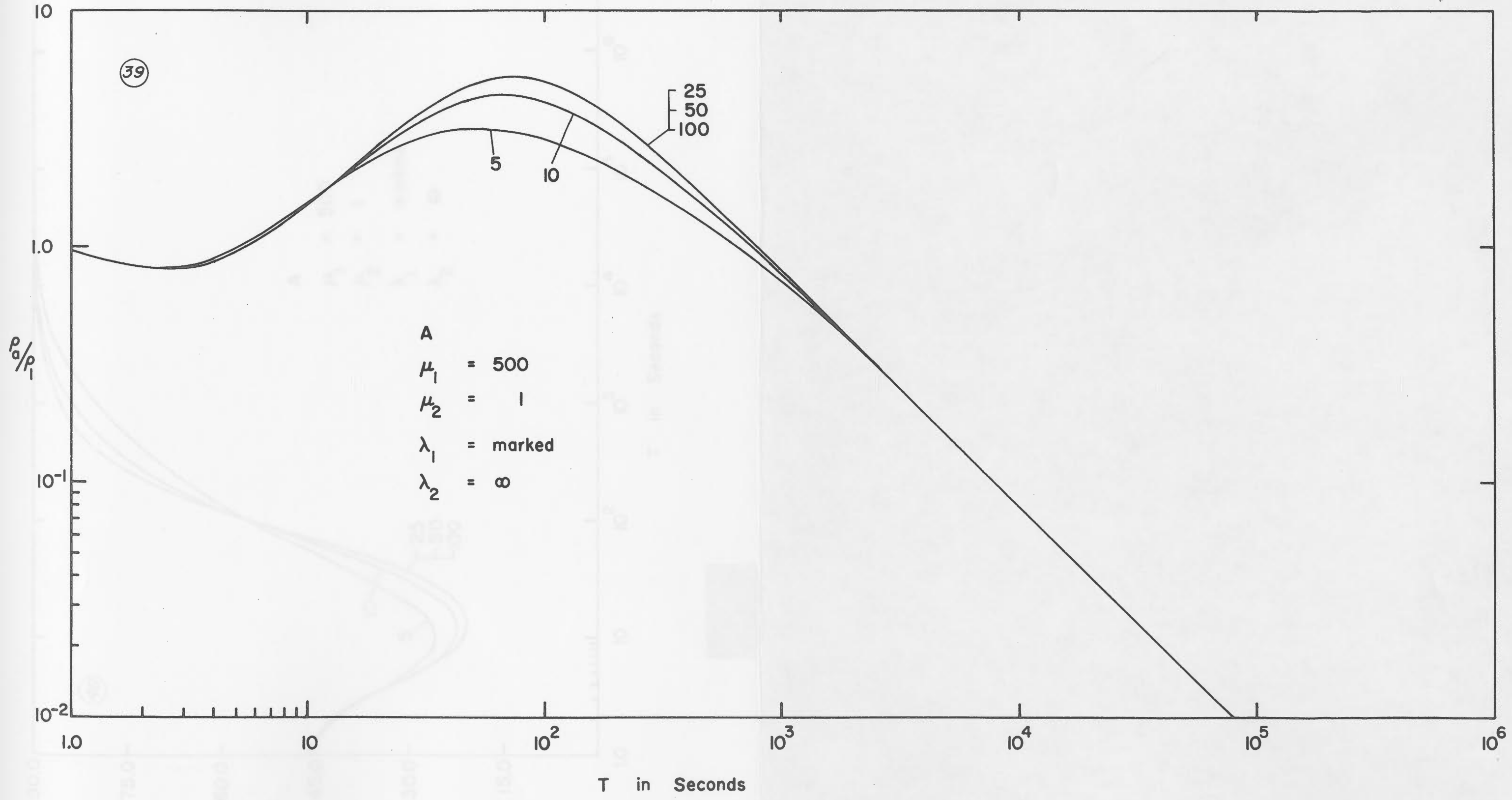
100
 80
 50
 10
 5

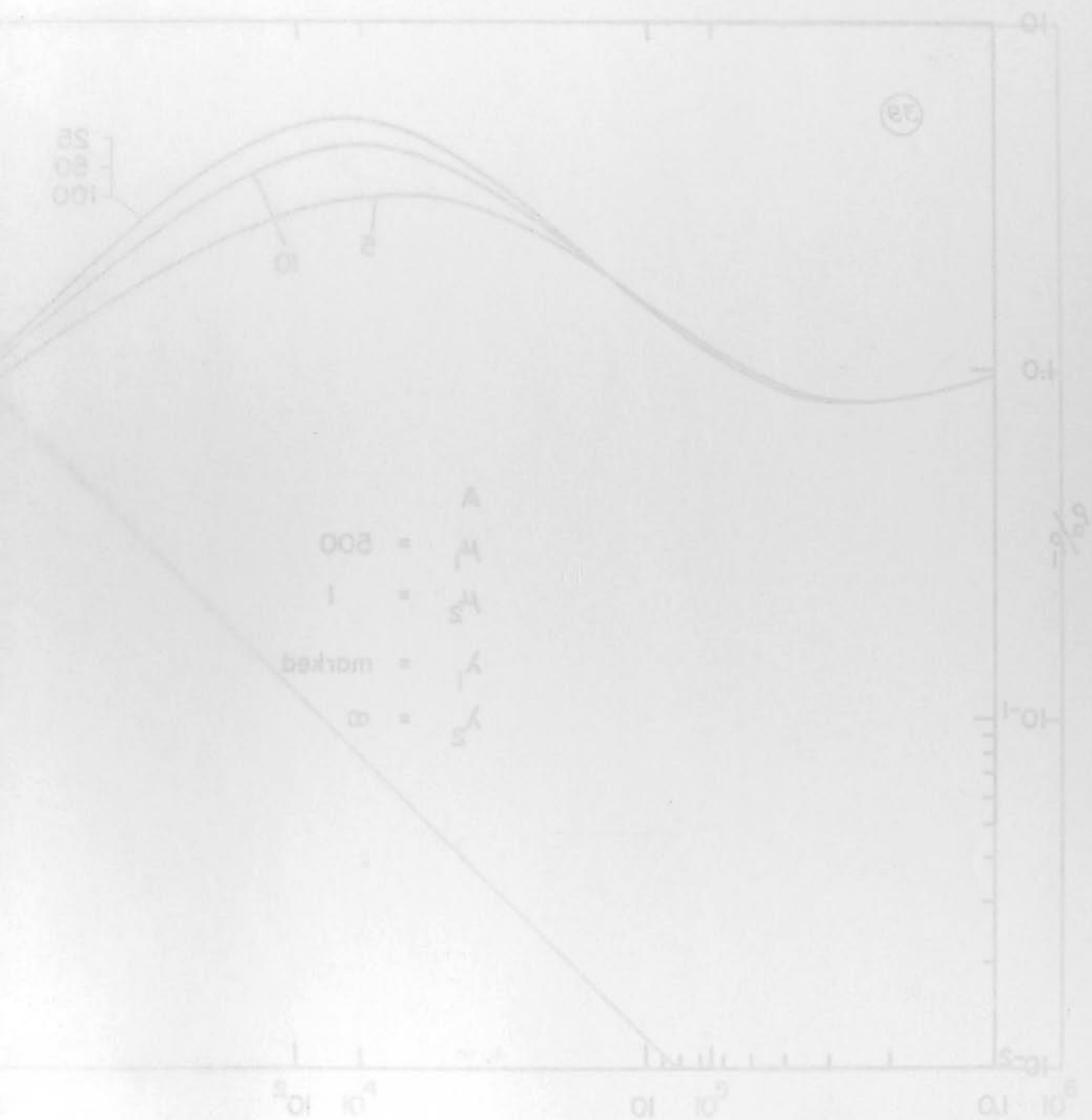
T in seconds



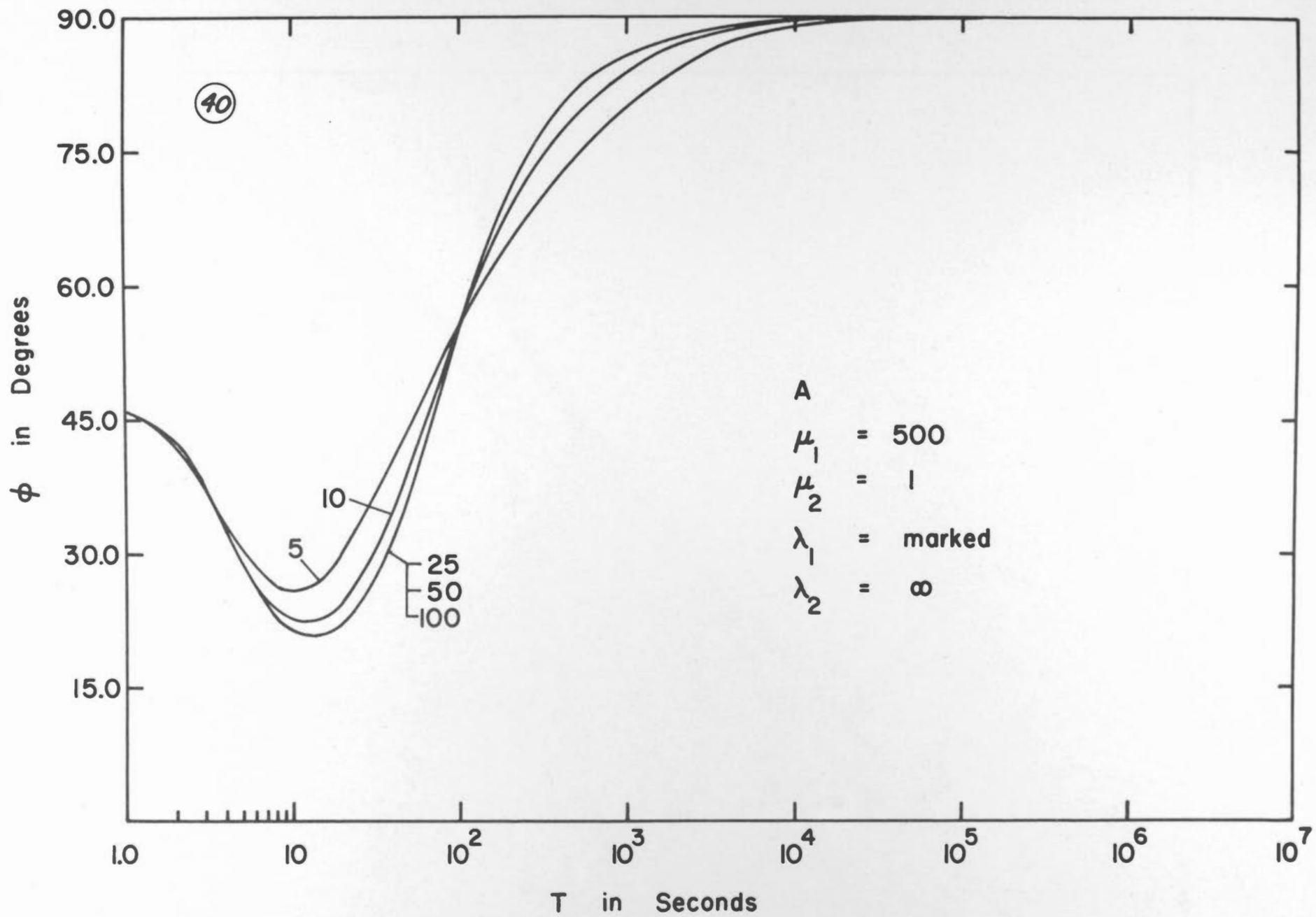
Abundance T



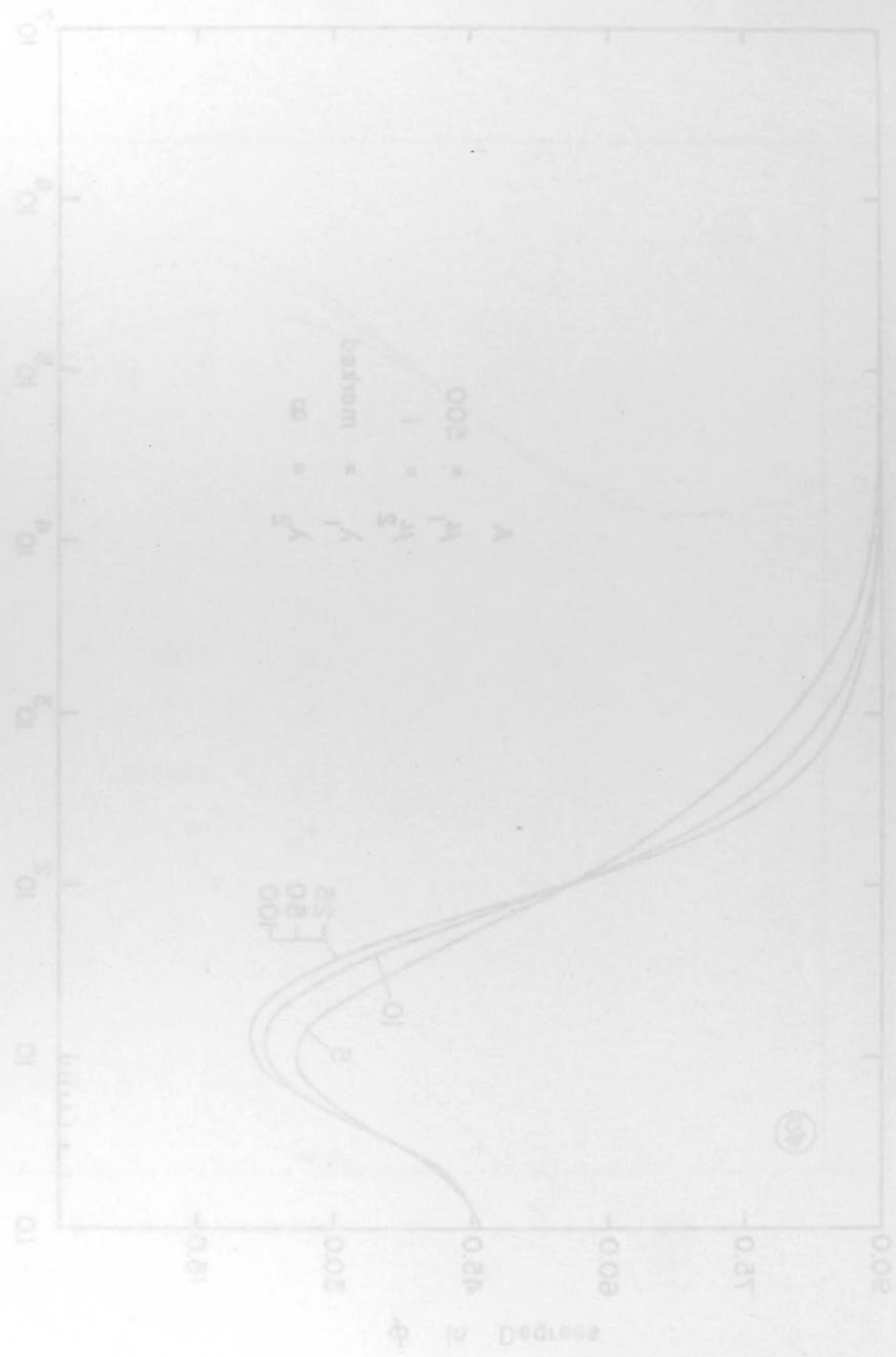


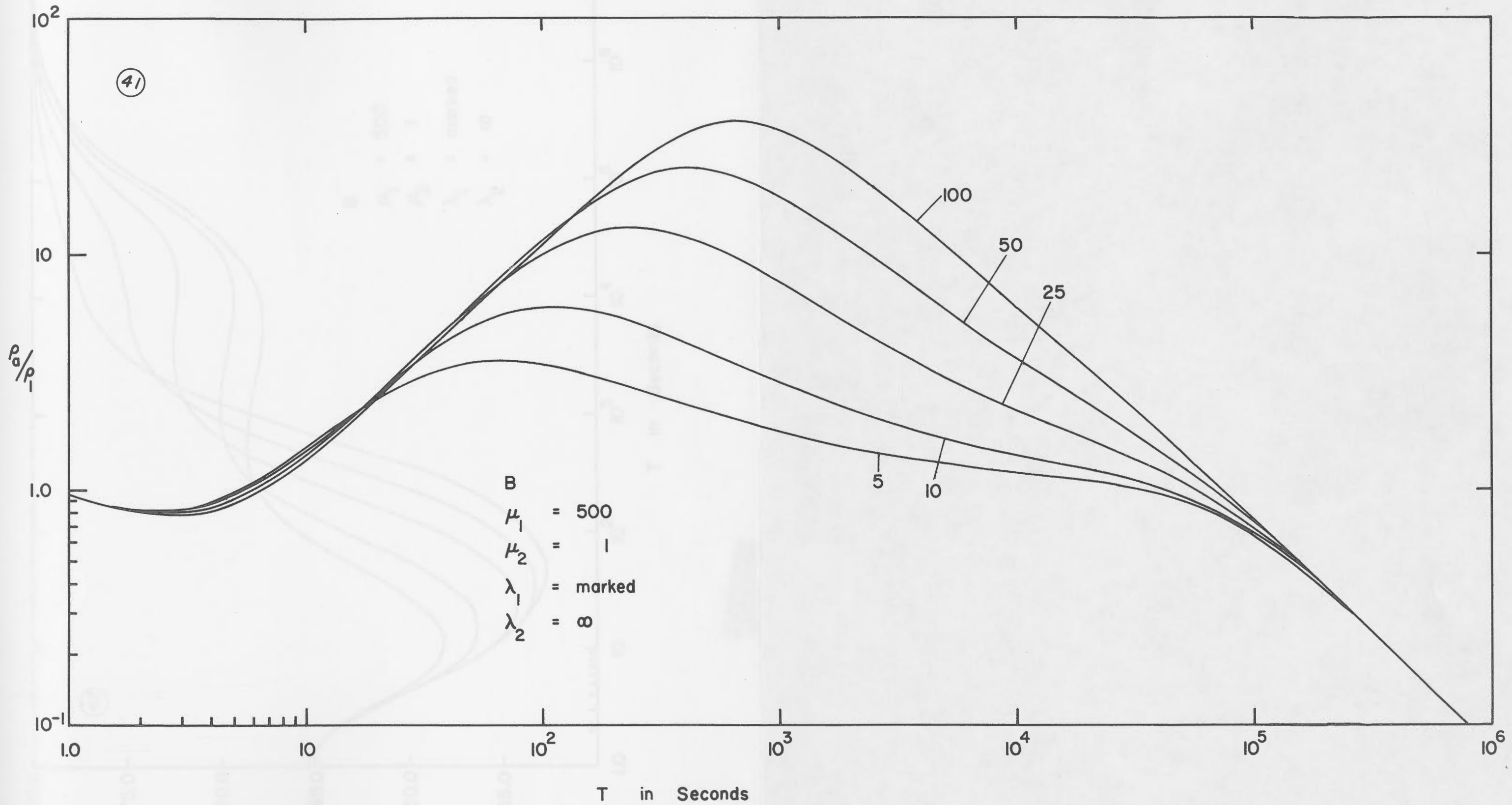


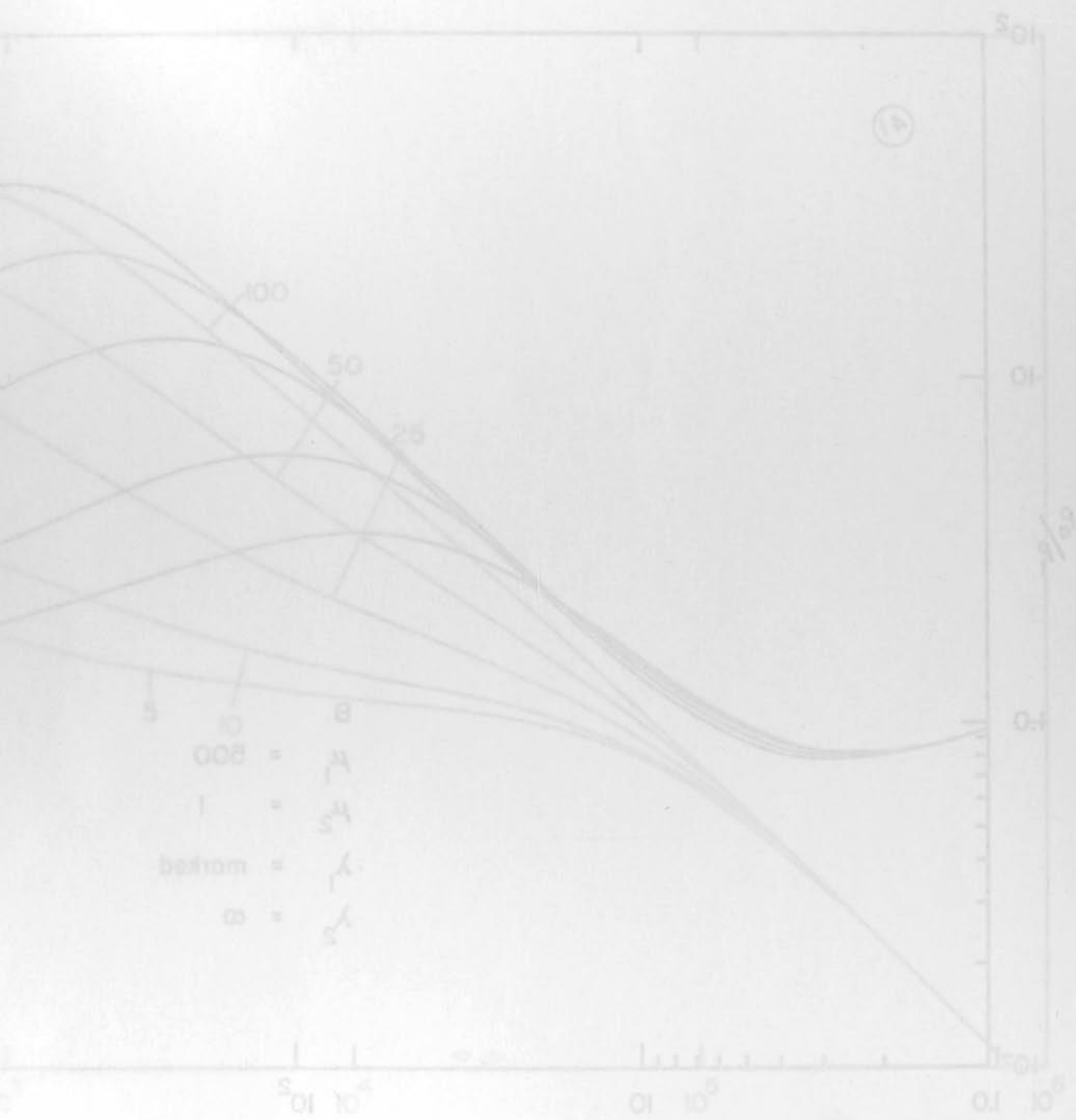
T in sec



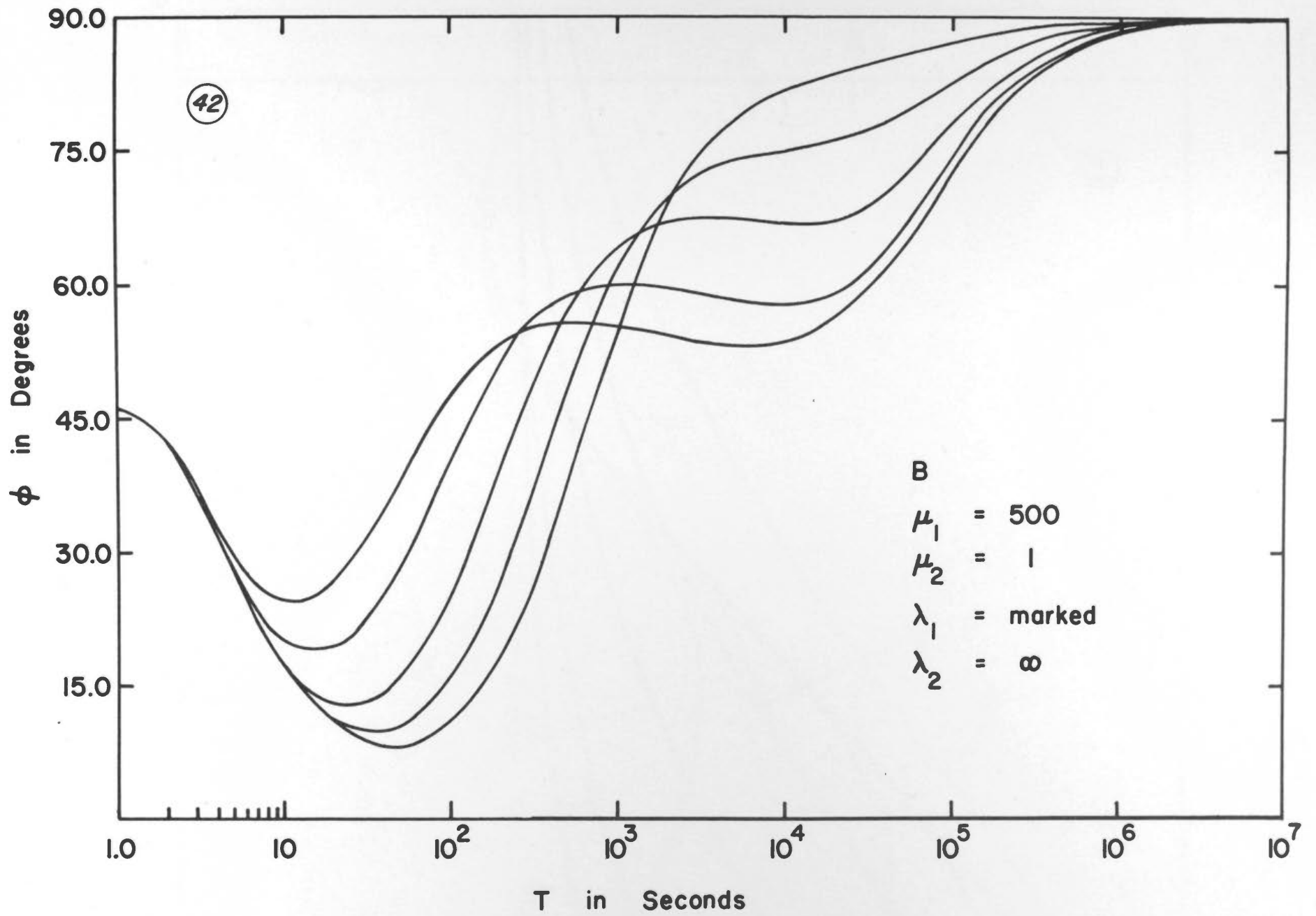
1 in seconds





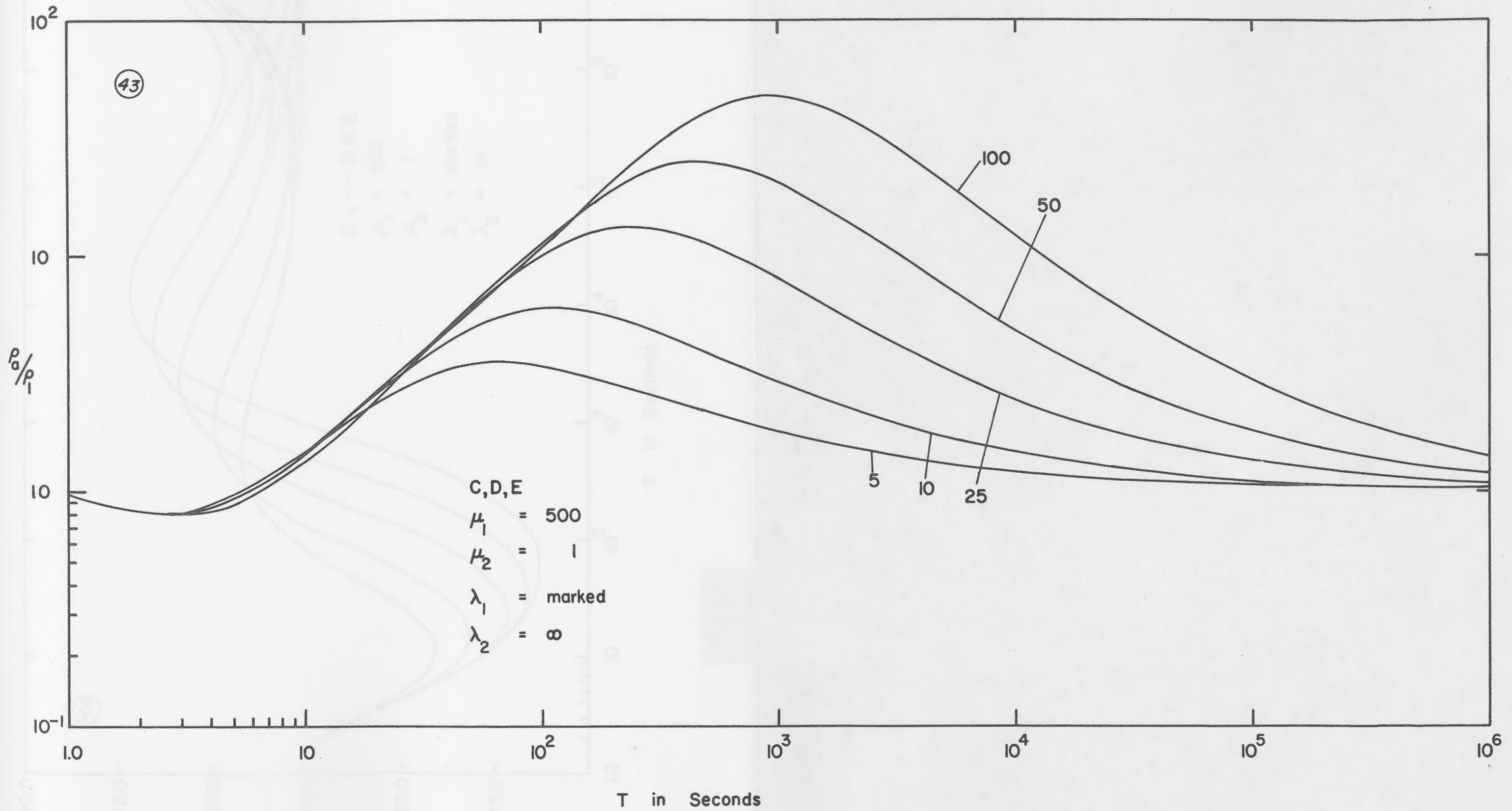


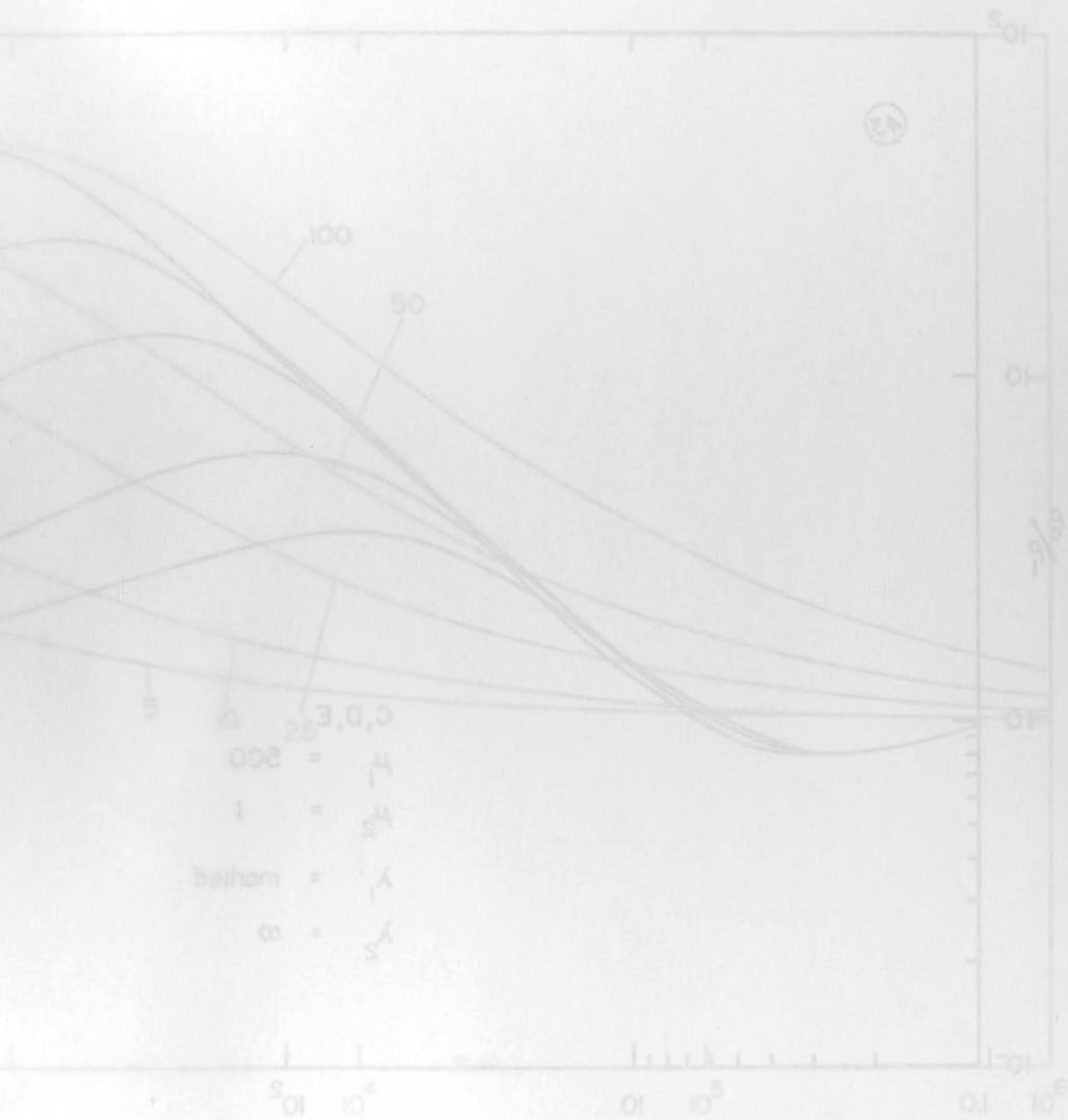
T in Seconds



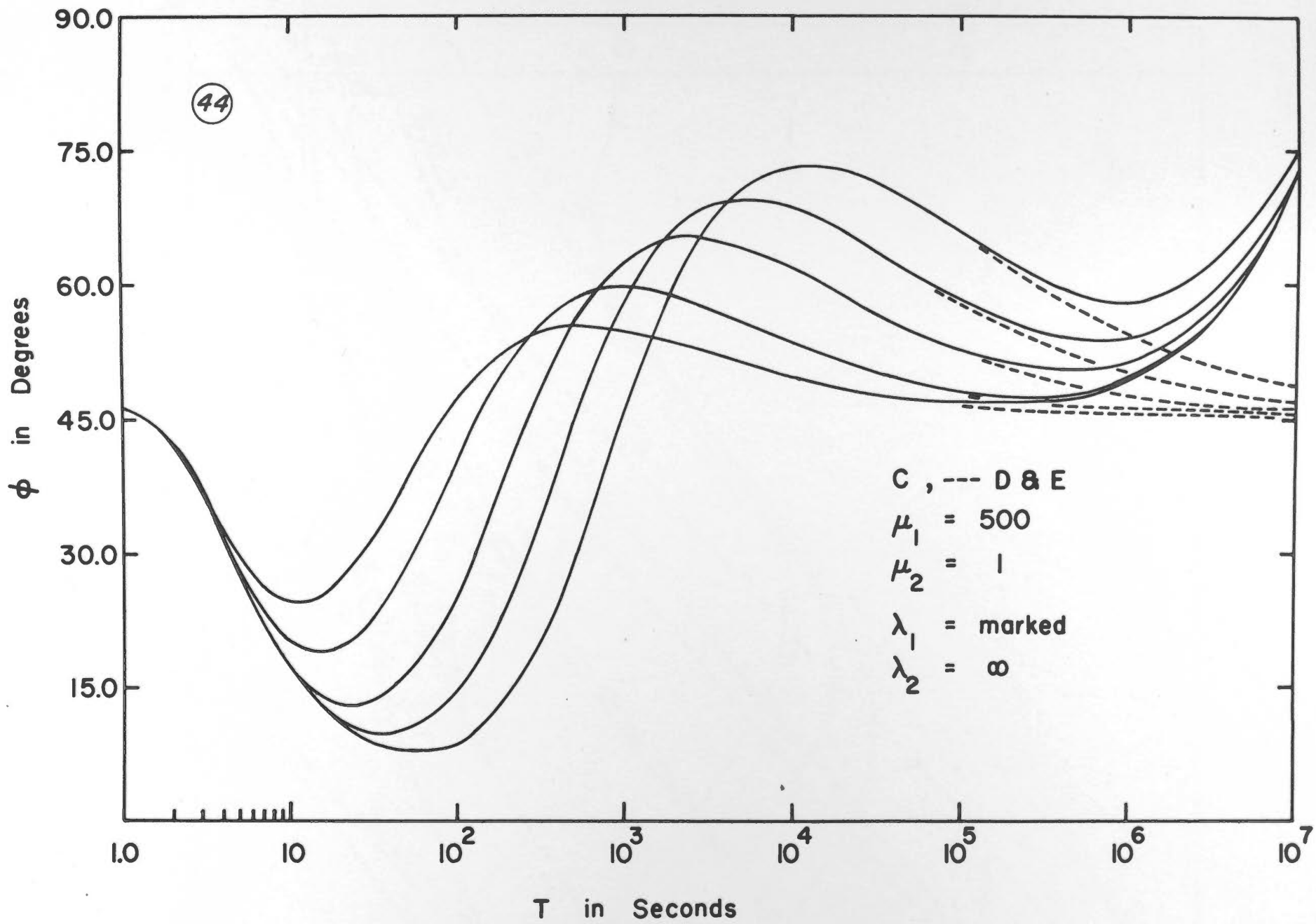
T in Seconds







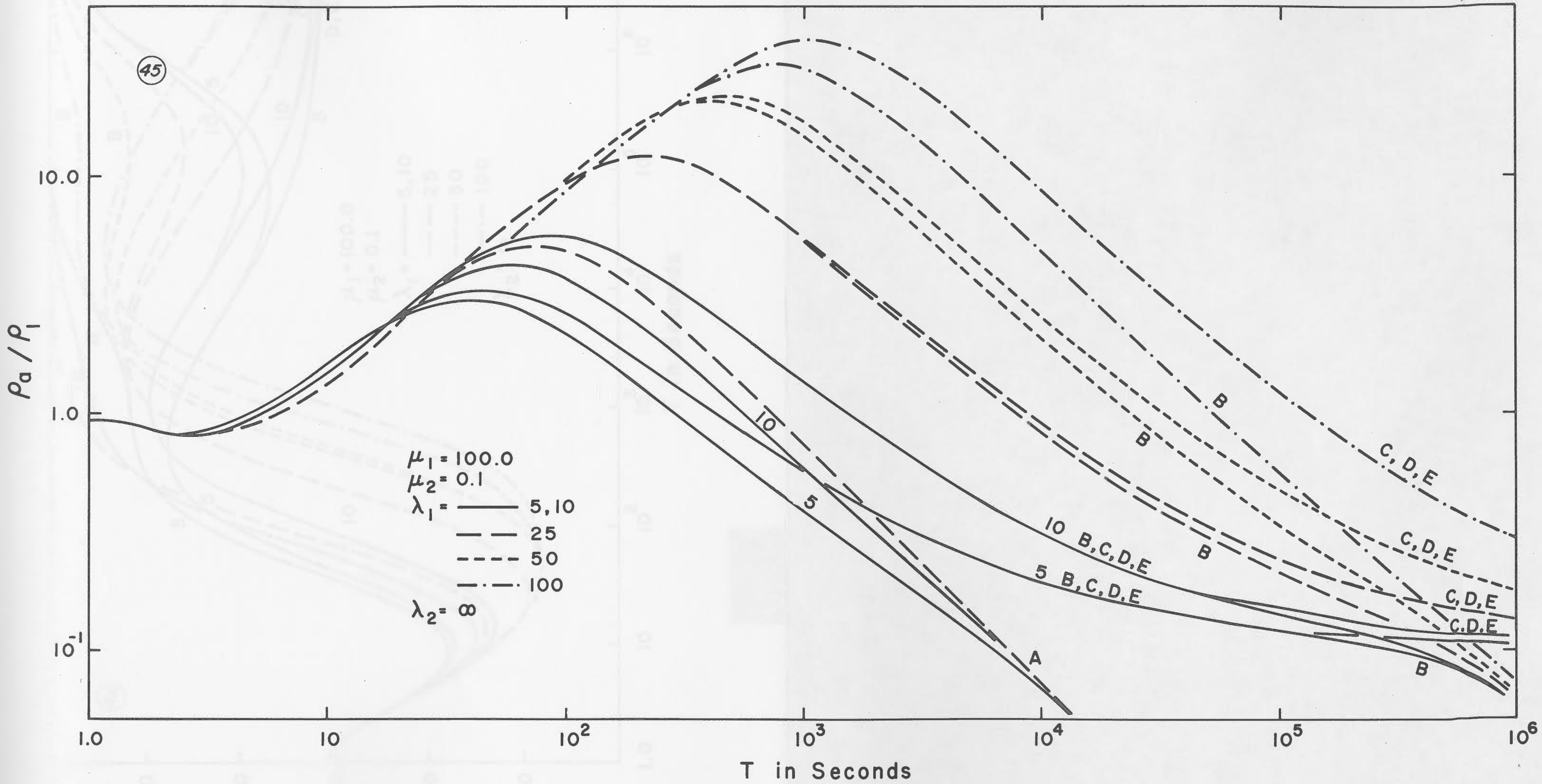
T m

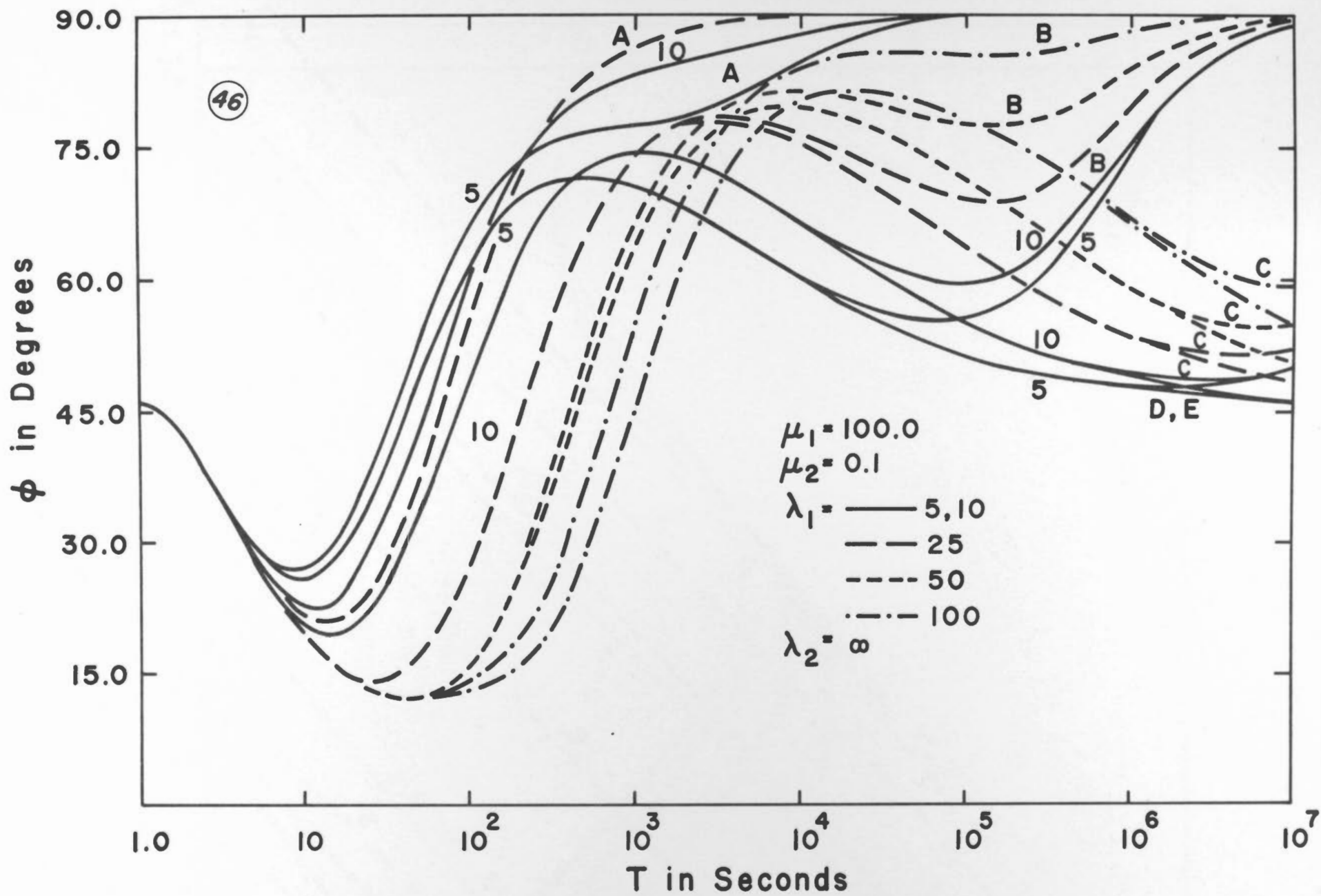


1 in 200000

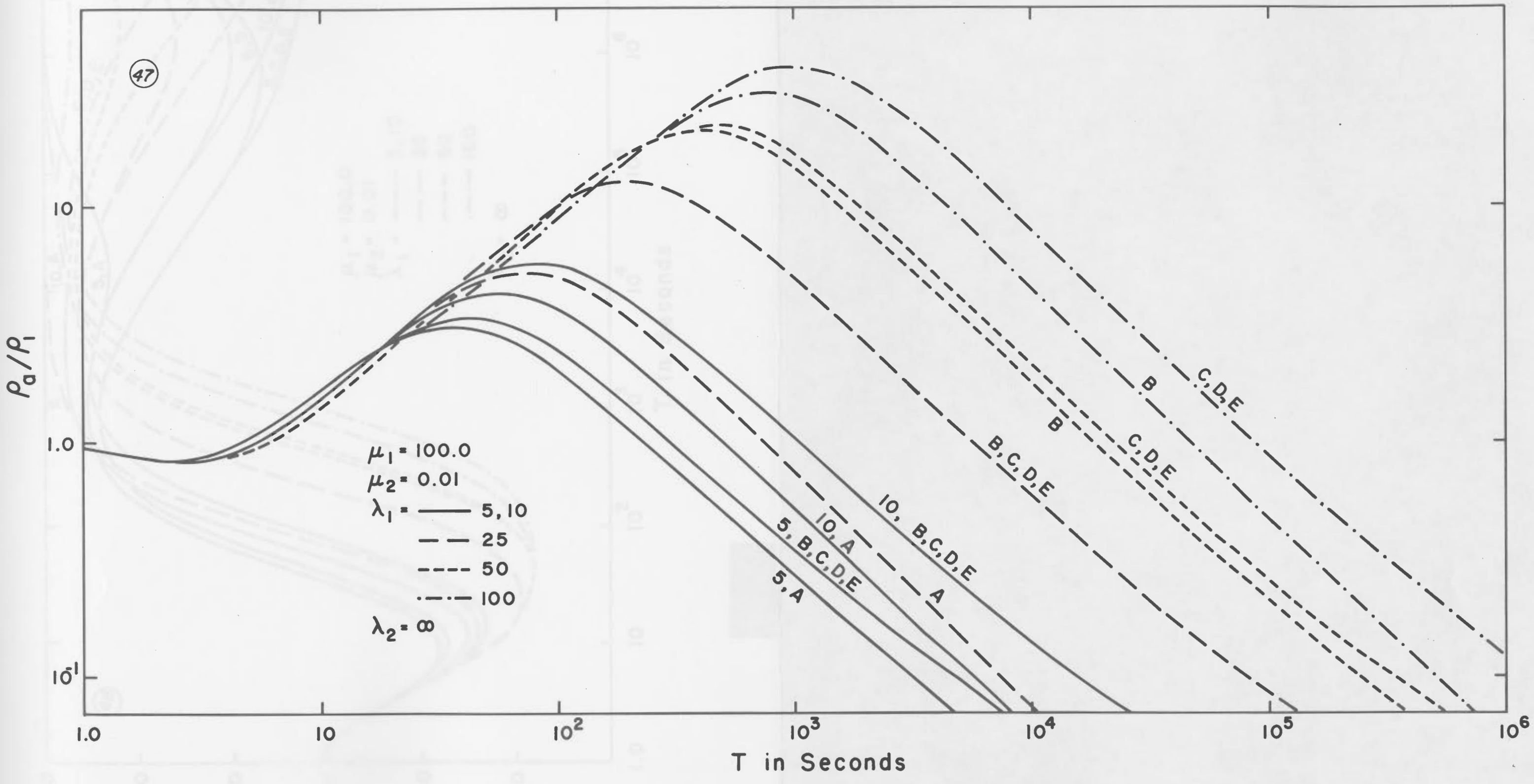


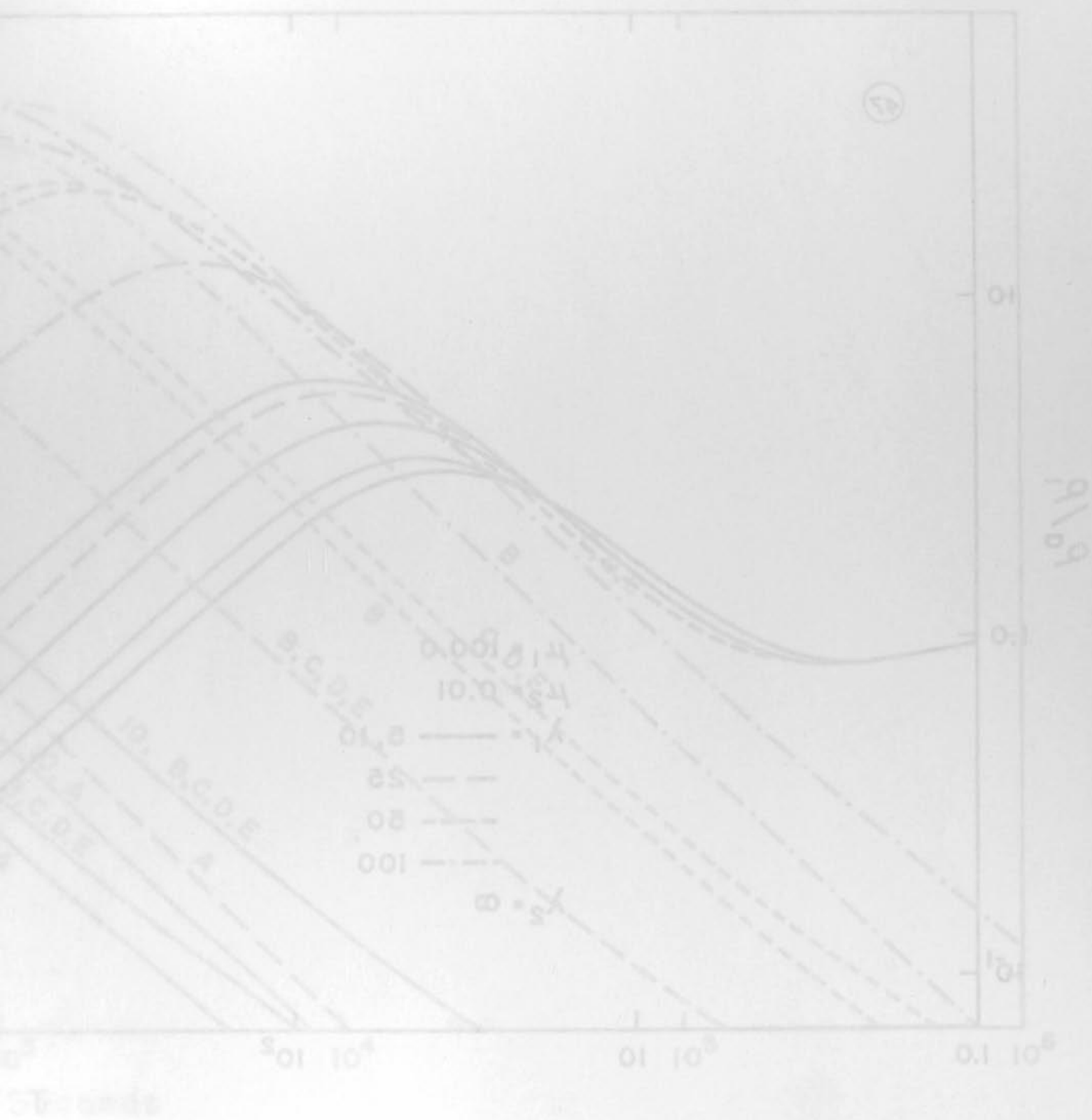
45

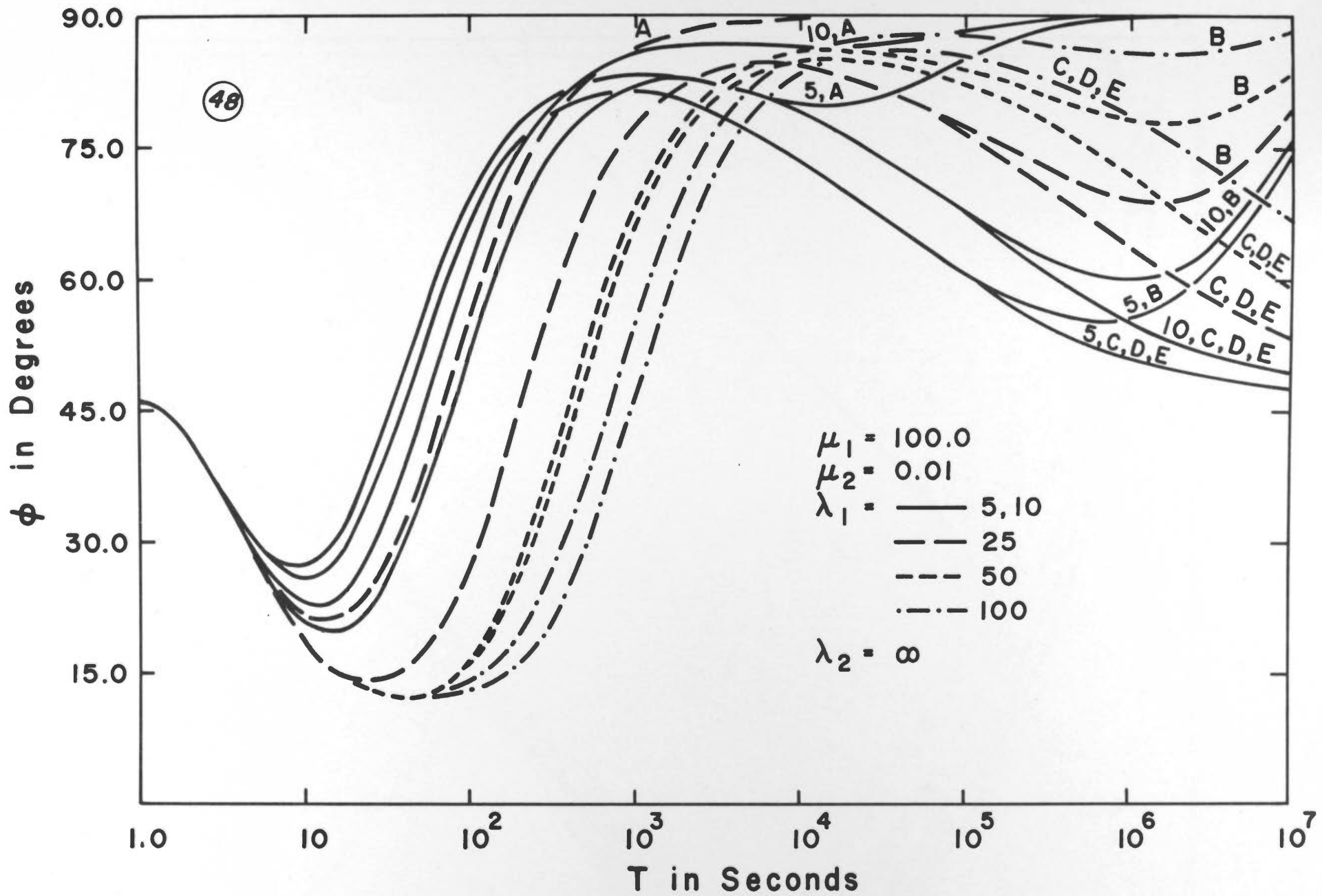


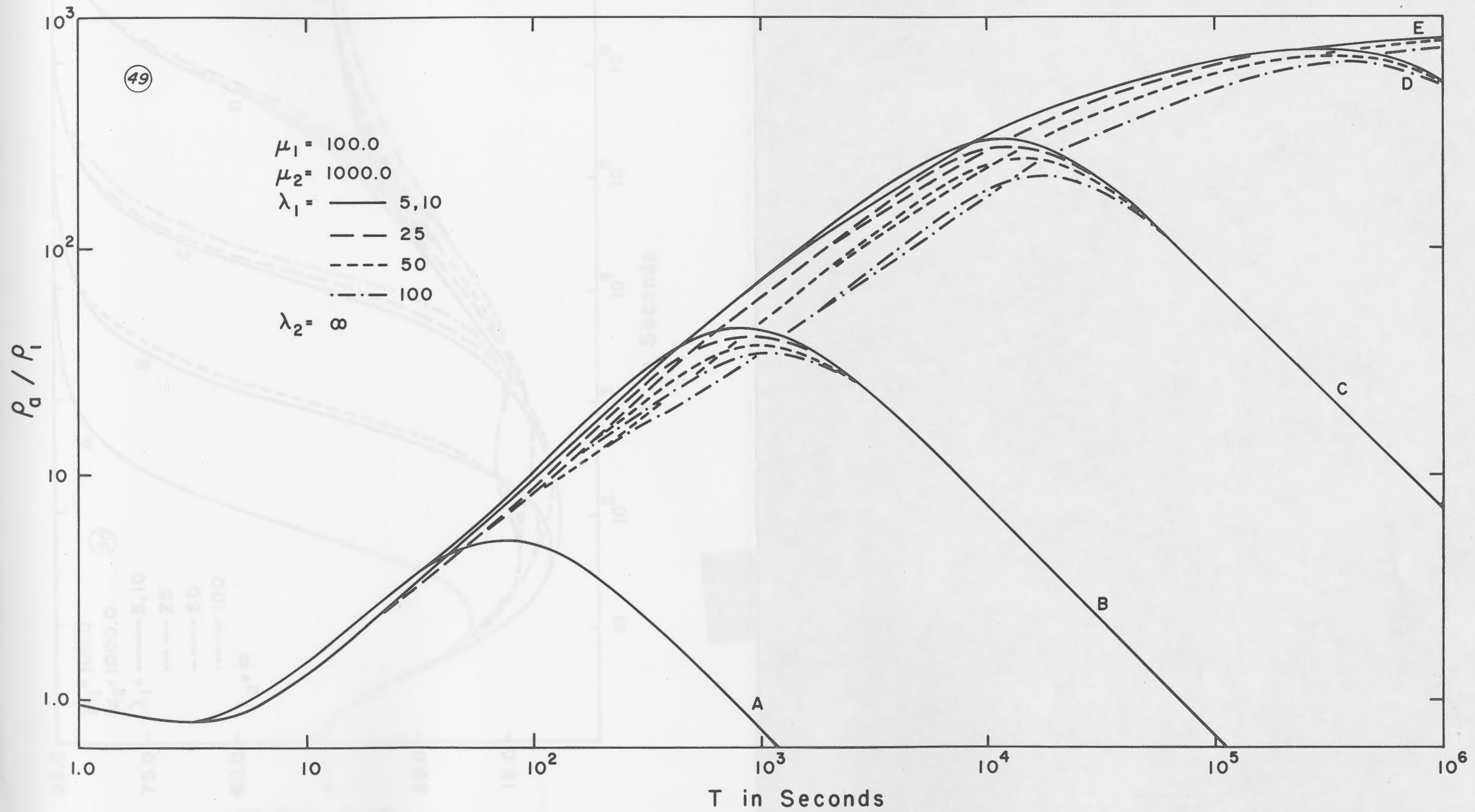


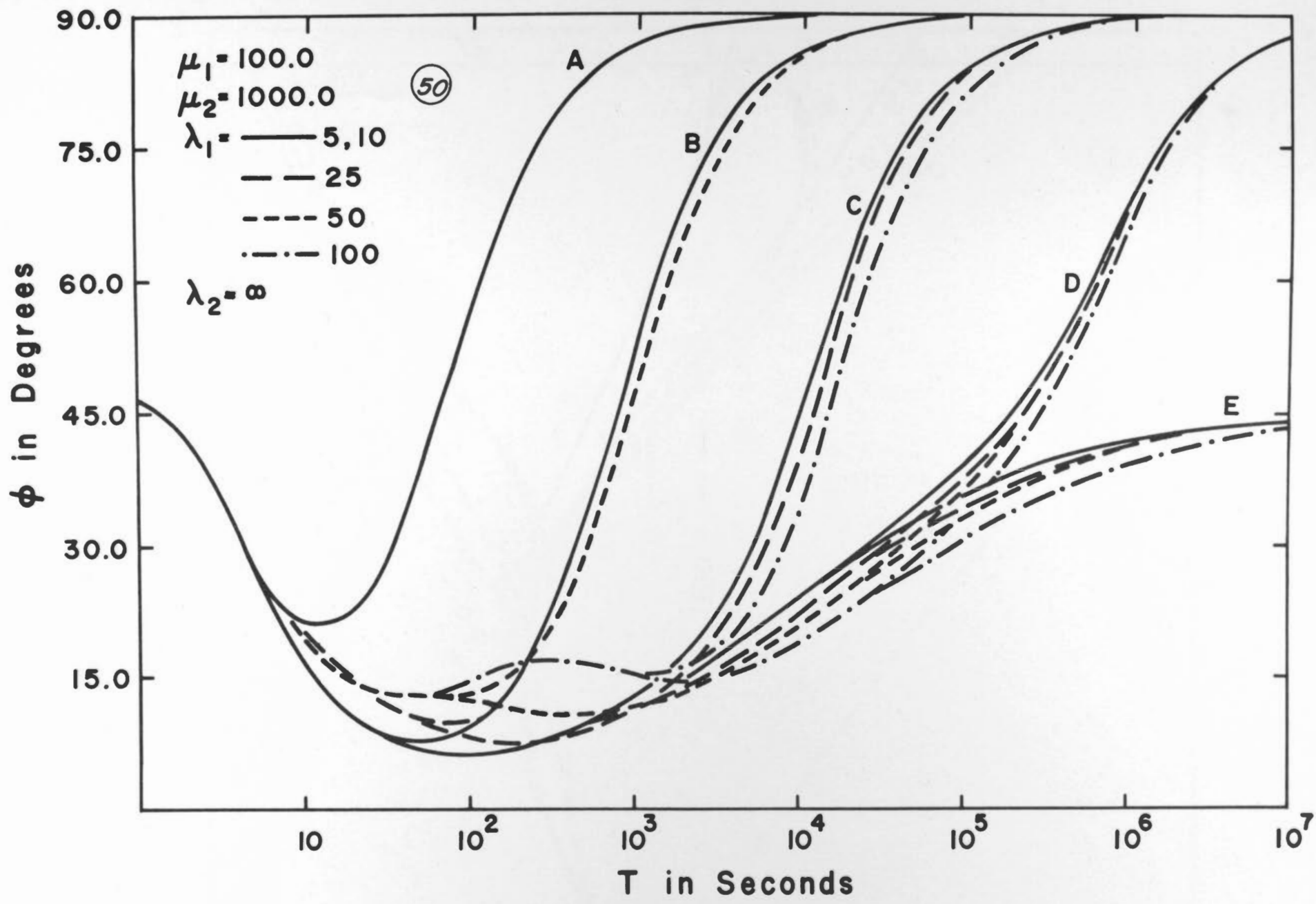
47

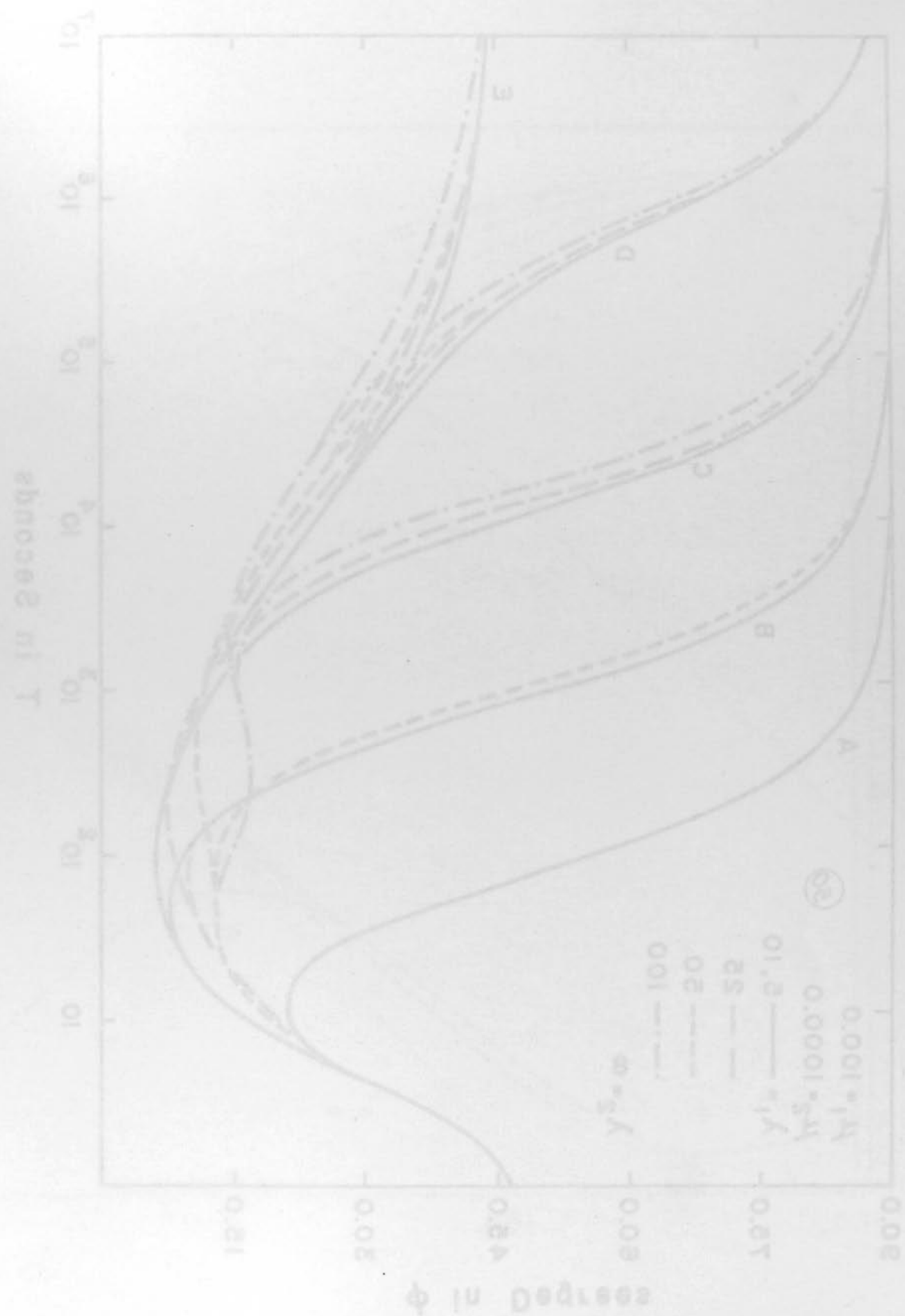


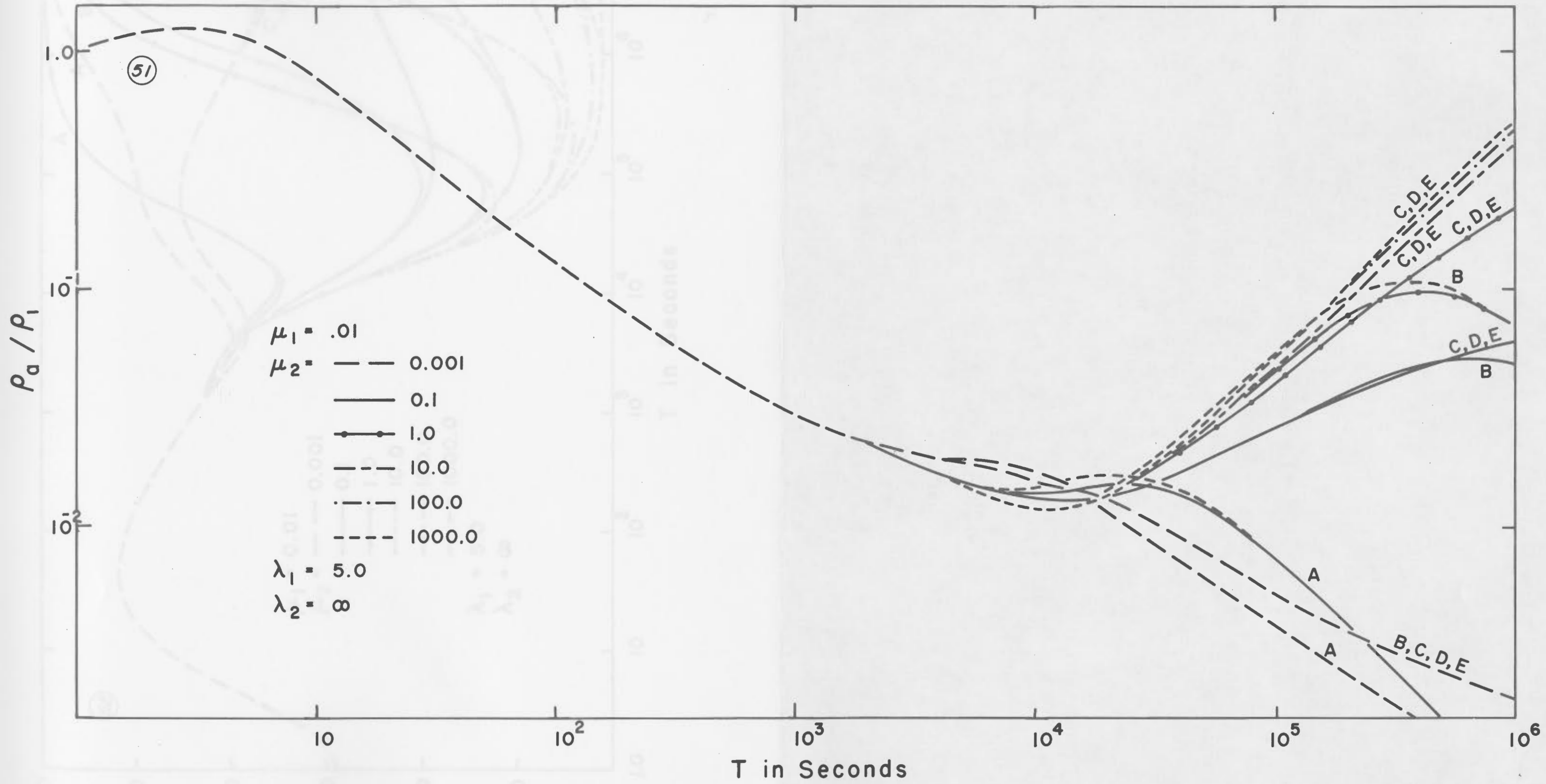


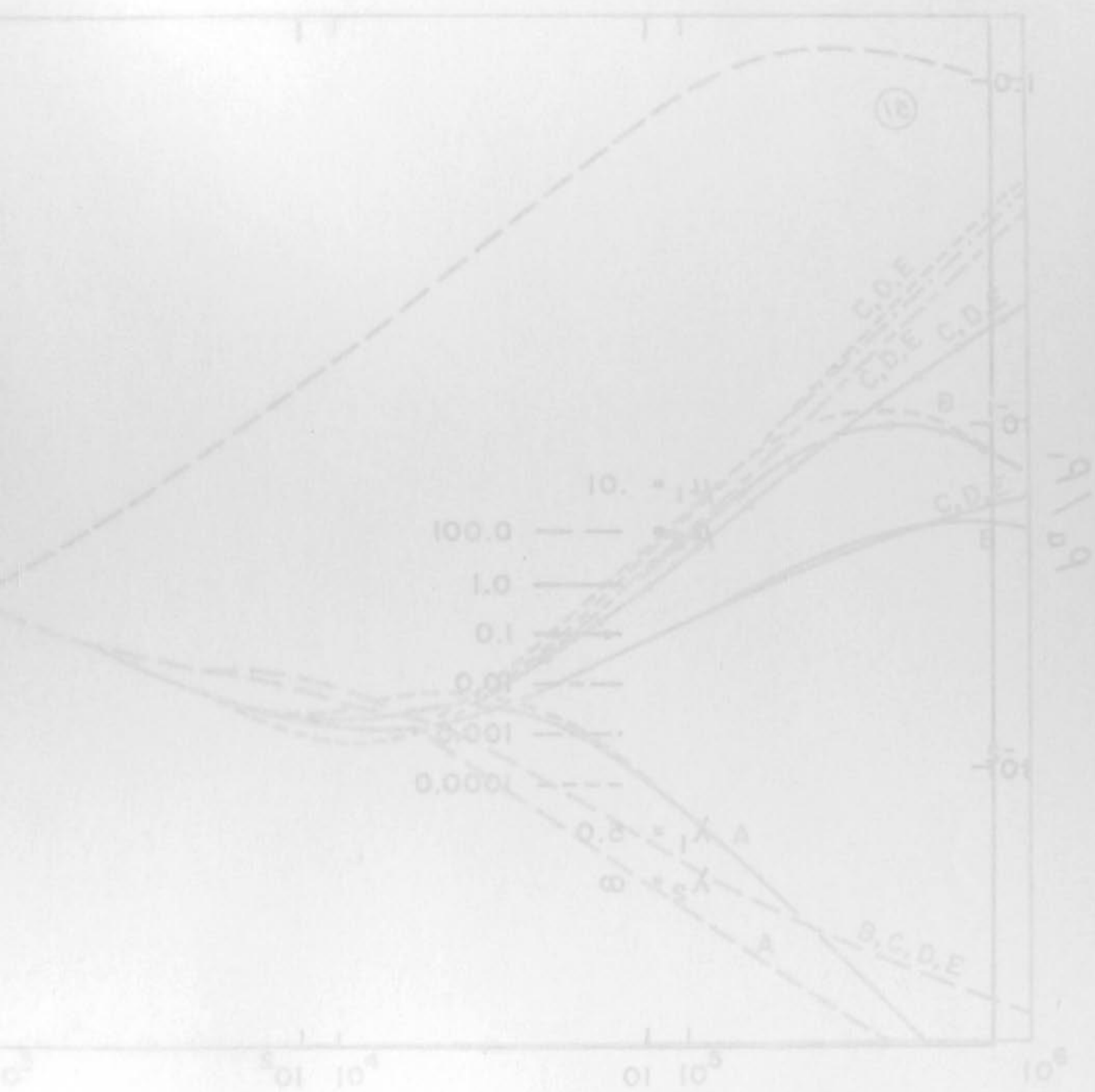


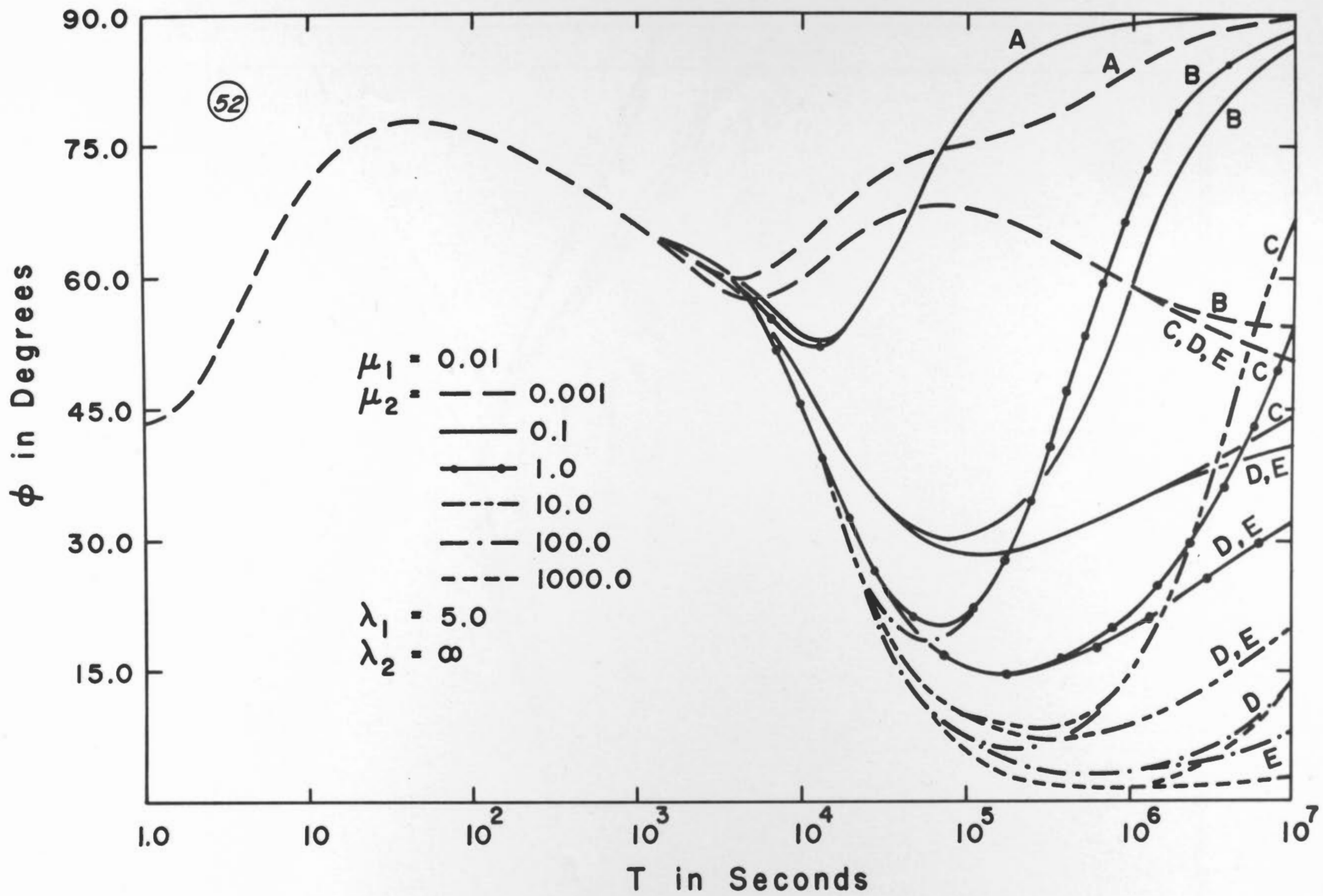




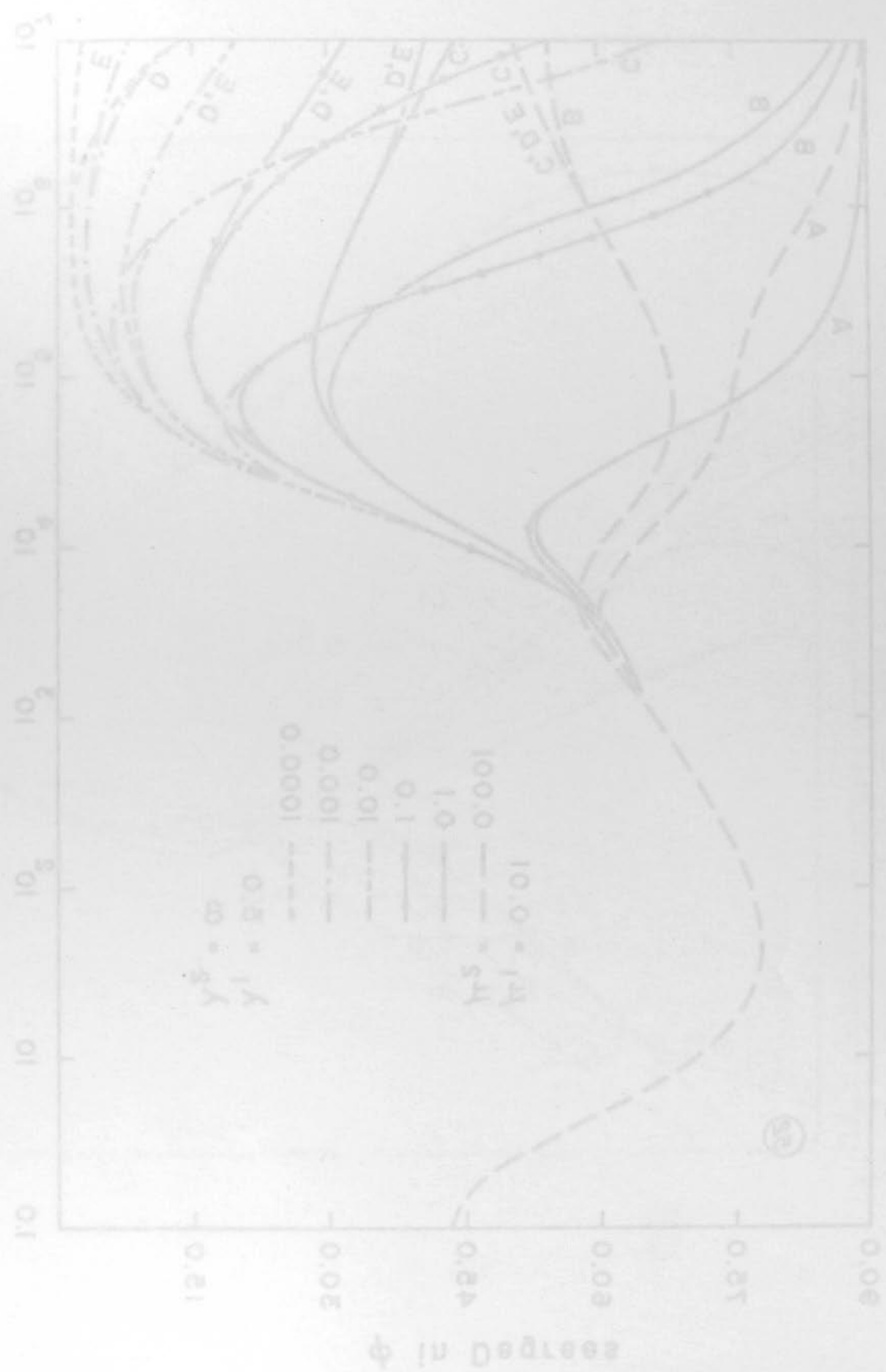




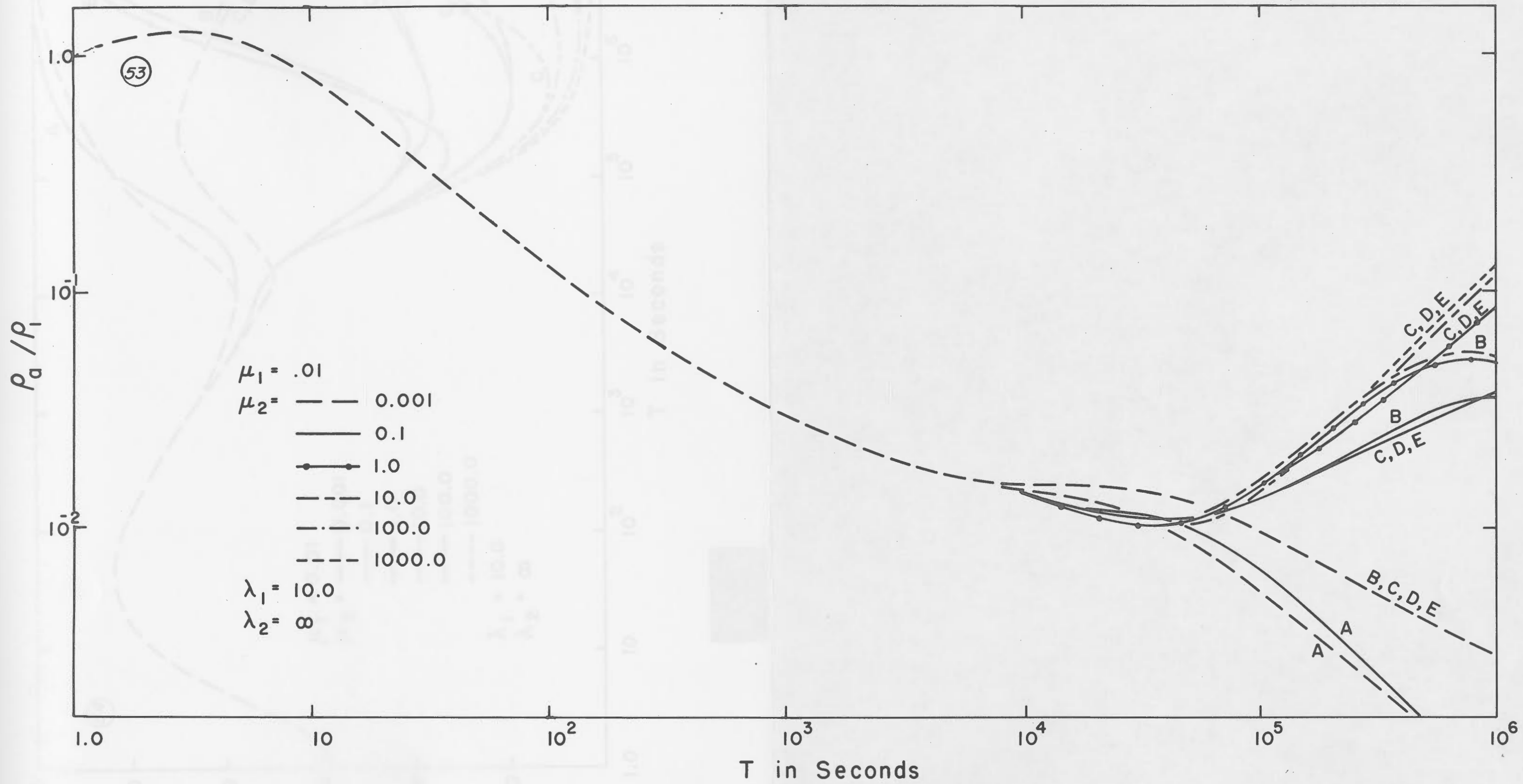


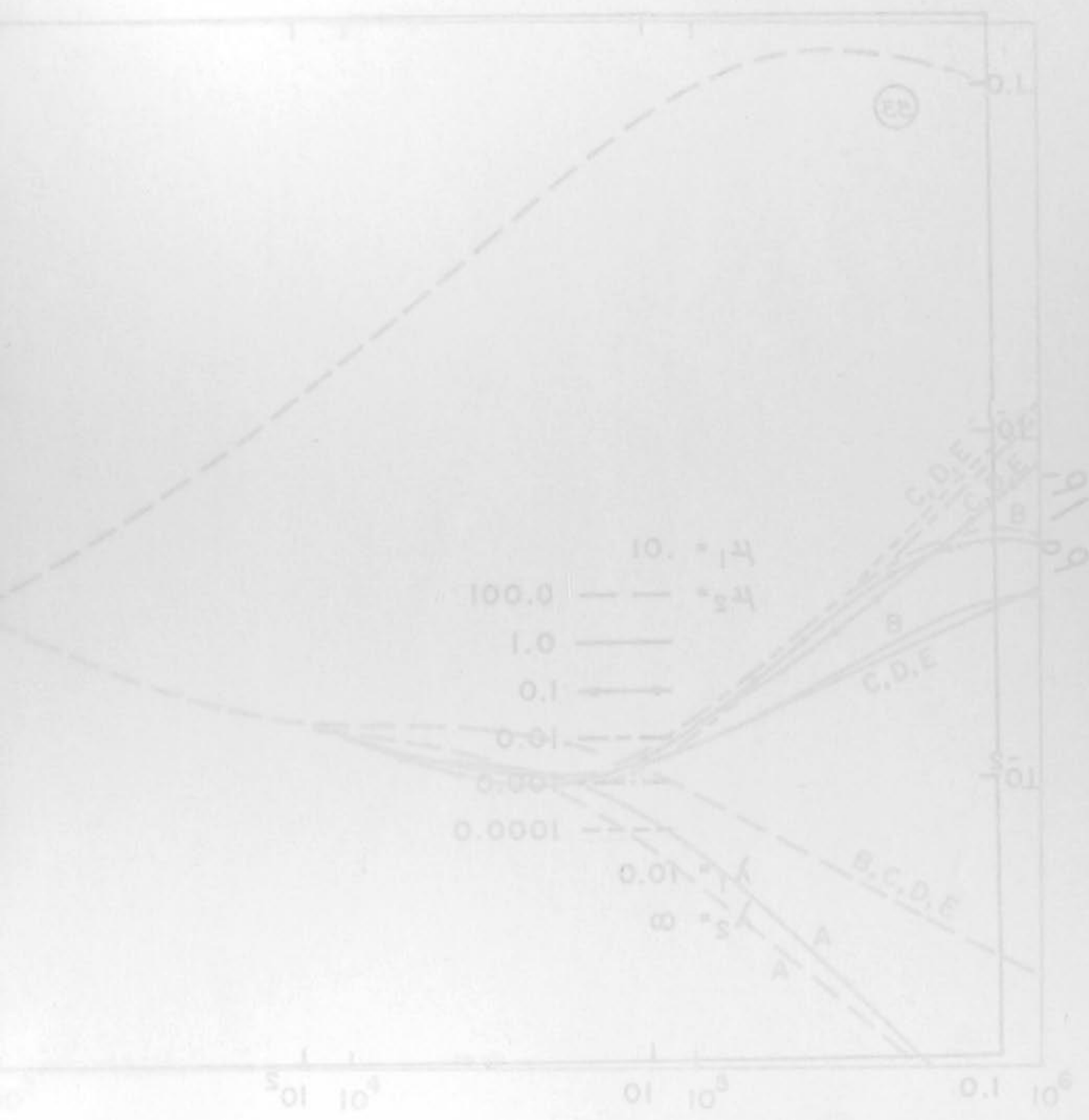


T in seconds

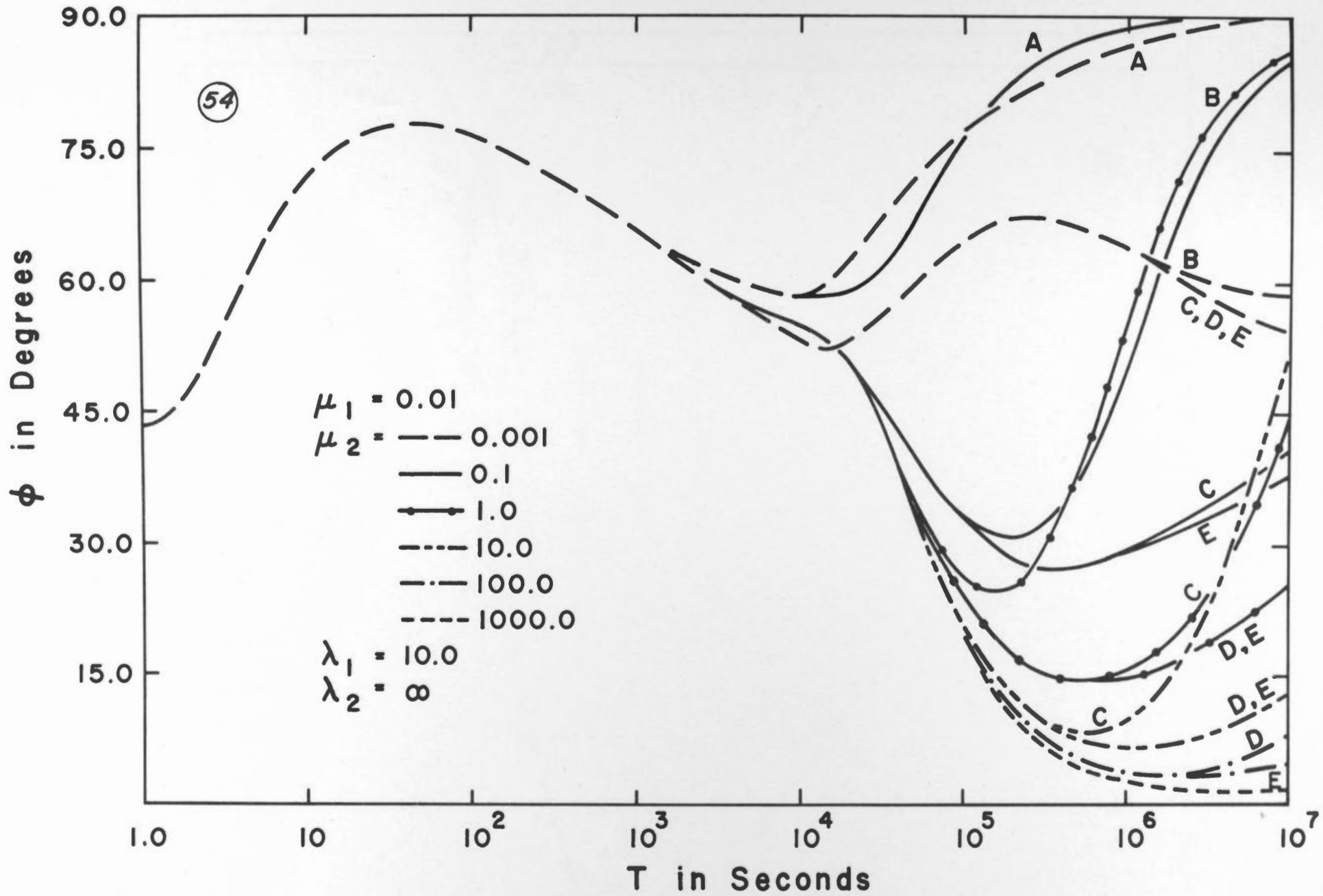


(35)



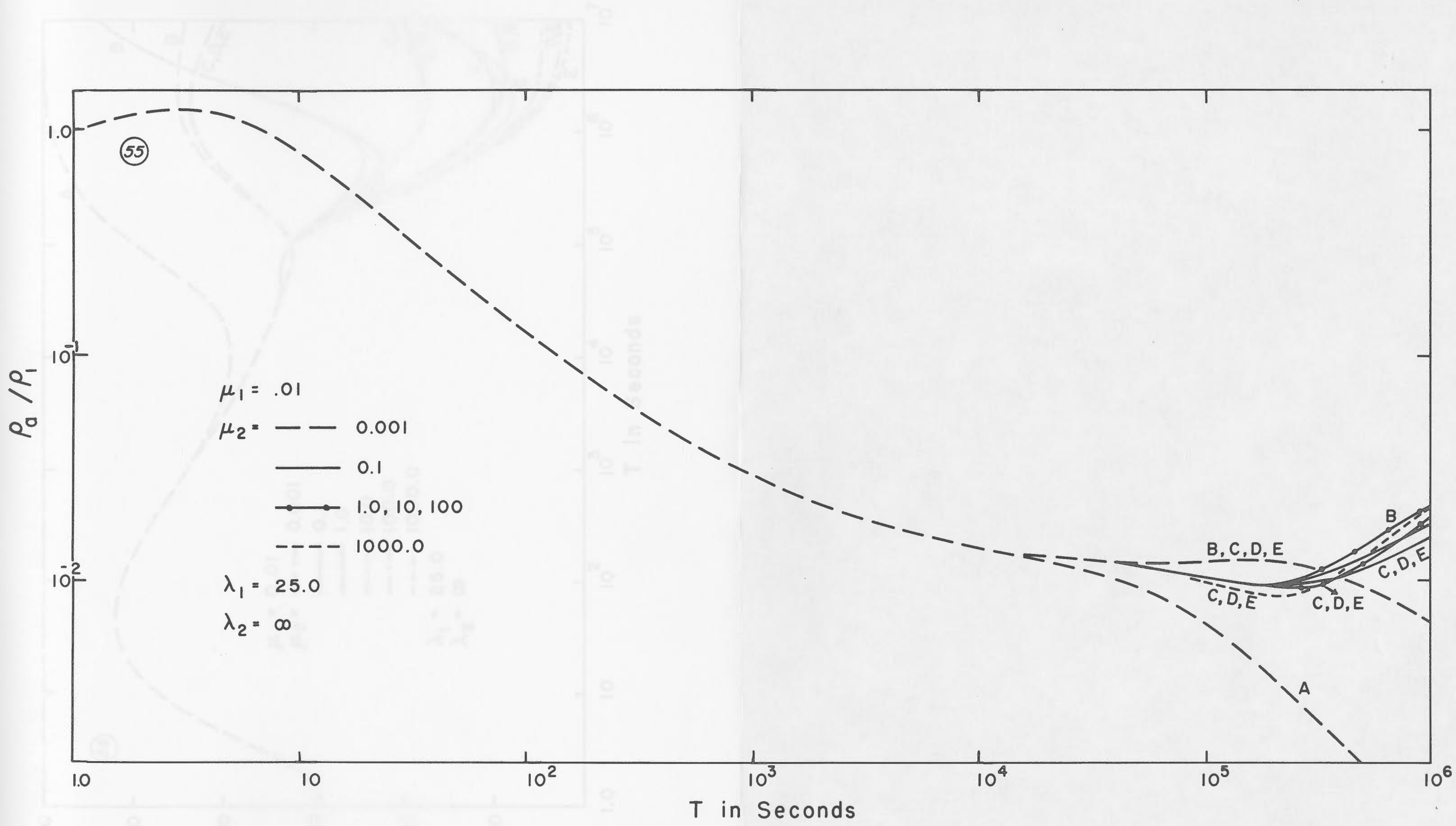


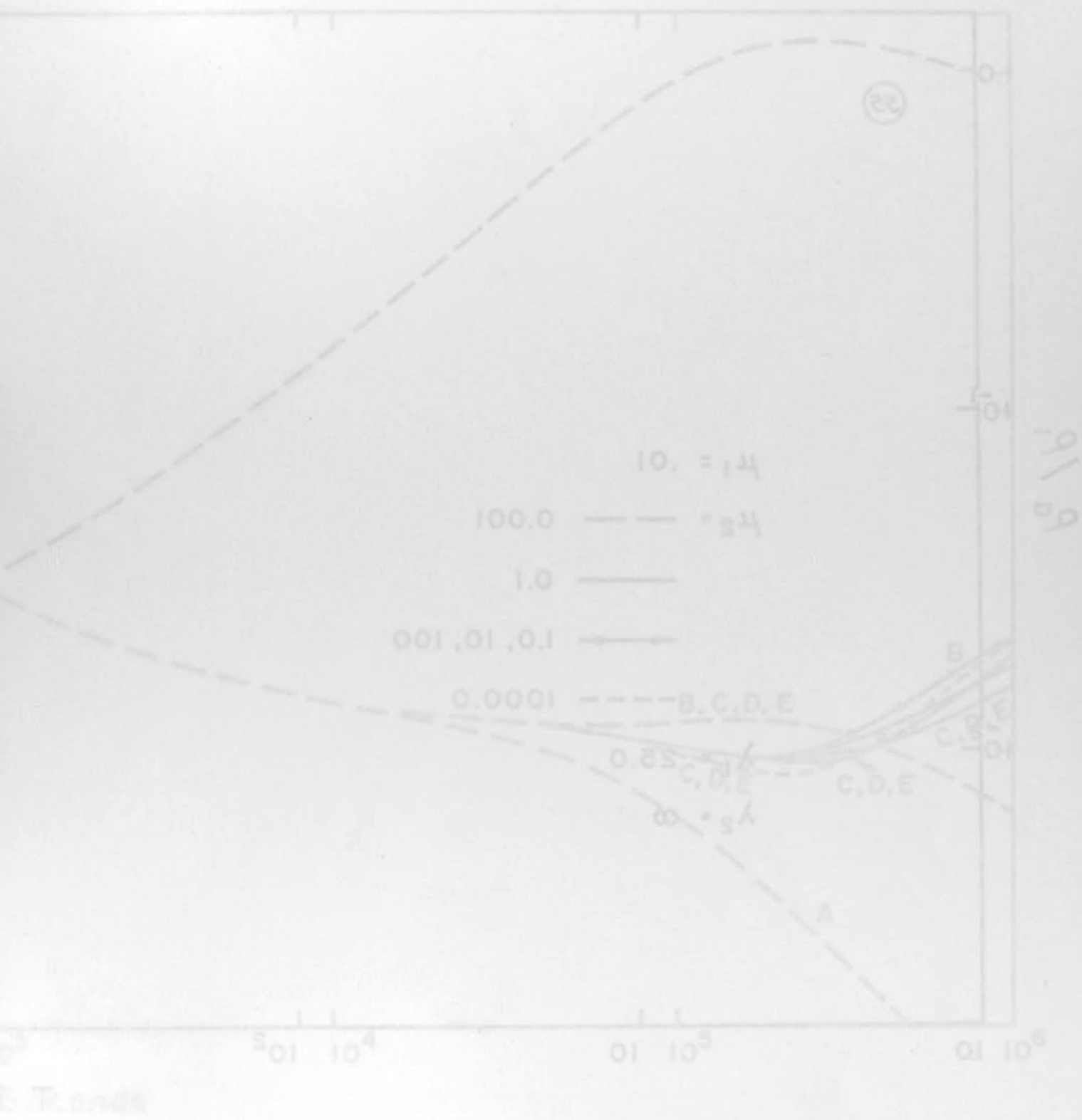
Speeds

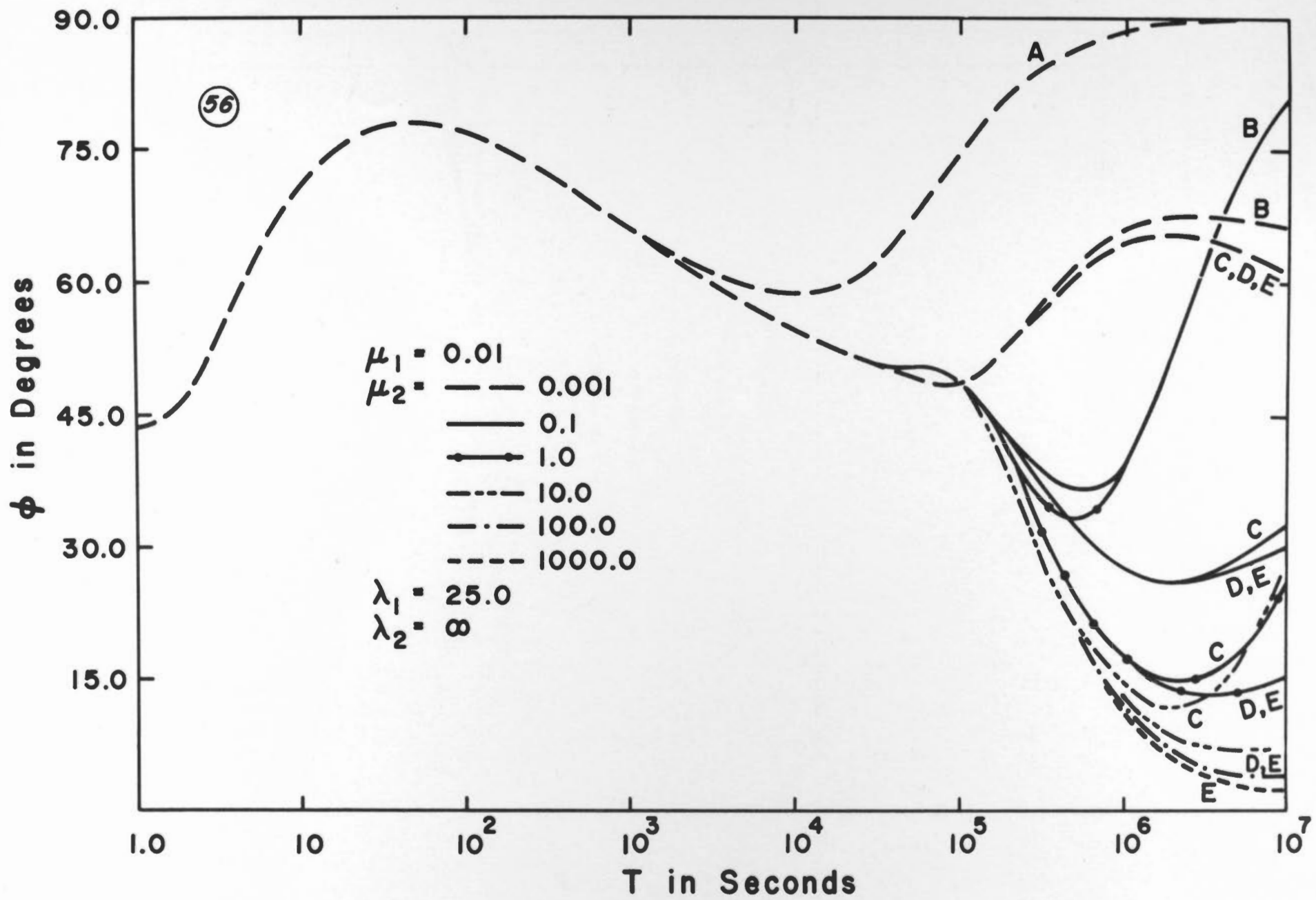


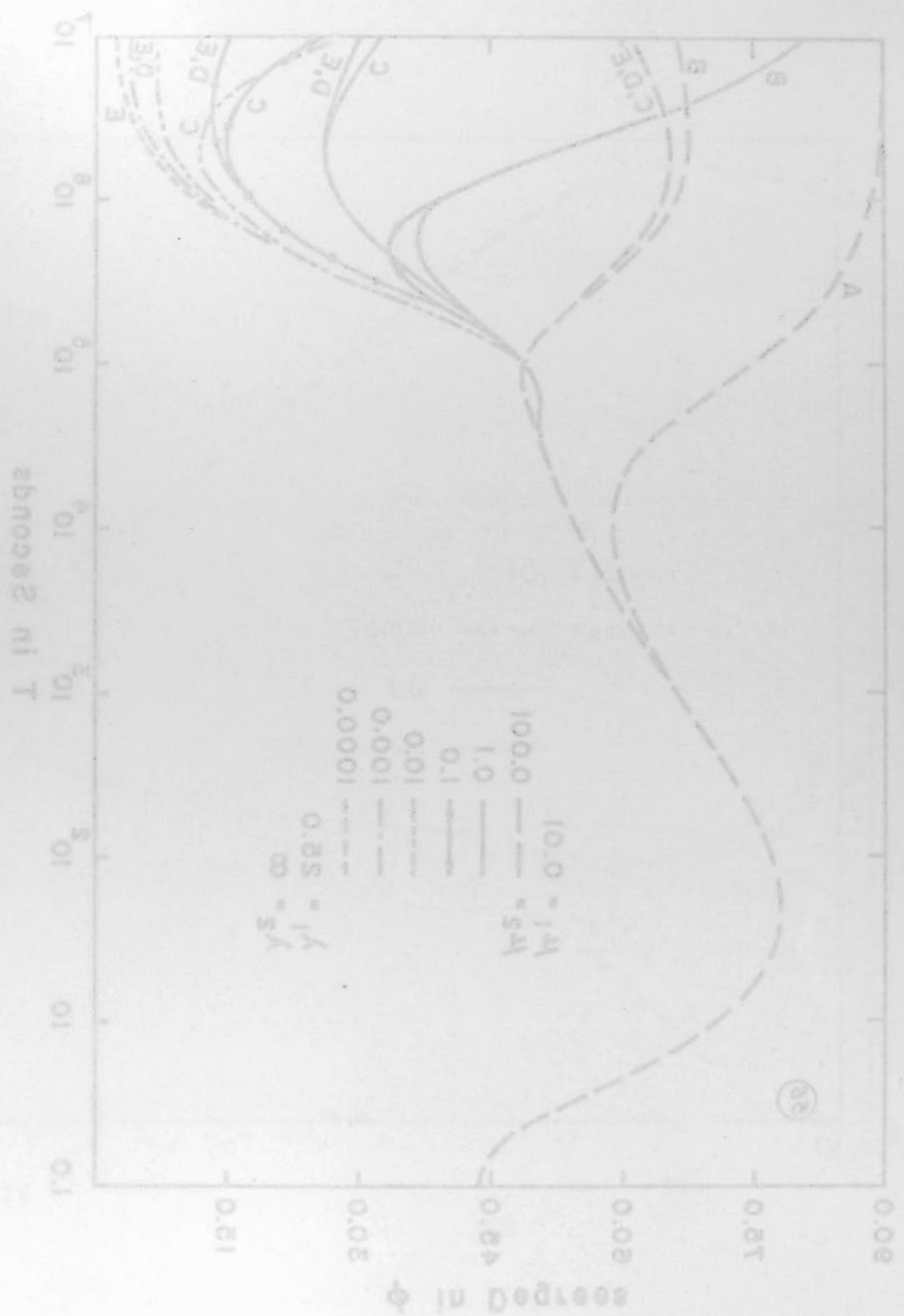
T in Seconds

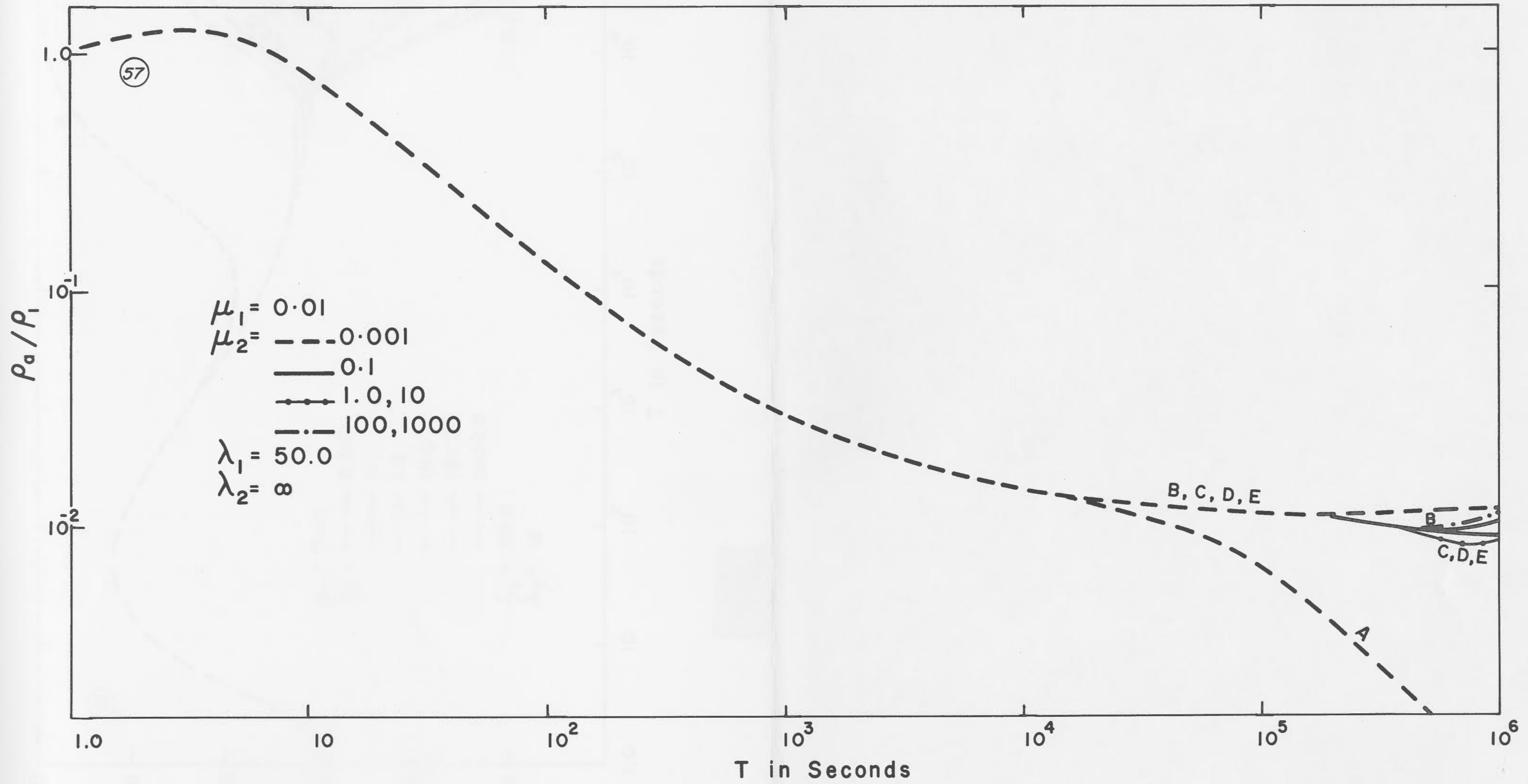


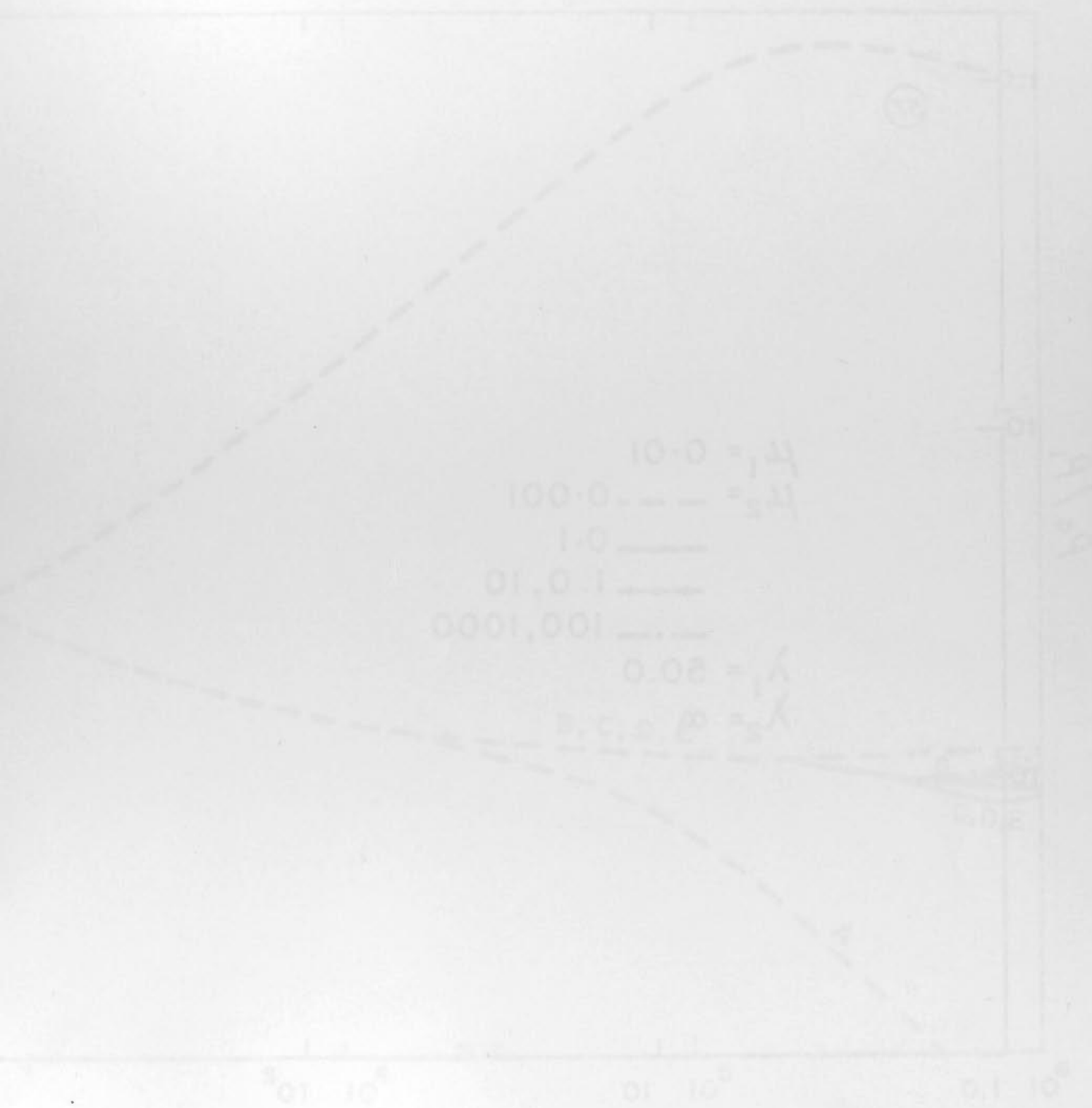












11/29

0.02

A

